INFORMATION TO USERS

This manuscript has been reproduced from the microfilm master. UMI films the text directly from the original or copy submitted. Thus, some thesis and dissertation copies are in typewriter face, while others may be from any type of computer printer.

The quality of this reproduction is dependent upon the quality of the copy submitted. Broken or indistinct print, colored or poor quality illustrations and photographs, print bleedthrough, substandard margins, and improper alignment can adversely affect reproduction.

In the unlikely event that the author did not send UMI a complete manuscript and there are missing pages, these will be noted. Also, if unauthorized copyright material had to be removed, a note will indicate the deletion.

Oversize materials (e.g., maps, drawings, charts) are reproduced by sectioning the original, beginning at the upper left-hand corner and continuing from left to right in equal sections with small overlaps.

Photographs included in the original manuscript have been reproduced xerographically in this copy. Higher quality 6" x 9" black and white photographic prints are available for any photographs or illustrations appearing in this copy for an additional charge. Contact UMI directly to order.

ProQuest Information and Learning
300 North Zeeb Road, Ann Arbor, MI 48106-1346 USA
800-521-0600

Methods for Pore Size Engineering in ZSM-5 Zeolite

David Ohayon

A Thesis

in

The Department

Of

Chemistry and Biochemistry

Presented in Partial Fulfillment of the Requirements

for the Degree of Doctor of Philosophy at

Concordia University

Montreal, Quebec, Canada

April 2002

Abstract

Methods for Pore Size Engineering in ZSM-5 Zeolite

David Ohayon

The desilicated form of the ZSM-5 was prepared by a process which involved the selective removal of silicon atoms from the parent sodium form zeolite in an aqueous basic solution of sodium carbonate. If the resulting material was activated at 700°C, its pore size was larger than that of the parent zeolite. The sample is called DS for: Desilication and Stabilization. The desilication treatment has the effect of lowering the Si/Al ratio, while keeping the zeolite structure essentially unmodified. The silicate material which had been removed was determined to be in large proportion sodium orthosilicate.

Ion-exchange of the Na-DZSM-5 with ammonium chloride gives us the more acidic form H-DZSM-5. An amount of 5 wt.% sodium orthosilicate is reinserted on the H-DZSM-5 zeolite and with a stepwise heating treatment to 700°C for 16-18 hours, the pore size decreases to 4.6Å. This process is termed DRS, which stands for: Desilication, Reinsertion and Stabilization. To get this pore narrowing, there is a reaction that occurs between the zeolite's and the orthosilicate's silanols during the thermal treatment. This reaction results from dehydroxylation and formation of siloxane bonds.

Selective adsorptive tests with the BTX aromatics and catalytic runs performed with methanol at various reaction temperatures, confirm the enlargement due to the DS treatment, and the pore narrowing as the result of the DRS treatment.

With the goal of better understanding the mechanism involved in the DRS process and to improve the success rate, we passed the sodium orthosilicate through an acid resin and then an amount of 8 wt.% of the resulting orthosilicic acid was reinserted into the H-DZSM-5. The sample was then activated to 700°C for a period of 16-18 hours and a measure of the median pore size gave us 4.4Å with an improved reproducibility. The reaction temperature between the zeolite's and the orthosilicic silanols was determined with the Differential Scanning Calorimetry/Thermal Gravimetric Analysis (DSC/TGA) instrument to be ca. 600°C. The product of this reaction gives us the formation of new siloxane bonds which are responsible for pore narrowing.

Selective adsorption tests with n-heptane and isooctane, catalytic runs performed with methanol at various reaction temperature, the determination of the constraint index and the internal space, confirmed the pore narrowing as the result of the DRS treatment.

Dedicated

To my Parents and all of
my Family for their love,
encouragement and confidence in me.
To my beautiful wife Sandrine you
have given me inspiration, so much love,
and the greatest gift in the world
an amazing baby boy named Joshua.

Acknowledgments

I would like to express my sincere appreciation and gratitude to Professor Raymond Le Van Mao for his support, patience, encouragement and teaching me how to become a real scientist.

I would also like to thank:

Drs. M.Lawrence and P.H Bird as committee members for their time and very valuable suggestions throughout my research.

Shawn Melancon, Philip Kletnieks and David Mc Cann for many hours of useful discussion, a great team environment and a very valuable friendship.

Tuan S. Le for teaching me many techniques which were very useful for me during my undergraduate project up to my Ph.D.

Office Staff, Ms. C.J Coutts, Donna Gordon and Kathy Ussas for their assistance and help whenever it was needed, solving many departmental problems that I have encountered during my various degrees at Concordia.

The many French students that have come and gone over the past 6 years, always leaving good souvenirs behind.

The Chemistry Department laboratory technicians that helped me through my research and demonstrating duties, especially Jim Kolikotronis, Rita Umbrassas and Franco Nudo.

The chemistry librarian, Ruth Noble, who was always there to help me and inform me on new methods to get very useful information for my research.

Finally, I wish to express my deepest gratitude to my parents for their love, moral support and understanding. I would also like to thank my wife for lifting my spirits when I was down, understanding me in all my stressful moments, never taking me too seriously and encouraging me to do a PhD.

Table of Content

Appendix

List of Figures

Chapter 2

Chapter 4

APPENDIX

List of Tables

Chapter 2

Chapter 4

Chapter 1

1.1 Literature Review on Pore Size Engineering in Zeolites.

The modification of the pores of a zeolite is a very important tool for various purposes such as in the separation of gas mixtures, ultra purification of gases, the storage and transport of unstable, dangerous or explosive gases.

The separating ability of zeolites can be achieved or altered by the molecular sieving caused by size and/or shape differences between the zeolite crystal aperture and the adsorbate molecule. In addition, selectivity can be caused by differences in the interaction energies between the adsorbate molecules in a specific zeolite, as well as the window effect which is induced by the adsorbate molecular configuration and the internal pore diameter.

Molecular Sieving Effect

i) The first modification method is by the cation exchange process. This works by changing the exchangeable cation in a zeolite, which may enlarge or narrow the pore openings as a function of the cation diameter. With zeolite A, divalent ion-exchange opens the aperture to full diameter, whereas exchange with a large univalent ion diminishes the opening's size. It has been shown that the pore reduction does not occur gradually with increasing extent of exchange, but rather suddenly at a level of about 25% potassium exchange as mentioned by Breck. [1]

ii) The second modification involves the preadsorption of polar molecules. If small amounts of polar molecules such as water or ammonia are preadsorbed in a dehydrated zeolite, and the adsorption of a second adsorbate can be drastically reduced. It has been shown that for zeolite A, there is a strong interaction between the zeolite's cation and the

dipole moment of the polar molecules which produce a diffusion block by clustering around the exchangeable cation in the zeolite's channels.

iii) The last modification is of the zeolitic framework. Pore size engineering can be achieved by a modification of the zeolitic framework resulting from one of these three techniques:

1) The first technique involves a modification by crystallographic changes where the molecular sieve behavior of a zeolite can be controlled by a hydrolytic process at elevated temperatures because of cationic migration. The water vapor which is in contact with the zeolite crystals at high temperatures results in a variation of the zeolitic adsorption characteristics. The amount of water vapor, pretreatment temperature and the pretreatment time can control the effective pore size of zeolites.

2) The second technique for pore size modification results from an internal and external modification by the implantation of additional groups in the zeolitic pores.
Some methods that help vary the pore systems are :
a) silanation, b) disilanation, c) boranation, d) implantation of boron-nitrogen compounds and e) modification by inorganic acids and their salts. [2]

3) The third technique is described in a paper entitled "Production of Porous Materials by Dealumination of Alumina-Rich Zeolites" by Le Van Mao et al.[3] They talked about a method that would enable one to get larger pores. This process used ammonium hexafluorosilicate (AFS) on alumina rich zeolites such as Ca-A. They started with an initial diameter of 17 Å and got larger mesopores after treatment which were in the region of 120 Å with fairly narrow peaks which suggest homogenous pore sized systems with much

higher void volumes. The authors then did a comparative study using the Na-X zeolite which has a higher Si/Al ratio with a diameter smaller than 17Å. They found that after treatment, mesopores of about 40Å were obtained and they got sharper and narrower pore size distributions than for the Ca-A/AFS treated sample. This could be explained by the fact that having a high Si/Al ratio prevented any serious damage to the zeolite pore system and this had the effect of increasing the pore openings of the treated Na-X only slightly compared to the treated Ca-A sample.

A mild and controlled dealumination of alumina rich zeolites gives a mesoporous materials with fairly homogeneous pore systems. Several advantages are associated with the AFS treatment and they are: 1) having only slightly diminished cation exchange properties, 2) having higher void volumes in the case of alumina-rich parent A zeolites and 3) having high thermal stabilities. [3]

As the catalytic reactions are concerned, selectivity in adsorption and reaction can be investigated by several techniques as shown by Forni [4] in a paper he published on the "Standard Reaction Tests For Microporous Catalysts Characterization". He discusses the fact that the choice of molecular sieves as dimensionally selective catalysts requires an as rapid as possible collection of reliable information on the porous structure of such materials. The information could be obtained by using either a crystal structure determination or selectivity of adsorption of some properly selected probe molecules. We know that the active sites are located within the pores, so the probability for the reactants to penetrate inside the pores and react depends on the pore size and the structure of the reacting molecules because the molecules need to be small enough to enter but also the molecules which are small enough

will be able to diffuse out of the pores as products. Several types of selectivity have been identified, they are: 1) Reactant Selectivity, 2) Product Selectivity, 3) Reaction Intermediate Selectivity and 4) Molecular Traffic Control Selectivity.

The method of characterizing the effective pore width of zeolites by catalytic tests was first employed by researchers at Mobil. The distribution of the reaction products using properly chosen, simple test reactions that exploit the acidic properties of the catalyst, make it possible for them to define the value of some characteristic parameters such as the constraint index (CI) and spaciousness index (SI). To get information on the relative pore dimensions of a catalyst, we have to compare its selectivity in a given set of probe reactions. We need to compare it to catalysts that have different dimensions to see if there exist differences of the parameter values.

For the constraint index, we have to compare the cracking of an equimolar mixture of n-hexane and 3-methyl-pentane on the acidic form of the zeolite. As long as the catalyst pores are sufficiently spacious, branched alkanes are cracked at higher rates than their unbranched isomers. The method has some drawbacks, the first being that the reaction suffers from a relatively fast catalyst deactivation for large pore zeolites and a temperature dependence for medium-pore zeolite. [4]

The CI value grows with decreasing pore diameter and in the presence of small amounts of noble metals in the catalyst. The modified constraint index (CI*) changes with the load of noble metal. For example, if we increase the platinum weight (%), this will have the effect of decreasing the CI* value. The actual pore size of the catalyst, then becomes lower at high platinum loading.

Another characteristic parameter is the spaciousness index (SI). The reaction involves the cracking of butyl-cyclohexane (BCH) and we measure the yield ratio of iso-butane/n-butane which is produced. This value grows with increasing pore size of the catalyst and is virtually independent of reaction conditions. It is a parameter which is sensitive enough to analyze the typical pore size of 12- membered ring zeolites.

Molecular sieving effects brings a change in the shape-selectivity of a catalyst. This will have the result to block off some molecules of specific sizes from entering or exiting the pore channel.

Shape selectivity was first described by Weisz and Frilette in 1960. P.B Weisz, N.Y Chen, V.J Frilette and J.N Miale were not only pioneers of shape selective catalysis, but they demonstrated its many possible applications such:
(1) undesirable impurities can be continuously converted to easily removable smaller compounds or harmless substances, (2) selectivity of a desired product can be increased and (3) coke formation can be reduced.

Small and uniform pores characterize zeolite catalysts. If most catalytic sites are inside the pore structure and if the pores are small, then the fate of the reactant molecules and the probability of forming product molecules are determined mostly by the molecular dimensions and configuration.

The importance of diffusion in shape-selective catalysis cannot be overemphasized. In general, one type of molecule will react preferentially and selectively if its diffusivity is at least one or two orders of magnitude higher than that of competing molecular types. Molecules which are too large, will be absolutely unable to diffuse through the pores. Even

those molecules which react preferentially have much smaller diffusivities in shape-selective catalysts than in the ones that have larger pores.

The early research that was performed to determine if the uptake diffusivity could determine unequivocally that intracrystalline diffusion was the rate-controlling process in a transient adsorption experiment. The scientists observed the effect of chain length of n-paraffins on diffusivity. This phenomenon was termed the window effect. It was hypothesized that the chain length of the paraffin molecule (ex: n-C_8H_{18}) exactly matched the dimension of the zeolite cage (ex: erionite). The entrapement of the molecule leads to a loss of its diffusional mobility. They believed that molecules that are either larger or smaller will not fit within the erionite and will consequently have a higher mobility. When the chain length exceeds 12 carbons, the chain length effects predominate leading to the expected monotonic decrease in diffusivity.

1.2 Objectives of the Research Work

Our objective was to develop a unique procedure for enlargement and narrowing of the zeolite micropores which would be simple, predictable, reproducible and applicable to a large number of zeolites or other crystalline silicates. The modification of the pore size using the DRS (narrowing) or the DS (enlargement) method, does not give us an enormous change in its size when compared to the pore size it starts off at. Using the parent ZSM-5 zeolite pore size as a starting point, the enlargement that we see with the DS method is no bigger than 0.6Å . The DRS method shows a pore reduction by up to 1Å. This however is sufficient to affect molecular sieving effects, adsorption/diffusion or reaction shape selectivity of

molecules whose sizes are close to the zeolite's pore dimension.

One of the most important questions that will be addressed in this thesis is on the subject of the mechanism that makes pore size modification possible, using a small amount of sodium orthosilicate which was removed in the preparatory step of the desilication. We are also going to discuss the mechanism that is involved when orthosilicic acid which is made from sodium orthosilicate is impregnated onto the desilicated zeolite. A detailed understanding will involve use of the DSC/TGA and FTIR techniques. In particular, a catalytic chamber will be adapted for the FTIR instrument for the analysis of the changes occurring with stepwise heating. According to Flanigen and Khatami, [5] the FTIR instrument could show many changes in the bands of the pore mouth siloxane bonds which are known to be in the region of 300-420 cm^{-1}. The surface siloxane region could also show some changes, when reinsertion of some silicate species is applied to the desilicated ZSM-5 zeolite. Their characteristic bands are in the region of 850-910 cm^{-1}. The information we get for both of these regions will give us a better understanding of the new siloxane bonds which have been formed during the critical step of the DRS process and which are responsible for pore mouth reduction.

At the same time, as we focus on the pore mouth region, we could also follow the terminal and bridging silanol bands which are in the region of 3600-3800 cm^{-1}. A decrease in the intensity of these bands means that these silanol groups react with the incorporated orthosilicate to form the siloxane bonds, which are known to be responsible for the changes in the pore mouth size.

A) The DS method results in a more extended desilication effect by using a longer desilication time than in the case of the DRS, so this more drastic, yet controlled process produces larger holes within the zeolite structure and the proportion of sodium pyrosilicate extracted is larger than that of the sodium orthosilicate. During the stabilization process, some small silicate species are broken off from one extremity, while still being weakly held to the structure at two points. When heat is applied, formation of siloxane bonds will occur when the silanols within the structure and the weakly held species react with each other. The silicate species and silanols from the zeolite structure undergo a reaction at a temperature of ca. 600°C to form strained siloxane bonds which probably have a larger Si-O-Si angle and a longer Si-O bond than in the case of the DRS.

B) Understanding the mechanism for the DRS process with the ZSM-5 zeolite, will help us better apply this method to other catalysts which have small, medium or large pores and that have a different Si/Al ratio. Choosing a zeolite for modification, we need to make this choice on the basis of its thermal stability which should be equal or superior to the stabilization temperature, the acid density and strength, the rate of deactivation and in what shape-selective reactions they could possibly be used in.

1.3 Organization of The Thesis

The thesis is divided into five chapters. In chapter 1, the literature review which is related to the subject of the thesis is reviewed briefly. The objective of the research is also elaborated in this section.

The background regarding the properties of the zeolites is included in chapter 2 as well as some theoretical aspects of the research.

The experimental details are given in chapter 3. The results and discussion of the thesis are presented in chapter 4. Finally in chapter 5, we have the conclusion.

Chapter 2

Introduction

2.1 Heterogeneous Catalysis

Catalysts serve to reduce energy barriers associated with a reaction that is thermodynamically feasible by providing an alternative pathway of lower activation energy. They alter the rate of a reaction without affecting its free energy since the ratio of the activities of the product and the reacting species is unaffected, so that there is a minimum expenditure of energy. Historically, it was thought that these catalysts emerged unchanged after altering the reaction rate, but developments in the ability to observe surfaces at an atomic level have demonstrated that there are changes in the topology and even composition brought about by catalytic activity. Catalysts have a tendency to become sintered, etched, eroded or covered with residues left behind by the interacting molecules.[6]

A catalyst could be defined as a substance that increases the rate of approach to equilibrium for a chemical reaction without substantially being consumed in the process.[7] In figure 2.1, we could see the changes in energy which are associated with a simple exothermic reaction. The velocity of a uncatalyzed reaction for the conversion of reactants A and B into product P may be expressed as:

$$-d[A]/dt = k\,[A]^n[B]^m \qquad (1)$$

Where: [A], [B] are the concentrations for reactants A and B. The terms n and m are the partial orders with respect to reactants A and B.

$$k = A \exp(-E_{hom}/RT) \qquad (2)$$

where: T is the temperature, R is the gas constant, E_{hom} is the activation energy for the homogeneous reaction, E_{ads} represents adsorption of the reactants onto the catalyst, E_{cat} is for the formation of the activated complex and E_{des} for the desorption of the products; λ_{ads} is the enthalpy of adsorption of the reactants and is taken to be exothermic, and λ_{des} being the enthalpy of desorption of products is taken to be endothermic. The reaction rate at a given temperature will be increased by finding some means of reducing E_{hom} or increasing the pre-exponential factor A in equation (2). In the presence of a catalyst which might chemisorb A or B or both, the system may follow an alternative reaction path of lower energy of activation E_{cat}. Here the system appears to pass through a new chemisorbed transition state. The overall energy change upon reaction is ΔH and is the same for the two pathways.[8]

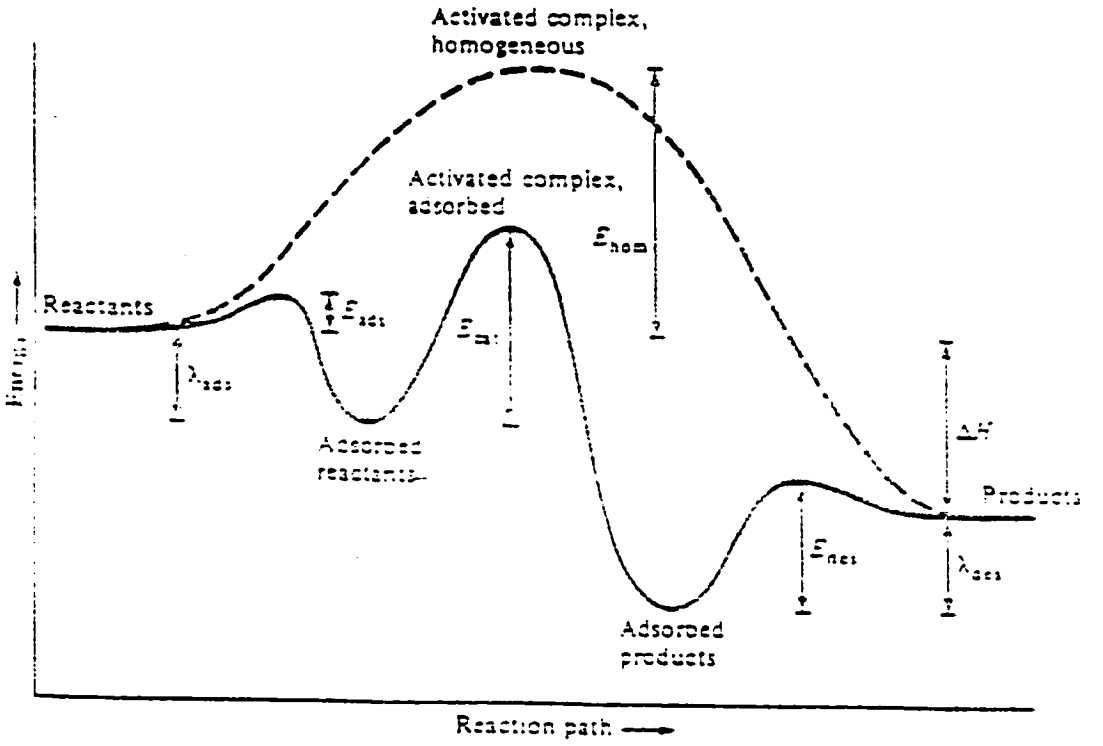

Figure 2.1 Energy changes associated with individual steps of a chemical reaction.

2.2 Catalyst Technology

2.2.1 From the Perspective of Petroleum Refining

Catalytic technology forms the backbone of the chemical and petroleum industries since many of the synthetic and refining processes are catalytically controlled. There is a major push to continue technological advances in the field of catalysis and the progression of catalytic developments continues. The major goal of a catalyst researcher is to develop novel catalysts for already existing processes, then to optimize the various components in their complementary role with respect to activity and selectivity with the emphasis on the minimization of the energy consumed and the pollution produced.

It is necessary to understand the processing of any catalytic reaction at an atomic level and to discover the mechanism by which catalysis proceeds so that one can design and construct the most efficient catalyst for a particular reaction.(Advanced surface analysis techniques are a key element for successfully developing and characterizing catalysts.)

How successful is a catalyst ? This depends on its ability to reduce the activation energy barrier for a reaction. Another approach is to develop a means of reducing energy consumption to effect the same results as more efficient catalyst..

The advantage of performing analysis in situ is obvious, if one considers the possible variations in catalytic behavior that actual conditions incur, compared to empirically optimized reaction conditions. The optimization of each parameter is directly controlled by the operator and can be manipulated in the desired fashion and the effects monitored. Under typical reaction conditions, however, the extent to which one can exert control over the reaction is limited. [9]

2.2.2 General Principles Relating to Zeolites

Zeolites are a class of porous crystalline aluminosilicates having a rigid three-dimensional framework with well defined cavities and channels of molecular dimensions ranging from 3 to 10 Å in diameter. The general formula for the composition of a zeolite in the hydrated form is :

$$M^{n+}_{x/n}[(AlO_2)_x (SiO_2)_y]^{x-} * z\ H_2O$$

where exchangeable cations M of valence n are used to neutralize the negative charge associated with the framework aluminum ions. Typical cations include alkali metals, e.g. Na^+, K^+, alkaline earth metals, e.g. Ca^{2+}, Ba^{2+}, NH_4^+ and H^+. Zeolites have been described as molecular sieves, which have open porous crystalline structures and ion-exchange capacities. Von Ballmos [10] defined zeolites as porous solids consisting of corner-sharing tetrahedra, representing a three-dimensional, four connected network with T- atoms at the vertices of the network and oxygen-atoms near the mid-point of the connecting lines. The crystal structure of a zeolite is defined by the specific order in which a network of tetrahedral units are linked together.[11]

The primary building unit of zeolite structures is a tetrahedron composed of a central Si or Al atom (commonly called T-atoms) surrounded by four oxygen atoms, namely $[SiO_4]$ or $[AlO_4]^-$. Figure 2.2 depicts the primary units represented by the vertices of the network and connected to each other by straight lines which schematically represent the T-O-T bridges. [12] These tetrahedra are joined so that each of the four oxygen anions is shared in turn with another silica or alumina tetrahedron to form a wide range of small secondary building units (SBU), as shown in figure 2.2 b). These SBU's are interconnected to produce a wide range

of tertiary building units or building polyhedra as seen in figure 2.2 c), which in turn are arranged in a three dimensional fashion to form extended characteristic frameworks of the various zeolite crystal structures (figure 2.2 d)). In these structural diagrams the corners of the polyhedra represent Si or Al atoms and the connecting lines the shared oxygen atoms. The combination of tetrahedra containing Si and Al atoms to form the aluminosilicate framework creates a negative charge on the Al atoms which is balanced by non-framework cations M^{n+} to give electrical neutrality.

Their acidity derives from the protons that are required to maintain electrical neutrality in the structure. The size of the zeolite pore opening is determined by: 1) the number of tetrahedral units, or, alternatively, oxygen atoms, required to form the pore; 2) the degree of puckering of the pore structure; 3) the shape of the pore (circular, elliptical and teardrop shape); and 4) the nature and the concentration of the cations that are present in or at the pore mouth.[13]

To date, about 38 naturally occurring zeolites have been identified and synthesized, but in the quest for the new catalysts more than 130 synthetic zeolites have been developed with a large variety of framework structures. [14,15] These structures have high thermal and chemical stabilities making them useful materials in a wide range of important industrial processes such as catalysis, separations, purification and ion-exchange.

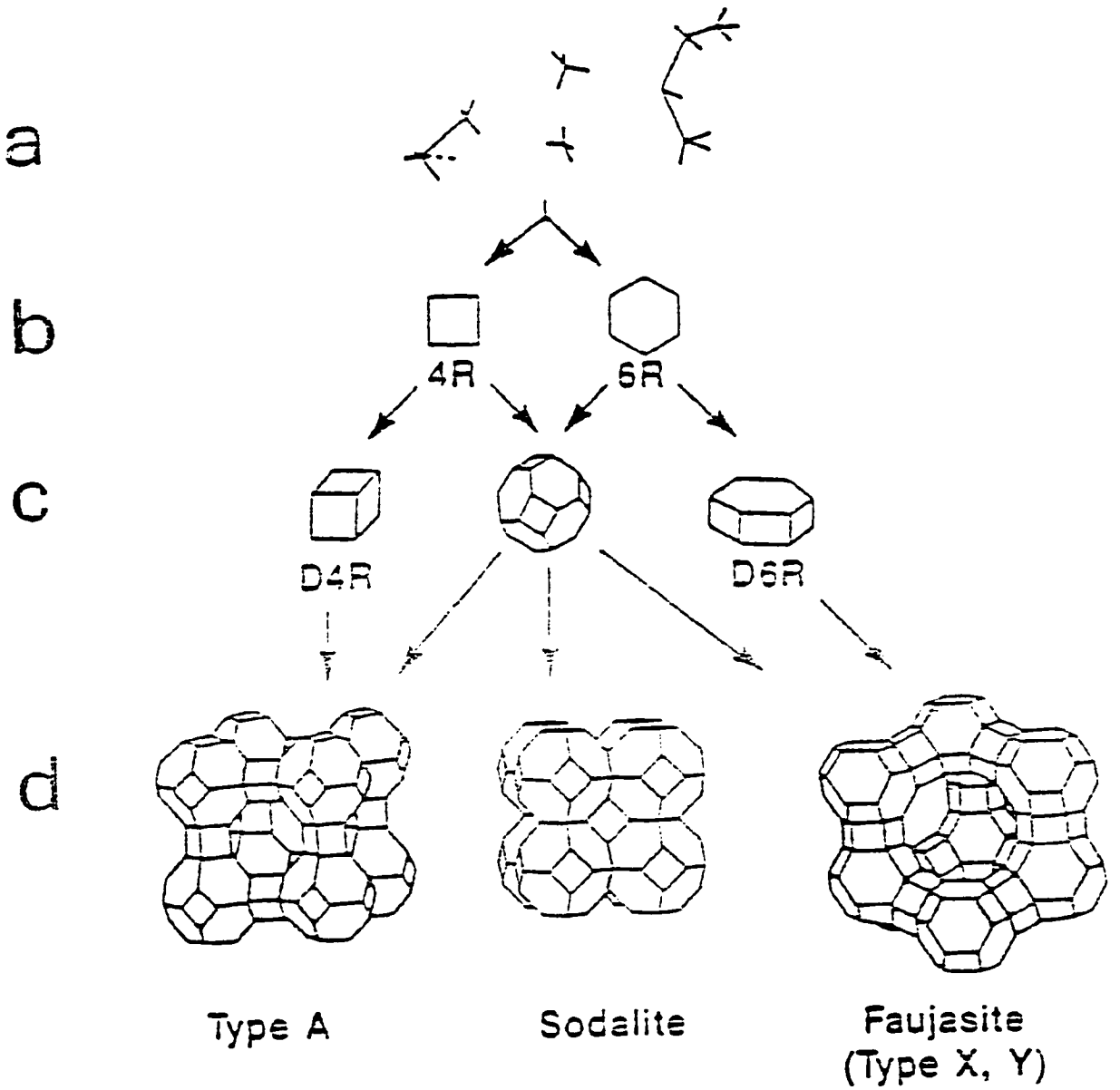

Figure 2.2 Structural composition of zeolite framework a)Primary Units, b)Secondary units, c)Tertiary units and d) Zeolite structures

In general, zeolites do not have Si/Al ratios below unity. This implies that each Al atom cannot have another Al atom in its second coordination sphere. This observation was rationalized by Loewestein in terms of the Al-O-Al avoidance rule on the distribution of Al atoms within the zeolite structure.[16] Such an arrangement of Al atoms involving two adjacent negative charges would create an electrical instability in the zeolite framework and is therefore ruled out.[16] The Si/Al ratio also represents a convenient way for classification of zeolites according to their silica and alumina framework contents. Generally, the higher the silica to alumina ratio, the more thermally stable is the zeolite.

According to Flanigen's notation[16], low silica zeolites are defined as having $2<SiO_2/Al_2O_3<10$; and high silica materials as generally having SiO_2/Al_2O_3 ratios greater than 10. [17] There are no known naturally occurring high silica zeolites. In fact, it was not until the late 1960s that zeolites with SiO_2/Al_2O_3 ratios greater than 10 were synthesized.

Silicoaluminophosphates (SAPOS) are less hydrothermally stable and acidic than their aluminosilicate counterparts. [18] Aluminophosphates ($AlPO_4$) are considered as non acidic and have been found to be even less thermally and hydrothermally stable than SAPOS. [19]

Owing to the existence of a three-dimensional channel network interconnected to cavities or voids, zeolites possess very large internal surface areas as determined from the BET nitrogen surface area technique.[20] The external surface area only represents a few percent of the total surface area which ranges from 400 up to 1000 m^2/g as observed for some of the most commonly used zeolites in heterogeneous catalysis:

a) zeolite X : 650 m^2/g b) zeolite Y : 750 m^2/g c) zeolite ZSM-5 :400 m^2/g

The important structural feature that make zeolites unique is the uniform size of pore apertures which have dimensions approximately equal to those of many molecules converted in catalytic processes as demonstrated in figure 2.3. The "molecular sieve" term for zeolites was given by McBain [20] in 1932 because they were able to discriminate between molecules on the basis of molecular size and shape. Molecules smaller than the aperture size can penetrate through the pore system while those larger cannot. Zeolites are classified according to the size of these apertures. In table 2.1, shows the number of oxygen atoms in the aperture of each zeolite and the aperture dimension. The size of the aperture is also dependant on the size of the exchangeable cations, for example with zeolite A, the effective pore diameter is 3Å when the cation is K^+, 3.8Å when it is Na^+ and 4.3Å when it is Ca^{2+}.

In figure 2.3, we could compare the relation between the cavity size and the zeolite dimensions. At the same time, relating the critical dimension of the hydrocarbons to the zeolite's cavity size.

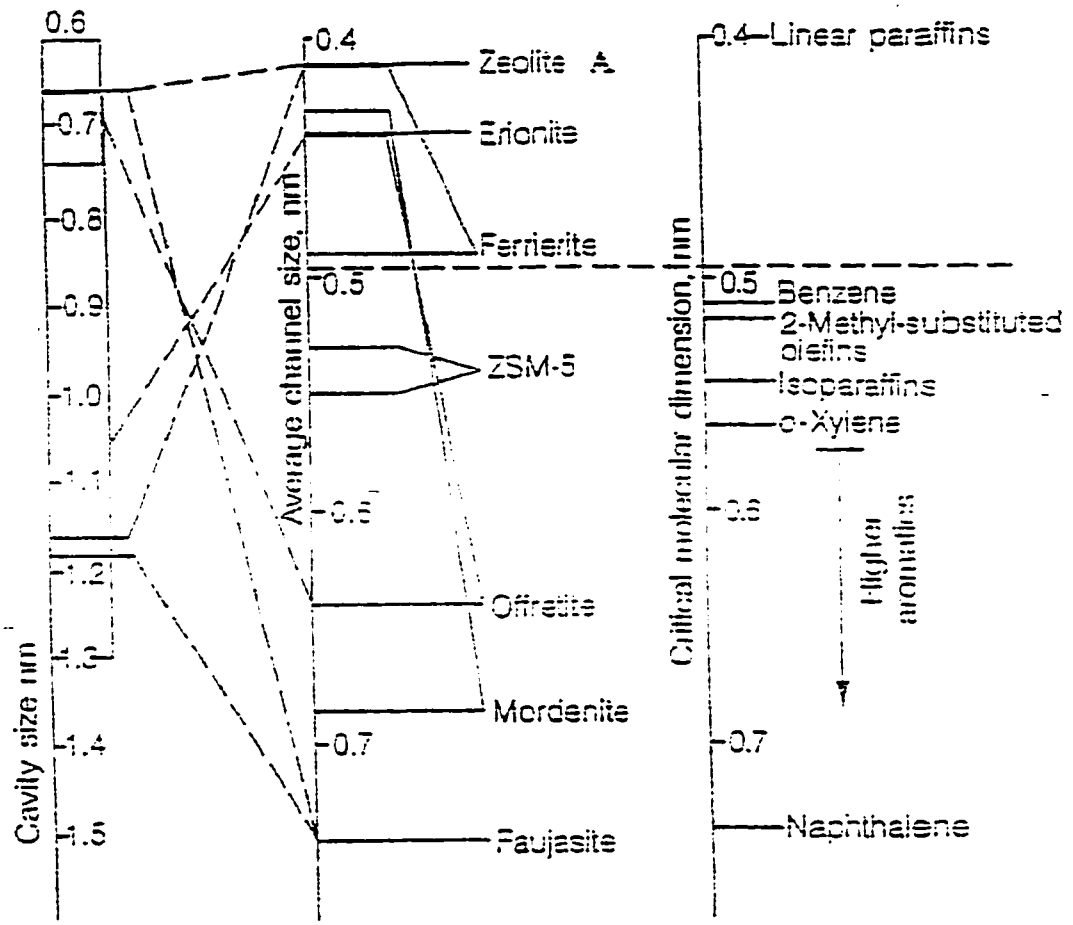

Figure 2.3 Pore dimension of zeolites and critical dimensions of some hydrocarbons [21]

Table 2.1 Zeolites and Their Pore Aperture Dimensions

Zeolite	Number of Oxygens in the Ring	10 × Aperture Dimensions, nm
Chabazite	8	3.6 × 3.7
Erionite	8	3.6 × 5.2
Zeolite A	8	4.1
ZSM-5 (or silicalite)	10	5.1 × 5.5 ; 5.4 × 5.6
ZSM-11	10	5.1 × 5.5
Heulandite	10	4.4 × 7.2
Ferrierite	10	4.3 × 5.5
Faujasite	12	7.4
Zeolite L	12	7.1
	12	7.0
Mordenite	12	6.7 × 7.0
Offretite	12	6.4

2.2.3 Zeolites as Catalysts

The use of zeolites as commercial cracking catalysts was first announced in 1960. By 1976, it was estimated that this development saved the petroleum industry and ultimately the U.S public more than 3 billion dollars in reduced petroleum and refining costs compared to the previously used silica-alumina catalysts. [22,23]

Zeolites have long been used for water softening and for drying (taking advantage of their ion-exchange capacities). Beside their large scale use as industrial catalysts in petroleum refining and chemical manufacture, zeolites have evolved as environmental catalysts in auto emissions control, [24,25,26] detergent (non-phosphate) builders [27], selective adsorbent, membrane synthesis [28] and as modifiers at electrode surfaces in electrochemical applications. [29,30,31]

2.2.4 Properties of Zeolites

One of the most important properties of zeolites is their ability to exhibit shape selective catalysis.[32] Their ability to combine molecular sieving properties with unusually high activity for acid catalyzed reactions such as cracking and dehydration, make them especially interesting. Their pore diameters vary between 3 to 8 Å and their pore sizes usually fall within a discrete range with a narrow pore size distribution. Since most catalytic sites are located within pores of the catalysts, the relative probability of forming product molecules depends on the accessibility of reactant molecules to the active sites. Other properties which render them efficient catalysts are their high internal surface area, usually well over 300 m^2/g depending on the zeolite, and the presence of ion-exchangeable cationic sites which allow the

introduction of various metal cations with variable catalytic properties. Replacement of metal cations with protons generates strong acid sites which are at the origin of catalytic activity in solid acidic catalysts.[33]

2.3 ZSM-5 Zeolite

The group of solids having the composition SiO_2, will be expanded by replacement of some of the Si atoms with Al. The compound SiO_2 is stable in the gas phase, having a structure with two Si=O bonds resembling that of CO_2. There is a large free-energy driving force for the self-association of the SiO_2 molecules, with conversion of the Si=O bonds into Si-O bonds. Many geometries of the resulting condensed structures exist, two of the best known being quartz and cristobalite and another being silicalite, which is closely related to zeolites. All of these are crystalline, with each Si atom in tetrahedral surroundings, sharing bridging oxygen atoms with neighboring Si atoms. Silica is a non-crystalline material also with the composition SiO_2.

The SiO_4 tetrahedra can be combined in many arrays with the sharing of oxygen atoms. When they are appropriately arranged, the result is the secondary building block of silicalite. When some Si atoms in this structure are replaced by the Al atoms, the resulting aluminosilicate is referred to as ZSM-5, a zeolite and an industrially important catalyst.[34] The name ZSM-5 is short for Zeolite Socony Mobil and the number 5 for the pore size of 5.6Å.

The ZSM-5 zeolite exhibits a two dimensional network of channels having a structure as illustrated in figure 2.4 . There exists two distinctive pore types intersecting each other and

both are formed by 10 membered oxygen rings. One pore type varies from 5.1x5.5 Å in straight channel ellipsoidal rings, the other zig-zags and has circular opening of 5.4x5.6 Å. It possesses a mean average pore diameter of 5.5Å with a Si/Al ratio ranging between 10 and 500 (see figure 2.4). Because of its pore structure, it exhibits a high degree of shape selective catalysis and has many useful applications in petroleum refining, particularly in enhancing the gasoline's octane number, when this zeolite is used as a catalyst additive in gas oil cracking.[35]

2.3.1 High Surface Area

The rate of a catalytic reaction is proportional to its active surface area.[36] Because of the high degree of porosity and their multichannel structure, zeolites exhibit extremely large internal surface areas relative to their total external surface area. This is a major factor, contributing to their efficiency as catalysts. It will provide a greater accessibility of reactant molecules to the active sites, where the reaction occurs. Occasionally a high surface area at the interface arises when two phases are coupled together under pressure leading to a contact synergy, thereby increasing the overall catalytic activity.[37,38]

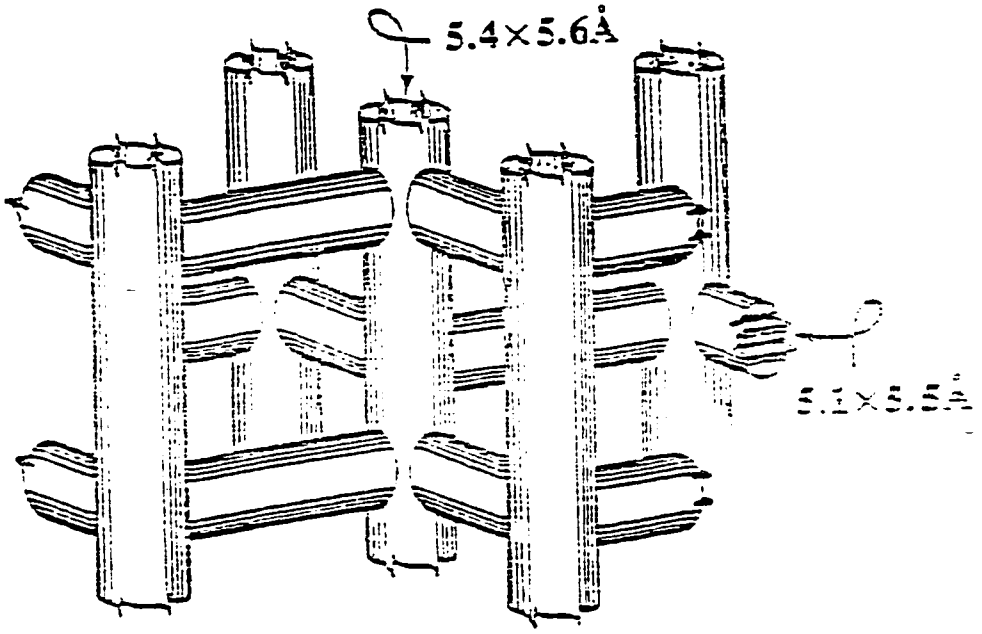

Figure 2.4 Structure of the ZSM-5 Zeolite

Table 2.2 Typical Surface Areas of Some Common Zeolites

Zeolite	Surface Area (m^2/g)
ZSM-5	300-400
A	650
Beta	400-500
X and Y	700
MCM 41	>1000

2.3.2 Acidity of the ZSM-5 and Other Types of Zeolites

There are two types of acid sites which classify the active sites in heterogeneous catalysis, they are: i) classical BrØnsted and ii) Lewis acid sites. According to the Lewis definition, an acid is a substance that can take up an electron pair to form a covalent bond. The Bronsted-Lowry definition states that an acid is a substance that gives up a proton and the strength of an acid is dependant on its tendency to give up a proton. [39]

Catalytic activity is connected to the following characteristics:
1) the strength of acidity, 2) the concentration of acid sites and 3) the accessibility of the bridging hydroxyl groups which are known to act as BrØnsted acid sites. [40]

Surface acid sites in zeolites are of two types: a) those capable of donating protons, as the bridging hydroxyl group in SiO(H)Al which is associated with tetrahedrally coordinated or framework aluminum atoms, or Bronsted acid sites (B.A.S) and b) those capable of accepting electron pairs from adsorbed species, like the tricoordinated Al^{3+} or Lewis acid sites (L.A.S). [41]These two types of sites are illustrated in figure 2.5. The acidity of zeolites will therefore be defined by two independent qualities, firstly the "strength" which is defined as the ease of proton transfer from the surface sites to the adsorbed base, or of an electron pair transfer from an adsorbed base to a surface and secondly by the amount of acid which is given by the concentration of the respective acidic sites assuming no diffusional limitations.[42] BrØnsted acid strength depends on the electronic charge of those protons associated with the bridging hydroxyl groups of SiO(H)Al in zeolite frameworks.

Each tetrahedrally coordinated aluminum atom contributes to one potential BrØnsted acid site but since the distribution of aluminum is not uniform, there exists a wide distribution of proton strength in zeolites.[43]

Therefore there are strong, medium and weak acidic sites on the H-ZSM-5 zeolite. The concentration of strong acid sites depends on the concentration of framework aluminum. An increase in calcination temperature (>500°C) of the zeolite leads to dehyroxylation, resulting in a decrease in Bronsted acidity and an increase in Lewis acidity. Using steam on the zeolite sample, results in a decrease in the concentration of strongly acidic OH groups.[44] According to Lowenstein's rule [45] for the distribution of aluminum in the tetrahedra of aluminosilicates zeolites, there are no near neighboring AlO_4^- tetrahedra in zeolites. They are always interspersed with SiO_4 to form an electrically stable structure. Zeolites with higher Si/Al ratios or low densities of proton donor sites have high proton donor strength.[46]

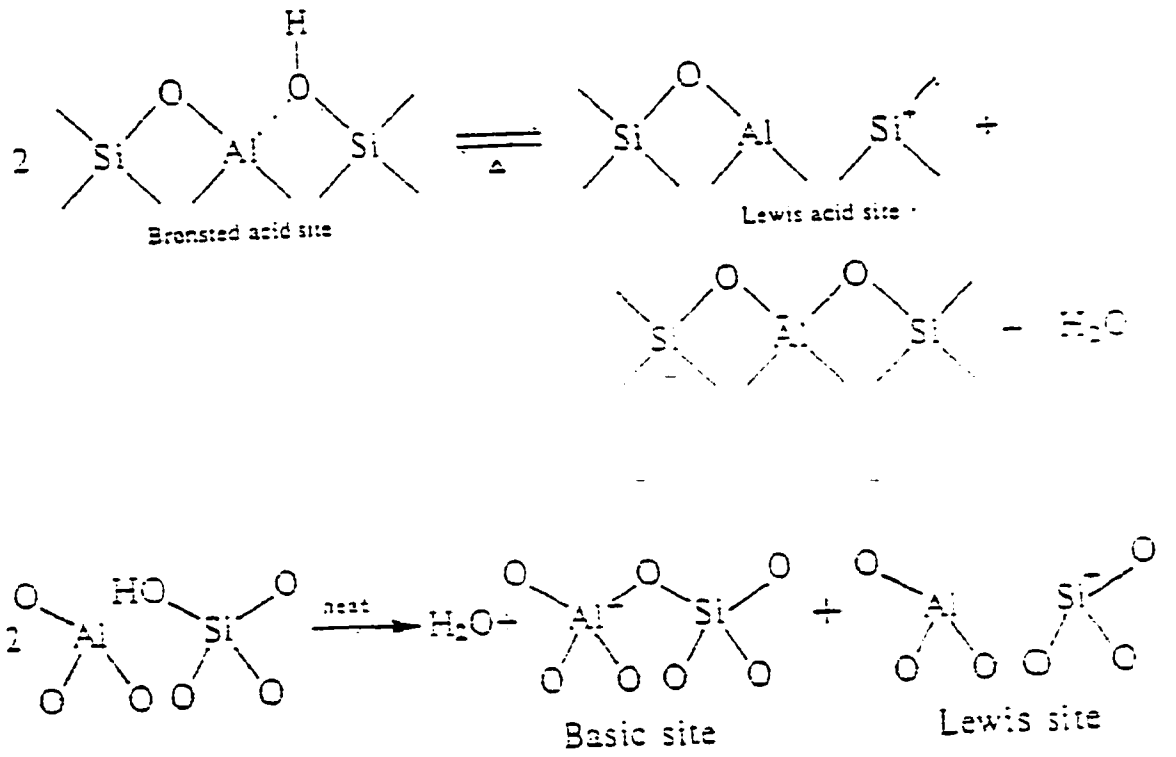

Fig. 2.5 Formation of Lewis acid site from Brønsted acid sites.

Doremieux-Morin et al.[47] proposed a scale for measuring the proton acidic strength of solid acids based on a calculated ionization coefficient obtained from simulated broad-line NMR spectra. BrØnsted acid sites are able to ionize water molecules to form hydronium ions (H_3O^+) which can be quantified. Different concentrations of water are adsorbed onto anhydrous zeolite under vacuum and the degree of ionization of water to form hydronium ions is directly proportional to the number of acidic sites present.[48]

Figure 2.6 shows a typical zeolite framework surface (a) as synthesized, where M^+ is either an alkali cation or an organic cation, (b) using the ammonium ion-exchange procedure, this produces the ammonium form, (c) thermal treatment (450°C) is used to remove ammonia producing the acidic form (d). The acid form in (c) is in thermal equilibrium with the form shown in (d), where there is a silanol group adjacent to a tricoordinated aluminum.

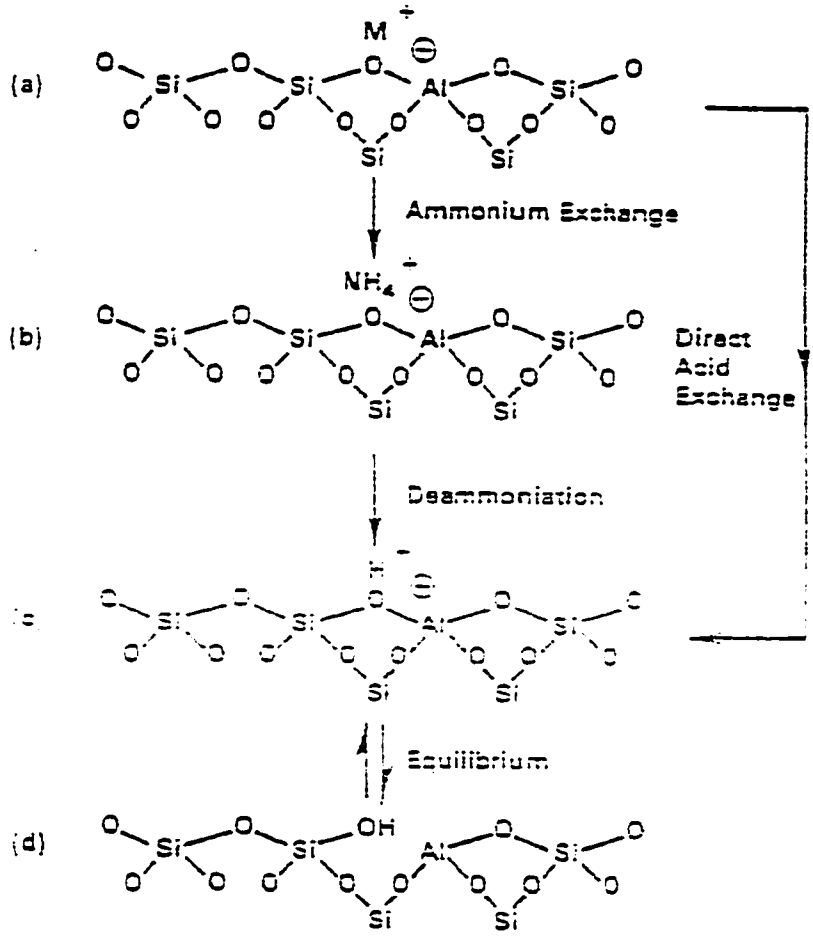

Fig. 2.6 Diagram of a zeolite framework surface

The catalytic activity of zeolites is also determined by : i) the strength of the acid sites, ii) their density within the zeolite matrix as well as iii) their accessibility. The strength of zeolite acidity is characterized by the varying ability at which protons are transferred from different surface acid sites to the adsorbed chemical species. It arises from the non-homogeneous distribution of aluminum atoms within the zeolite structure as indicated by Electron Microprobe Analysis (EPA) and X-Ray Photoelectron Spectroscopy (XPS), showing a higher aluminum concentration on the surface compared to the bulk of zeolite crystal mainly for those larger than 5 microns.[49,50]

The result is a wide range of acid strength in zeolites, commonly classified as strong, medium and weak by the characterization technique of ammonia temperature programmed desorption (NH_3-TPD) [52] , FTIR spectroscopy[53] and a catalytic test reaction of n-hexane cracking.[54]

Many properties of ZSM-5 such as its ion-exchange capacity and hyrophobicity are dependent on its chemical composition (Si/Al ratio). Its attractiveness as catalyst is due to its intrinsic acidity arising from its low aluminum content which can be varied over a large range of concentrations giving rise to catalytic activities that can be predictably changed over many orders of magnitude. According to Olson et al.,[55] the ion-exchange capacity and catalytic activity increases with the aluminum content.

Figure 2.7 shows the variation of acid strength for hexane cracking with aluminum content of the zeolite. There is a very obvious, linear relationship between the n-hexane cracking activity and the aluminum content. On the other hand, the hydrophobicity increases with the decreasing aluminum content.[56]

According to Barthomeuf et al.[57], a lowering of the Si/Al ratio is congruent with an increase in the number of acid sites, but the acidic strength of bridging hydroxyls in SiO(H)Al species increases as the aluminum content decreases because of the isolated nature of the latter in these zeolites. It has been found by Barthomeuf et al. using experimental data on the topological densities of isolated AlO_4 tetrahedra in zeolites that the limiting Si/Al ratio for the preparation of the ZSM-5 is 9.5. [57,58] Some of the benefits which are associated with a high Si/Al catalyst are: oil refining, organic synthesis and include superior efficiency, easier separations and handling as well as greater stability.

Table 2.3, illustrates the large scale processes that are catalyzed by the ZSM-5 zeolite in the fields of petroleum, synthetic fuels and chemicals.

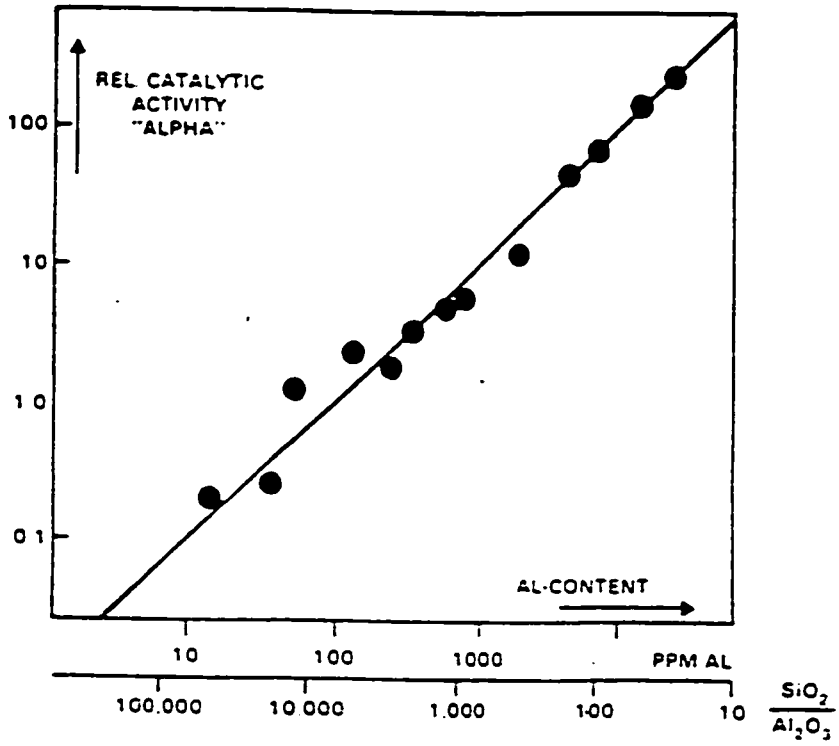

Fig. 2.7 Variation of acidic strength with aluminum content

Table 2.3 Large Scale Processes Catalyzed by ZSM-5

Petroleum:

Catalytic Cracking

Distillate Dewaxing

Light Paraffins to Aromatics

Refining

Synthetic Fuels and Chemicals:

Methanol to Gasoline

Olefins to Gasoline and Distillate

Dehydration of Ethanol

Chemicals:

Xylene Isomerization

Toluene Disproportionation

2.4. Diffusion in Zeolites

Pore diameter in molecular sieves usually depends not only on the number of tetrahedra in the ring. The actual pore size is dependant on the type of cation present. Cations occupy positions which block part of the pores. Adsorption inside these pores cannot occur until the adsorbate molecules are small enough to move freely into and within the pores.[59] When the molecules in the pore are nearly the size of the passageway, the diffusing molecules are never away from the influence of the wall, and the rate of diffusion becomes relatively slow. This has been variously termed restricted diffusion or configurational diffusion. In contrast, Knudsen diffusion occurs in pores and is, sufficiently large that the mean free path is much greater than the pore size, but sufficiently small that the molecular motion which occurs by free flight interrupted by momentary adsorption and desorption on the wall. A qualitative representation of the diffusion in the pores of solid is shown in figure 2.8.

We have to note that diffusion in zeolites is more complex than Knudsen diffusion or bulk diffusion and the activation energy is usually much greater than that for Knudsen diffusion or bulk diffusion. [60] Some typically reported values of diffusivities at 350°C in ZSM-5 for p-xylene, o-xylene and mesitylene were > 10^{-7}, 10^{-10} and 10^{-12} cm^2/s respectively.[61]

For most amorphous porous solids, it is generally accepted that the driving force for molecular diffusion in these solids is the local concentration gradient, $\partial C/\partial x$, or the gradient of chemical potential in the case of adsorbed molecules. The diffusion coefficient or diffusivity, D, is the proportionality constant relating the rate of diffusion or the molar flux, J or $\partial J/\partial t$, to the driving force as expressed by the well known Fick's first equation:

$$J = \partial n/\partial t = D\partial C/\partial x$$

When the size of the pores is 1μm or larger, which is much larger than the mean free path of molecular collision, the diffuse process in the solid occurs as if in the gas phase moderated by an occasional collision with the walls of the solid. The mean free path for gas molecules is proportional to T/P ; it is around 1000Å at Standard Temperature and Pressure (STP); 100Å at 10 atm and 20°C.

Gas diffusivity is proportional to temperature and inversely proportional to pressure and the square root of molecular weight. Diffusion in the gas phase is much faster than in the liquid phase. Bulk phase diffusivities are in the range of 10^{-5} to 0.3 cm^2/sec for liquid and gas, respectively.

For high surface area amorphous solids, the pore sizes are small relative to that of the mean free path of the diffusing molecules. As is often the case for gas diffusion through microporous solid media at atmospheric pressure, the molecules collide with the pore wall much more frequently than with each other and, in the limit, each molecule diffuses independently with the mean free path determined by the pore diameter. The diffusion coefficient thus becomes independent of molecular concentration or pressure. This is known as the regime of Knudsen diffusion.

$$D_{knudsen} = 1/3 \text{ (mean thermal speed of molecule)(pore diameter)}$$

Knudsen diffusivity increases with the square root of temperature and inversely with the square root of molecular weight. Mass transport in the macropores of many industrial catalyst pellets and extrudates fall in the Knudsen diffusion regime and for orientation purposes. Knudsen diffusivity falls in the range of 10^{-1} - 10^{-4} cm^2/sec.[61]

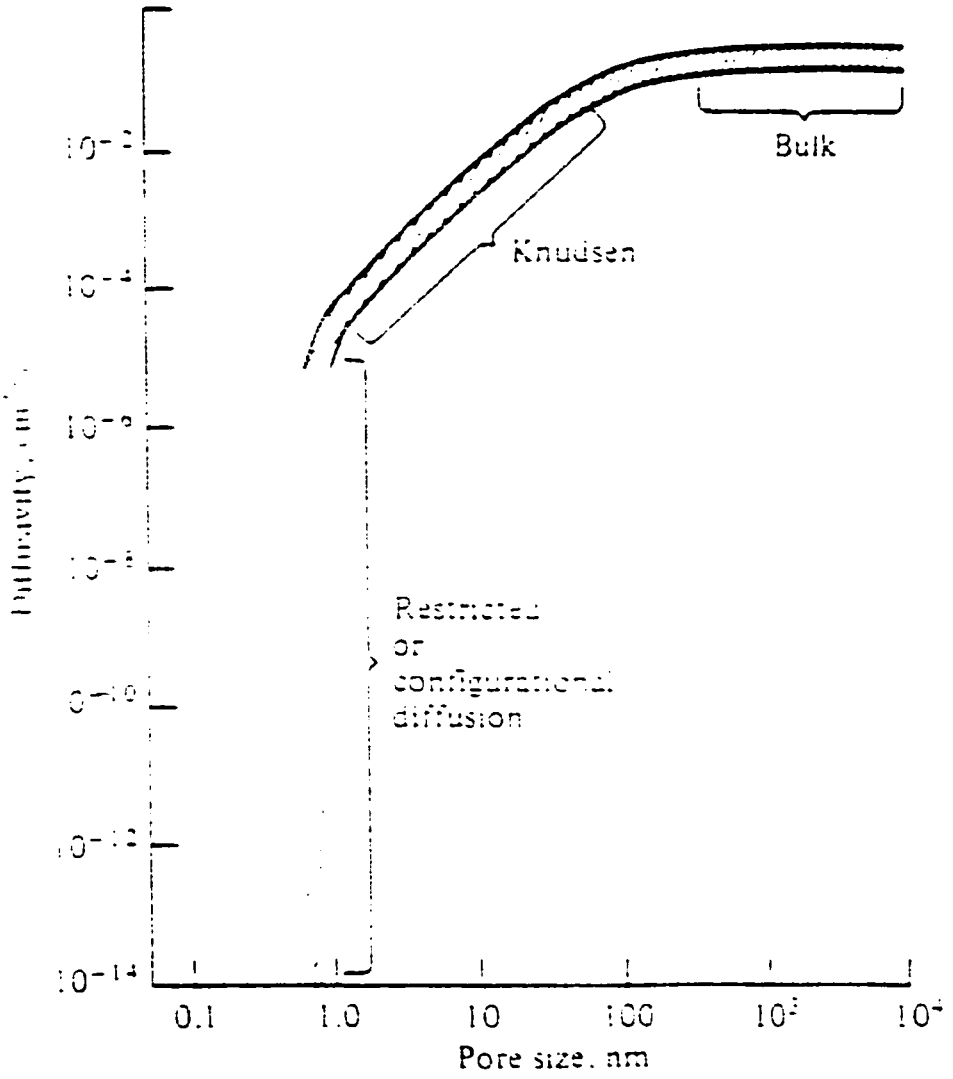

Figure 2.8 Effect of Pore Size on Diffusivity

2.5 Shape Selectivity

High crystallinity, regular pore structures and sizes are among the properties which render to zeolites their greatest advantages over other catalysts. Because of their specificity and selectivity for certain reactions and their ability to discriminate and exclude undesirable reactions from occurring, they achieve very high yields of particular products. It is possible to distinguish four different types of shape selectivities based on decreased diffusivity of either reactant or product molecules, which ultimately diminishes the reaction rate of the formation of the product:

First, certain reacting molecules may be excluded from diffusing into the zeolite pores and are thus unable to gain access to the active sites because of pore limitations (figure 2.9 a)). This type of molecular exclusion is known as reactant selectivity. Alcohol dehydration which requires weak acid sites is a typical case of reactant shape selectivity where secondary alcohols are excluded from the narrow pores of Ca-A zeolite.

Secondly, if the product molecules formed are too bulky to freely diffuse out of the pores and into the surrounding media limiting the formation of certain products, this leads to a phenomena known as product selectivity (figure 2.9 b)). The trapped products are either converted into less bulky products or they deactivate the catalyst by blocking its pores. A very good example of this is the methylation of toluene for which the ortho and meta products may not be formed depending on the pore size of the catalyst.

The third situation which arises is the formation of transition states which are restricted in movement by the size of the zeolite's pores. The kinetic effect arises because of the local environment around the active site. Since neither reactant nor product molecules are

prevented from diffusing through the pores, only the formation of the transition state is hindered. This is termed "restricted" transition state selectivity or spatio selectivity (figure 2.9 c)). An interesting example is the acid catalyzed transalkylation of dialkylbenzenes.

The fourth situation is a type of molecular traffic control which may occur in zeolites with more than one type of pore system such as ZSM-5. Reactant molecules may enter through one pore system and product molecules may diffuse out through another (figure 2.9 d)). In this way counter diffusion is greatly minimized. This is illustrated in the alkylation of toluene over a modified ZSM-5 zeolite.[62]

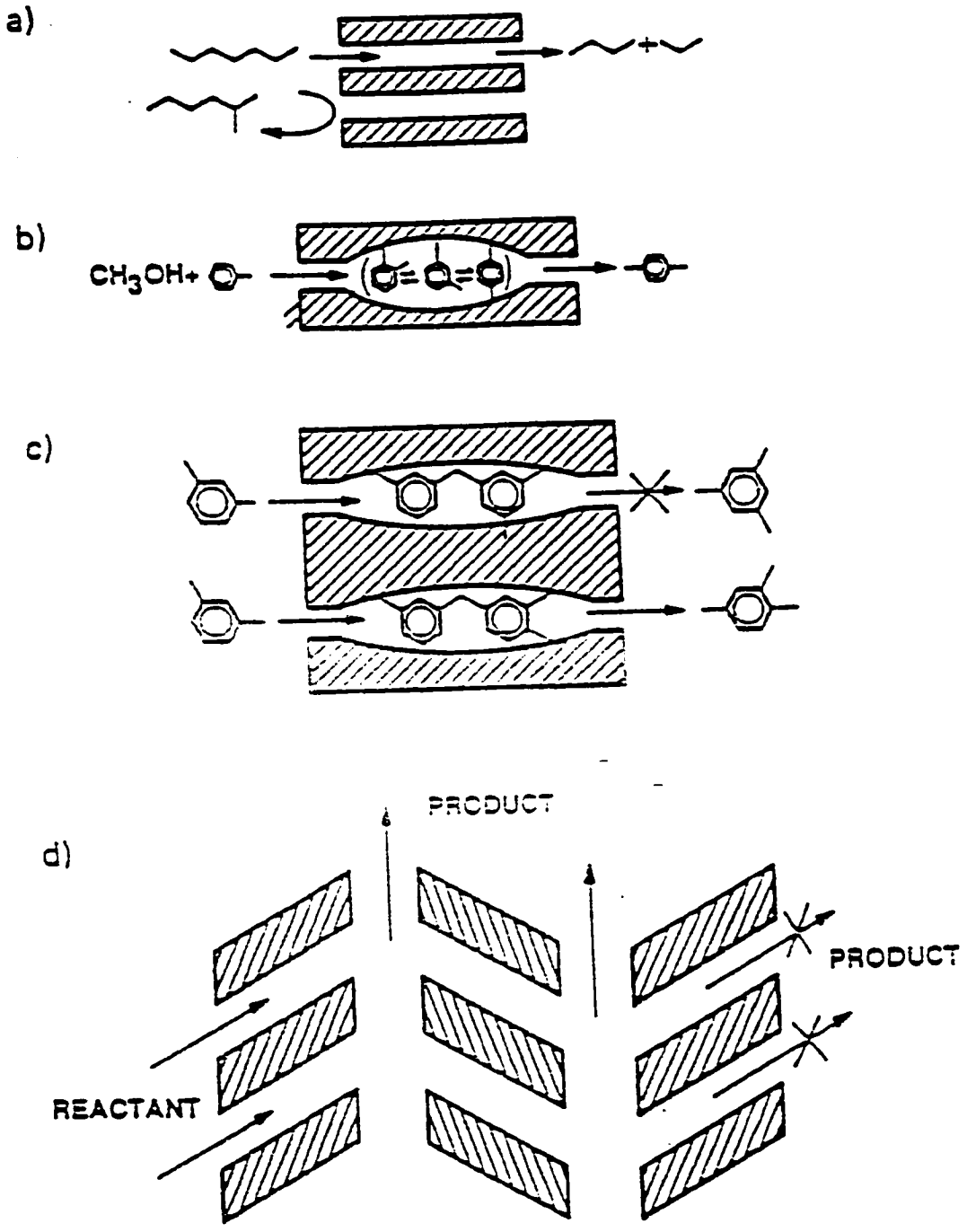

Figure 2.9 Shape Selectivity of Zeolites (a),(b),(c) and (d)

Figure 2.10 shows us the correlation between the effective pore size of various zeolites in equilibrium adsorption over a temperature range of 77 K to 420 K, with the kinetic diameters of various molecules from the Lennard-Jones potential relation.

In principle, the sizes of molecules can be determined by calculating their equilibrium diameters from the known molecular shape, bond distances, bond angles and Van der Walls radii. For a comparison with zeolite pore dimensions, however, the use of the kinetic diameter seems to be much more popular.[63] The kinetic diameter for spherical, non-polar molecules can be obtained from the Lennard-Jones potential which describes the potential energy of interaction between two molecules in dependence of their distance from each other.

$$\Phi(r) = 4\ \varepsilon[(\sigma/r)^6-(\sigma/r)^{12}]$$

In this equation: σ and ε denote the characteristic diameter (collision diameter) and the characteristic energy of interaction (the maximum energy of attraction between two molecules), respectively. Numerical values for σ and ε can be derived from the second virial coefficient, from viscosity data or from the critical parameters of the pure substance. [64,65]

A schematic graphical representation of the Lennard-Jones potential is shown in figure 2.11. At large separations, the attractive component, proportional to $(1/r)^6$ is dominant and describes the dipole-dipole interaction. For small distances, the repulsive forces proportional to $(1/r)^{12}$ predominates. The kinetic or collision diameter σ is the smallest distance between two molecules. The maximum energy of attraction (ε) occurs at the minimum distance r_{min} with $r_{min} = 2^{1/6} \times \sigma$ (see figure 2.11). While the use of the kinetic diameter is often appropriate

for truly spherical molecules, it is not very well suited for more complex molecules such as n-alkanes. In these cases, the use of the minimum cross-sectional diameter is recommended.[66] The contribution of the external surface of a zeolite crystal to its overall catalytic activity has often been questioned. With crystals larger than 1 micron, their external surface area relative to their intracrystalline surface area is so small (<1%) that surface activity can be ignored. However, for small submicron crystals, external surface sites could be a significant fraction of the total surface area. If the external surface sites are catalytically either the same or more active than the intracrystalline sites, then shape selectivity of a zeolite could conceivably be changed by these surface sites. One such speculation was advanced by Frankel [67] who proposed that the acid sites located in the "half cavities" or the external crystal surface of the ZSM-5 could be active for a second type of shape selective reaction. These sites were speculated to be responsible for the formation of such molecules as ortho and meta xylene, 1,2,4,5-tetra methyl benzene and 2,6 or 2,7 dimethylnaphtalene. However, the data as presented appears insufficient to support their proposal, because in the absence of information on diffusion coefficient and reaction rates, one cannot rule out the effect of diffusional constraints or product selectivity. Furthermore, the surface sites are probably less active than tetrahedrally coordinated internal sites.[68]

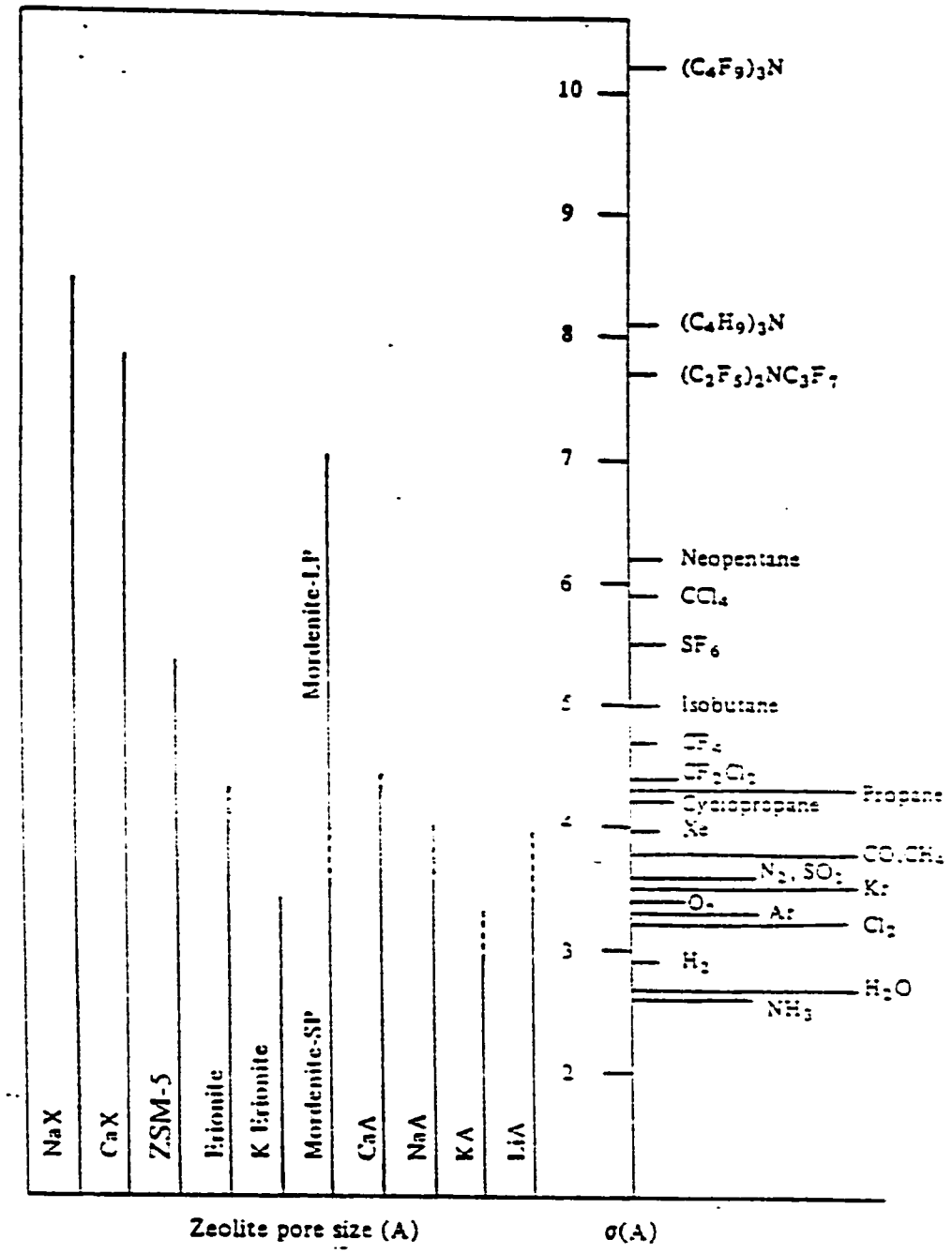

Figure 2.10 Correlation between the effective pore size of various zeolites with the kinetic diameters of various molecules based on the Lennard-Jones relationship.

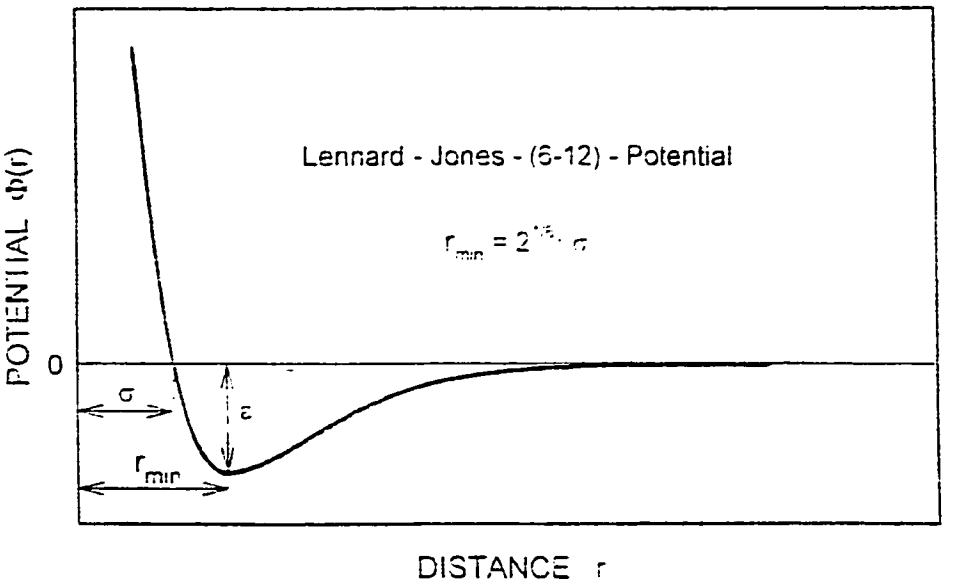

Figure 2.11 Schematic representation of the Lennard-Jones Potential

Table 2.4 Kinetic Diameters and Pore dimensions of some organic molecules and Zeolites respectively

Molecule	Kinetic Diameters (Å)
CO_2	3.30
CH_4	3.80
C_2H_6	3.90
$n\text{-}C_4H_{10}$	4.30
$i\text{-}C_4H_{10}$	5.00
Benzene	5.85
Cyclohexane	6.00

Zeolite	Pore Dimensions(Å)
Chabazite	3.6 x 3.7
Erionite	3.6 X 5.2
A	4.1
ZSM-5	5.4 X 5.6 ; 5.1 X 5.5
ZSM-11	5.1 X 5.5

2.6 Adsorption in Zeolites

The void spaces in the crystalline structure of zeolites provide a high capacity for adsorbates, which are referred to as guest molecules. The sorption capacity is a conveniently measured property that is used to identify zeolites. [69]

Almost all of the catalytic active sites are located inside the pores and channels of the zeolite crystals. In a typical catalytic process, the diffusion of reactant molecules to these active sites occurs according to the following steps:

1) Diffusion of reactant molecules from the bulk phase to the crystal interface

2) Diffusion of reactants through the pore system

3) Adsorption at the active site

4) Reaction of the catalyst-reactant complex

5) Desorption of product molecules from the active site

6) Counter diffusion of products from the pore system to the crystal interface

7) Transfer of products from the crystal interface to the bulk phase

Steps 3) to 5) are strictly chemical and consecutive to each other while the transfer steps 1) and 7) are strictly physical and occur separately from the chemical reaction.[70] The transport steps 2) to 6) which occur inside the pore system cannot be separated from the chemical steps 3) to 5) and they take place simultaneously with the chemical reaction. Figure 2.12 illustrates the possible different physical and chemical steps starting from a reactant A and ending in a reaction product B via heterogeneously catalyzed reaction paths.

In zeolitic diffusion, adsorbed molecules continuously interact with the surrounding pores and with adjacent molecules. The nature of these interactions determines the equilibrium and transport properties of the adsorbed phase.

A zeolite that contains more than one type of adsorption site, each with a different adsorption energy, is called energetically heterogeneous. Energetic heterogeneity can stem from a number of sources, including: (1) the presence of lattice defects, (2) differences in the positioning of framework aluminum species in the lattice, and (3) the topology of the lattice atoms relative to the configuration of the guest molecule. Regarding the last point, the lattice may be such that the potential energy in the zeolite may exhibit more than one local minima as the molecule goes through the channel. An example of this is the adsorption of butane in ZSM-5. There are two kinds of adsorption sites, one is in the channel and another is located at the intersection. [71]

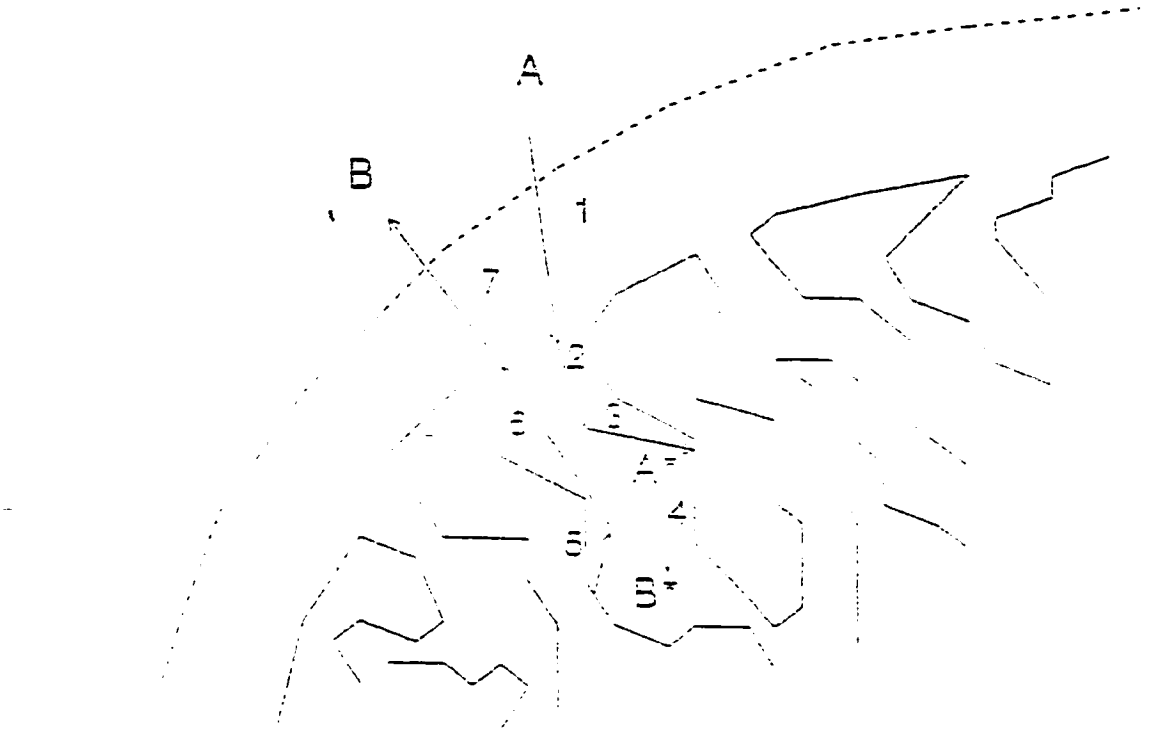

Figure 2.12 Chemical and Physical steps involved in the catalysis reaction of A –B

*(Where the * indicates the active sites)*

2.6.1 Window Effect

Gorring[72] was the first to have discussed the principle of window effect. His publication was entitled:"Diffusion of Normal Paraffins in Zeolite T". He tested the diffusion of paraffins in potassium T zeolite versus the chain length at 300°C. He noticed that the diffusivity decreases rapidly from ethane to propane, rises for butane, then drops to a minimum at C_8.The close sheathing of the n-octane molecule by the hexagonally shaped erionite cage yields a configuration where the molecule just fits the cavity. It is in a low-energy trap defined by the cage with the primary energy barrier to diffusion deriving from the 8-membered rings forming the cage's exit/entry ports. Entrapement in the cage leads to low mobility for just fitting molecules. Above nC_8, diffusivity rises rapidly reaching a maximum at C_{12}, then decreases again. He concluded that n-dodecane molecule was moving through the zeolite lattice at about 140 times the velocity of the n-octane molecule despite the difference in size, because due to its size it extends through the 8-ring and this results in a surmounting of the energy barrier by virtue of the molecular size alone.In fact, at 300°C, n-dodecane has a diffusivity six times greater than that of propane at the same temperature. The high values of diffusion coefficients in the nC_{11}-C_{12} range relative to the much lower values at nC_8 and nC_{14} indicate that the zeolite presents a "window of high transmittance" to molecules of a certain critical length but not to those either shorter or longer. This phenomena will be designated as the "window effect". The window effect is seen to persist over wide ranges of temperature. Although higher temperatures tend to decrease the depth of the window, the effect is still readily apparent at the catalytically interesting temperature of 450°C.

2.7 Methanol to Olefins and Gasoline (MTO/MTG)

The conversion of methanol into hydrocarbons using zeolite catalysts has attracted significant research attention since the publication of the landmark paper by Chang and Silvestri in 1977. [73] It resulted in the Mobil process, which has been commercialized in New Zealand for offshore natural gas. The plant has converted natural gas to methanol for more than a decade in continuous operation, the methanol was then processed into premium gasoline. In relation to the MTG conversion, the so-called methanol to olefins (MTO) reaction was developed. The Mobil MTO process can be considered as an intermediate step in the MTG process, but was demonstrated only on a semi-industrial scale in the 1980's due to the low olefin selectivities. One of the major drawbacks is the very rapid promotion catalyst deactivation.[74]

Mobil's MTO process is based on the discovery that by reducing the acidity of the zeolite and raising the operating temperature above 500°C, the relative rate of olefin formation reactions and aromatization reactions are different enough so that a C_2 to C_5 olefin yield as high as 80% has been obtained by Chang et al.[75]

The zeolite-catalyzed formation of hydrocarbon from methanol is represented by the general scheme:

$$n/2[2\ CH_3OH \rightleftharpoons CH_3OCH_3 + H_2O] \rightarrow C_nH_{2n} + n[CH_2]$$

The overall reaction may be regarded formally as a 1,1-α elimination affording H_2O and reactive C_1 intermediates which then combine to form hydrocarbons. The structure of the C_1 entity, as well as the mechanism (as shown in figure 2.13) by which the initial C-C bond

is formed are matters of continuing controversy.[76] One of the many discussed routes to form olefins is by using the Steven's rearrangement. Georges Olah [77] refutes the fact that this rearrangement even exists. His experiments based on labeling, showed that the ylide undergoes bimolecular methylation to form the ethyldimethyl oxonium ion intermediate rather than using a intra molecular Steven's rearrangement.

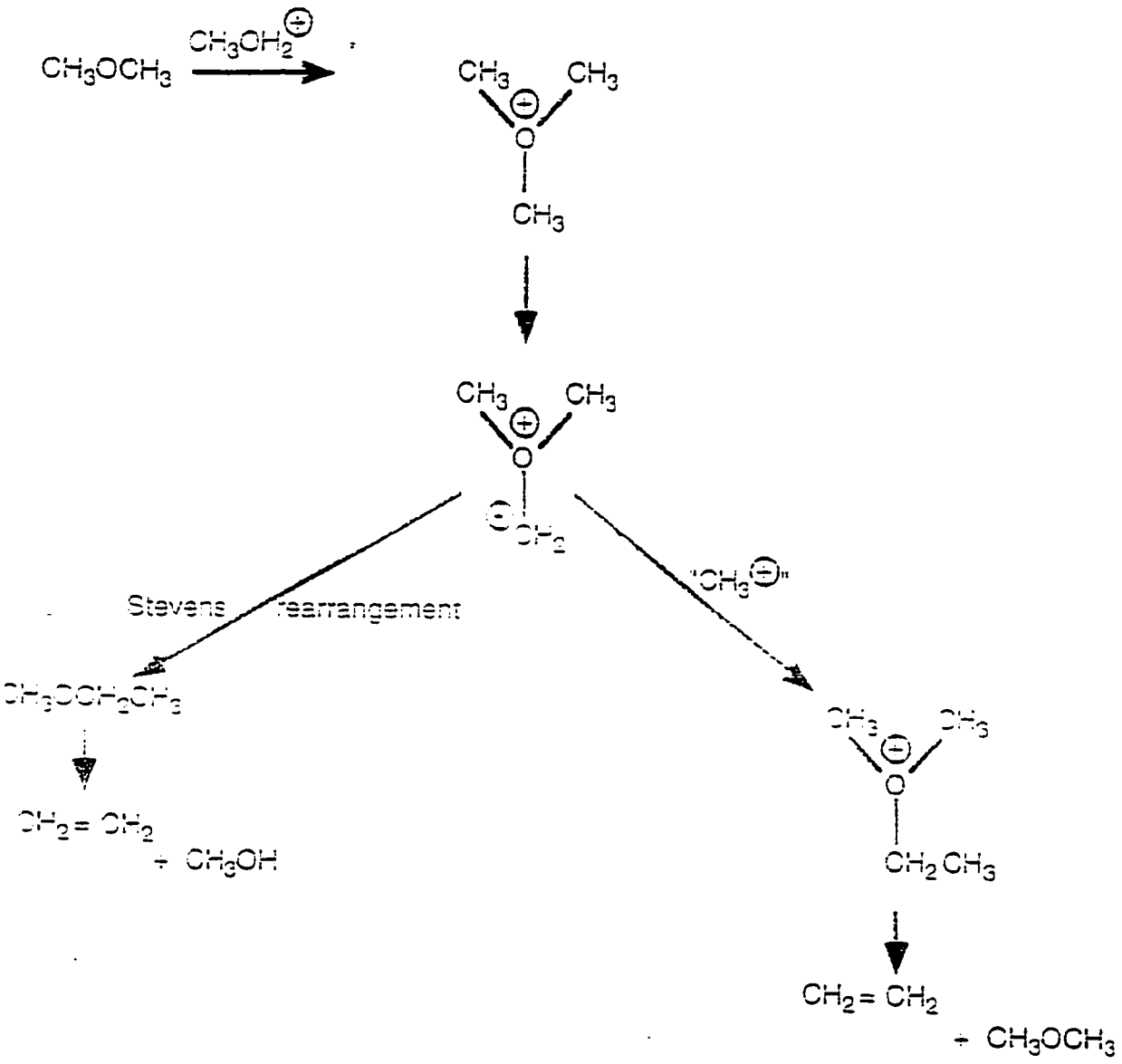

Figure 2.13 Ethylene formation via β-elimination

The MTG reaction mechanism has been a subject of controversy for nearly 2 decades, with no clear resolution as shown by the disagreement between Olah and other researchers. Speculation has focused mainly on two questions: 1) Formation of the initial C-C bond and 2) whether ethylene is the first alkene formed. Reactions forming aromatics and alkanes from alkenes are generally agreed to follow classic carbenium ion pathways, with concurrent hydrogen transfer. A recent survey has identified nearly three dozen mechanistic schemes in the literature. In general, the proposed mechanisms fall under one or more of the following categories: Carbene-carbenoid, carbocationic, oxonium ylide, free radical and concerted reaction.

Derewinski et al. [78] proposed that when methanol is passed over a poisoned catalyst only dimethyl ether is produced. This shows that the formation of the first C-C bond from C_1 species requires the participation of acid centers stronger than all other steps and once they have been poisoned, the reaction chain does not initiate itself. When however, trace amounts of ethanol were added, total transformation of methanol was observed on a poisoned catalyst, on which no reaction of pure methanol occurred. This could be explained by the fact that the presence of ethanol has an initiating effect on the reaction of methanol, which enables the by-passing of the most difficult step of the reaction chain as shown on figure 2.14.

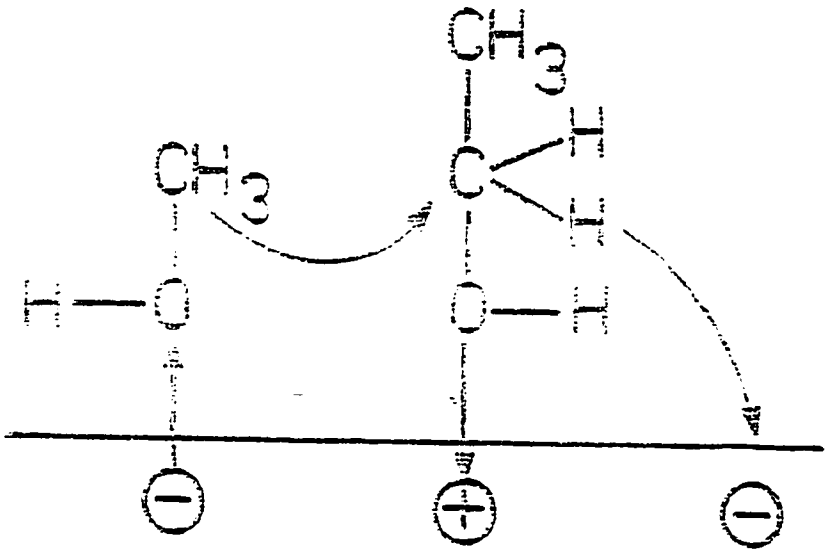

Figure 2.14 Presence of ethanol and its initiating effect on the methanol reaction

2.7.1 Coke Formation

Zeolites can become deactivated by carbonaceous deposits (coke) that cover catalytic sites and/or block pores. The coke structure varies with conditions, but consists essentially of ill-defined polyaromatic compounds. With time, and especially with increased temperature the hydrogen-carbon ratio of the coke usually decreases and the coke becomes more resistant to removal by oxidation.[79] It is well understood that they have low hydrogen content and often behave as insoluble solid like deposits that remain strongly attached to the catalytic surfaces. The carbonaceous deposits that accumulate on the zeolite catalysts can be classified as either "hard" or "soft" coke. Hard coke is generally derived from aromatic hydrocarbons that are present in the feed or that are generated during the reaction It is typically formed at high temperatures (> 427°C) by reactions that occur within acidic zeolites.

In contrast, soft coke is generally formed by oligomerization or alkylation reactions involving olefins and paraffins or naphtenes. Soft coke is normally formed at low temperatures and usually within the zeolite. The compounds that constitute soft coke might normally be soluble in hot solvents, the branched nature of these compounds prohibits them from being extracted from the zeolite. Typical of soft cokes would be those deposits formed during the ZSM-5 catalyzed MTG reaction. Soft cokes have hydrogen-to carbon (H/C) atomic ratios that are greater than 1.0 and typically greater than 1.25, while hard cokes have H/C atomic ratios that are typically less than 1.25. There seems to be a general consensus that hard coke forms through intermediate aromatic structures of increasing size and complexity.[80] Hard coke formation involves initial adsorption of highly unsaturated hydrocarbons followed by condensation and elimination reactions. These reactions normally

proceed by olefins interacting with adsorbed condensed ring aromatics to form paraffins and hydrogen deficient hard coke.

Derouane [81] has proposed the scheme shown in figure 2.15. Because the coke may grow into stacking complexes with dimensions comparable to the size of the pores, the activity of the catalyst may not be solely proportional to the remaining fraction of the acid sites. Indeed, continuous coke buildup on the surfaces of the pore reduces local diffusivities, thus reducing activity. In sequential reactions, the product selectivity may also be impacted. Ultimately, pore blockage causes the most significant effect on activity by both lengthening the diffusion path and rendering some of the active sites inaccessible for reaction.

There are several experimental investigations that have determined that coke forming reactions lead to increasing diffusional limitations and pore blocking of zeolite catalysts. Butt et al. [82,83] studied the conversion of cumene over coked mordenite samples. They concluded that diffusivities decreased more than a factor or two during the coking process and that the changes were not linear with the weight percent of coke on the catalyst. By using a scanning electron microscope, they observed significant pore blockage near the outer surface of the catalyst. No coke was found in the particle interior. Guisnet and Magnoux [84] examined the effects of pore structure on coking and on how coking changed the diffusivity. They concluded that steric constraints during the formation of coke molecules are more pronounced in the relatively narrow pores of zeolites like erionite than they are in the large zeolite Y supercages. The connectivity of the pore system also plays a significant role in determining the effect of coke deposition. When the pore system consists of non-intersecting channels such as in mordenite, pore blockage occurs rapidly. The first coke molecules formed

in the large channels are retained. One coke "molecule" is sufficient to inhibit the reactant diffusion to the active sites that line the channels. When the pore system of interconnected channels as is the case of the ZSM-5, the coke initially builds up adjacent to the acid sites and may limit access to them. Subsequently, there is blockage of the sites at the channel intersection in which the coke is situated. Finally, at high coke content, it places itself on the outer surface of the crystalline solid and this will block access to the sites of the channel intersections in which there are no coke molecules. With small pore systems, coke accumulates mainly on the exterior of the crystal and at the pore mouth. The kinetics of coke deposition is frequently described by the empirical Voorhies equation: [85]

$$W_c = k_c * t^{n_c}$$

where: W_c= amount of coke deposited (wt%);

k_c = coking rate constant (wt% min^{-n_c})

t = time-on-stream (min)

n_c = deactivation exponent (n_c>0)

A zeolite catalyst is usually regenerated by oxidizing the coke with air or air diluted with nitrogen. This process may also be more or less shape selective. In a comparison of removal of coke laid down by cracking of n-heptane on H-Y, H-mordenite, or H-ZSM-5, Magnoux and Guisnet in 1988 ascribed low oxidation rates on H-ZSM-5 to blockage of pore intersections by coke, that restricted oxygen recirculation. Whereas relatively high oxidation rates on H-Y zeolite were attributed to free circulation of oxygen through the supercages.[85]

2.8 Major Industrial Applications of Pore Reduced Zeolites

Zeolites, which have a cagelike structure of precise geometry with pores of uniform shape throughout the entire crystal, are molecular sieves that can be used for separating gas mixtures by molecular sieving effects or selective adsorption and for shape-selective catalysis reactions.[86]

Discovered in 1956, by Plank and Rosinski [87] the large scale applications of zeolites as catalysts only began in 1959 with Union Carbide using Y zeolite as an isomerization catalyst and in 1962 using the X zeolite as a cracking catalyst. They incorporated a small amount of zeolite in the standard silica/alumina catalyst. This significantly improved the cracking performance of crude oils in the production of petroleum.[87] It has been since that time that zeolites have been used in the oil refining and petrochemical industry, because of their superior activity, stability and selectivity in major conversion and upgrading process as compared to their amorphous equivalents.

Over the last 20 years, the shape-formation of substituted aromatic molecules over medium-pore zeolites were intensely studied by industrial as well as academic institutions. Starting with the pioneering work by Chen et al. [88], the interest was mainly focused upon ZSM-5 as a catalyst and was leading to several commercial processes. Thus, the kinetics of the alkylation, disproportionation and isomerization reactions of aromatic molecules leading to xylenes and diethylbenzenes are well established. The unique property of ZSM-5 is to produce p-dialkylbenzenes in selectivities exceeding thermodynamic values by far.

In the following sections, we are going to analyze the results that were achieved in literature concerning p-xylenes by several different chemical modification methods on reactions such as xylene isomerization, alkylation and disproportionation/transalkylation.

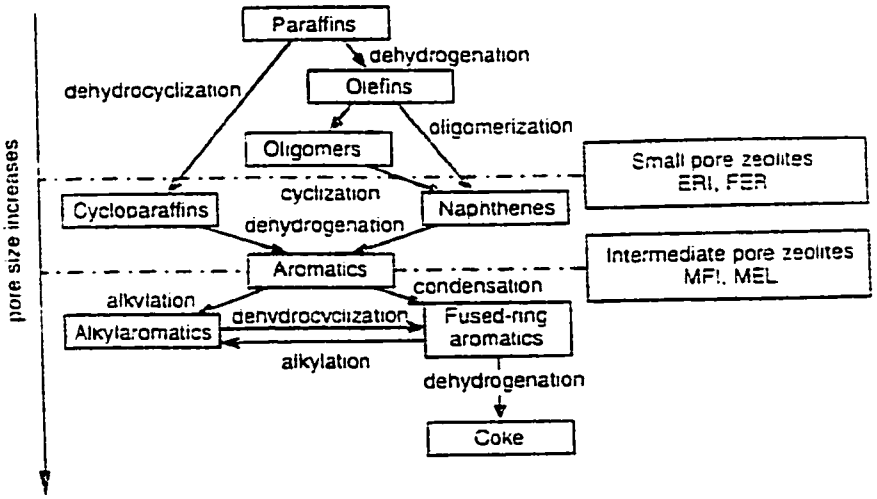

Figure 2.15 Reaction pathways leading to exclusion in small and medium pore zeolites and coke deposition in large pore zeolites.

2.8.1 Isomerization

A mixture of the xylene isomers and ethylbenzene is readily available as the C_8 aromatic fraction of catalytic reforming. Isomerization and transalkylation of alkylaromatics are used commercially to a large extent in the production of important petrochemicals. Xylene isomerization, allows one to meet the high demand for p-xylene which is used as a precursor for polyesters by converting the much less used meta and ortho isomers to the para (see figure 2.16).

The properties of the ZSM-5 zeolite, allow it to act as an effective molecular sieve with characteristic adsorption properties. By modification with certain chemical reagents, the production of p-xylene is favored compared to the two other isomers and the value is greater than at its thermodynamic equilibrium. This is in sharp contrast to results obtained with a variety of Friedel-Crafts catalysts which causes isomerization to occur but is also accompanied by a transalkylation reaction giving toluene, trimethylbenzene and a mixture of xylene isomers.[89] Usually the proposed mechanisms were deduced from detailed kinetic measurements, which only allow indirect conclusions with respect to the proposed mechanism. This is well reflected in the quite controversial discussion documented in papers by Chen et al. and Kaeding et al.[90,91]

Young et al.[92] discussed the subtle role of steric constraints in the pores of the molecular sieve and the role of diffusion and secondary isomerization in enhancing the selectivity to molecules with the highest diffusivities. Although the three isomers can enter the pores of the ZSM-5, diffusion measurements indicate that the diffusivity of para-xylene is $> 10^3$ faster than that of ortho and meta (p>o>m). [93,94]

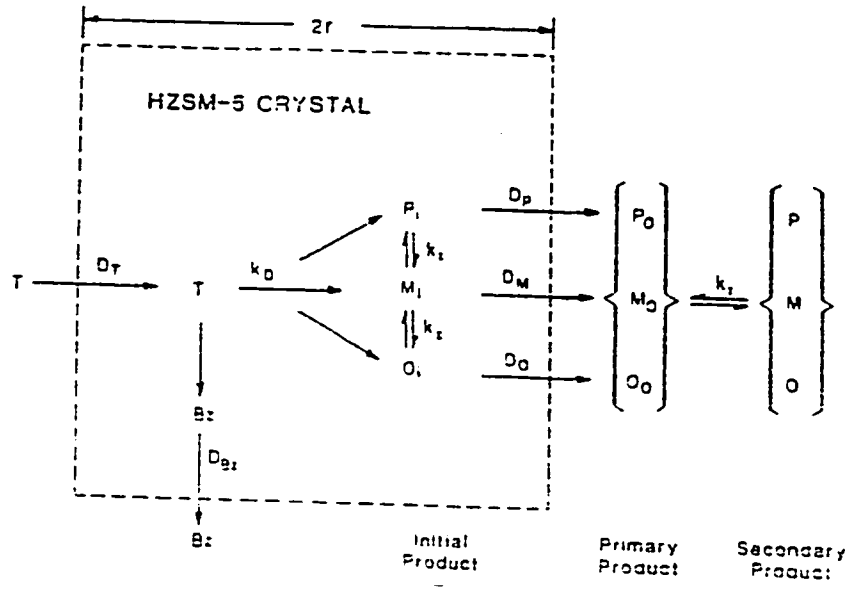

Symbols:

D = Diffusion Coefficient
k = Rate Constant
r = Crystal Radius
Bz = Benzene
T = Toluene
P,M,O = Para-, Meta, and Ortho-xylene

Subscripts:

I = Isomerization
D = Disproportionation
i = Initial Product
o = Primary Product

Figure 2.16 Different products formed from toluene over ZSM-5

Mirth and Lercher [95] used m-xylene as a reactant. The I.R spectra suggested that this is the main isomer in the adsorbate. This would suggest that the diffusion of all main products (para and ortho) out of the zeolite is fast in comparison to their rate of formation. They determined that all acid sites which are capable of adsorbing m-xylene are concluded to have the same catalytic activity. The isomerization of m-xylene gives a product ratio of 2 for para/ortho for all temperatures below 200°C. They concluded that the preferential formation of p-xylene is not due to a lower energy of activation, but rather due to differences in the transition entropies.

Zakett et al.[96], discussed the effect of chemical modification on the ZSM-5 selectivity. By impregnating the zeolite with aqueous phosphoric acid to add a phosphorous atom or using magnesium acetate to insert magnesium within the zeolite framework, it has been shown that this had the effect of increasing production of para-xylene. It has been proposed that these chemical treatments function in part by reducing the pore openings and the channel dimensions of the ZSM-5 crystals, favoring the formation of para isomer and permitting it and small molecules to diffuse out of the catalyst at a rapid rate.

Young et al.[97] from Mobil Chemical Company reported their findings for para selectivity with phosphorous (7.1%wt.) to be approximatively 91% and with magnesium (9.4%wt.) they found 81% of the para isomer. These values were for a reaction temperature of 600°C. It should be noted that with an un-modified ZSM-5 zeolite, the equilibrium composition of the para-xylene compared to the other isomers is 24%.[98]

Hibino et al.[99] showed that the isomerization of o- xylene gave more para than meta-xylene over ZSM-5 zeolite. The proportion of para to ortho ratio increased with addition of

silicon alkoxide reaching a maximum for 13.3% of silica deposited. The formation of large molecules such as trimethylbenzenes was completely suppressed.

2.8.2 Alkylation

Zeolite catalyzed alkylation of aromatics with ethene was first reported by Wise in 1966. He used rare earth exchanged faujasite, and this was followed by Becke et al. in 1973 who used mordenite.

Alkylation of benzene is accompanied by the polymerization of ethene. Hence a high molar ratio of benzene to ethene is necessary to minimize the polymerization of ethene and the formation of polyalkylated benzenes, which cause rapid catalyst deactivation as reported by Wise.

ZSM-5 is a class of zeolite that inhibits the formation of polyalkylated benzenes normally formed in significant quantities with non shape selective catalysts. This unique property led to a more stable catalysts and improved the product selectivity far superior to all previously available catalysts. The catalyst is used in the ethyl benzene process jointly developed by the Mobil and Badger company.[100]

For the methylation of toluene, it is commonly accepted by researchers that an activated form of methanol (methoxonium ion) reacts with weakly adsorbed toluene. The two models that explain the high selectivity to p-xylene found with ZSM-5 molecular sieve catalyst. They proposed either restrictions for the transition state to form meta and ortho xylene and/or diffusional constraints of the bulkier isomers.[101,102,103,104] It has been shown by Lercher et al.[105] that both proposals are not ideally fulfilled. They believed that the product

distribution in toluene methylation is neither controlled by the size of the transition state of the various xylenes, nor did they observe the xylene isomers in their equilibrium concentration in the catalyst pores. This would mean that the product selectivity would be determined by the different rates of diffusion. They acknowledged that any increase of the diffusional constraints, would increase the concentration of the ortho and meta- xylenes in the pores and enhance the para-selectivity. This diffusional constraint may be achieved by external coating or adding functional groups.

Young et al.[106] talked about modifying the pore size of the ZSM-5 with phosphorus from the $P(OCH_3)_4$ compound. They established the fact that para selectivity changes greatly if compared to the unmodified catalyst. They performed additions of phosphorous which ranged from 0 to 6 % and they found the maximum result to be at 5.6%, with a production of para- xylene that reached 93% of the total isomer content at 550°C. For temperatures lower than 550°C, the modified zeolites produced ortho-rich xylene mixtures. At temperatures higher than 550°C, the selective catalyst tends towards 100% para-xylene, whereas less selective catalysts generally tend toward equilibrium of xylene composition.

Hibino et al.[107] worked on depositing by chemical vapor deposition (CVD), different amounts of silicon alkoxide on H-ZSM-5 They wanted to see what kind of xylene selectivity they would be getting for the alkylation of toluene with methanol. They also believed that the external acid sites were inactivated by the deposition of the silicon alkoxide. Using these modified catalysts, they noticed that methanol was completely reacted for any amount of silicon alkoxide added and the conversion of toluene decreased with increasing amounts of silica. Small amounts of benzene, ethyl benzene, ethyl toluene and trimethylbenzene were also

formed. An increase in the deposited silica drastically changed the xylene isomer distribution. At 13% silica deposition, the para-xylene reached 81% and the other two isomers were greatly reduced compared to thermodynamic equilibrium values. This catalyst produces the isomer with the smallest dimension in each class of alkyl aromatics.

Kaeding et al.[108], who have studied extensively the alkylation of toluene on H-ZSM-5, have proposed that an equilibrium mixture of xylenes is formed as the primary product in the pores. Then by narrowing the pores, selectively only the para-xylene exits.

Yashima et al.[109,110] have a different view, they think that the primary product formed in the pores are para-xylene and they are then isomerized on strong acid sites in the pores. It is the reduction of strong acid sites in the pores that cause high para-selectivity.

Furthermore, Theodorou and Wei [111] have suggested that p-xylene is selectively produced in pores of H-ZSM-5, and the secondary isomerization of p-xylene proceeds only on the external surface. This means that to produce p-xylene, the external surface acid sites need to be inactivated.

2.8.3 Transalkylation/Disproportionation

Ethyl benzene is always present in commercial xylene streams. The relative rate of transalkylation of ethyl benzene to the disproportionation of xylene is an important factor in determining the selectivity of the catalyst.

The transalkylation of ethyl benzene proceeds readily over medium pore zeolites. Karge et al.[112] used ethyl benzene transalkylation as a test reaction for the determination of acid sites in ZSM-5 and found a linear relationship between the conversion and the aluminum content of the zeolite. Meshram et al.[113] discussed the fact that toluene conversion and the number of acid sites increase with increasing aluminum content in H-ZSM-5 zeolites, indicating that the surface acid sites are indeed active centers for toluene disproportionation. In 1985, Kaeding et al.[114] used ethyl benzene in the disproportionation reaction and found high concentrations of para-diethyl benzene and no ortho-diethyl benzene with ZSM-5. This is unlike with mordenite, which gave an essentially equilibrated di-ethyl benzene composition.

Young et al.[115] discussed the fact that the transalkylation reaction to form benzene and xylene within the pores is relatively slow, with benzene diffusing out of the pores rapidly. The xylenes would then isomerize rapidly within the pores. Para-xylene diffuses out the fastest, while meta and ortho move at a much slower pace inside the pores. The latter two xylenes would have to form p-xylene to escape from the channel system. They reported that with non-modified ZSM-5 type catalysts, they achieved equilibrium for the xylene mixtures in toluene disproportionation. Modifying the ZSM-5 with boron, increased the production of p-xylene to a level of 80% at 700°C. Using magnesium as a modifying agent gave 75% of p-xylene at 550°C.

Olson and Haag [116] reported evidence of diffusion control for p-xylene selectivity in toluene disproportionation over non-modified and modified ZSM-5 catalysts. It is believed that a good correlation exists between a diffusion related parameter and p-xylene selectivity in toluene disproportionation.[117,118,119] They determined that p-xylene selectivity increased with an increase in temperature. It was explained in terms of changes in the parameter $k(R^2/D)$ (where k= reaction rate , R is the crystallite radius and D= diffusivity), it is expected that the selectivity between species of differing diffusivities increases with $k(R^2/D)$.

Hibino et al.[120] used H-ZSM-5 and the SiHZSM-5 which was modified with 13.3wt.% of silica, to see what proportion of xylene isomers they would produce for the disproportionation of toluene. They found that the deposition of silica did not change selectivities to benzene and xylenes, but drastically altered the distribution of xylenes. The interesting part of all of this is that as the amount of silica increased, yields of meta and ortho xylenes decreased but that of p-xylenes increased. Specifically, the yield of p-xylene over SiHZSM-5(13.3%) was double that over non-modified HZSM-5, under the same conditions.

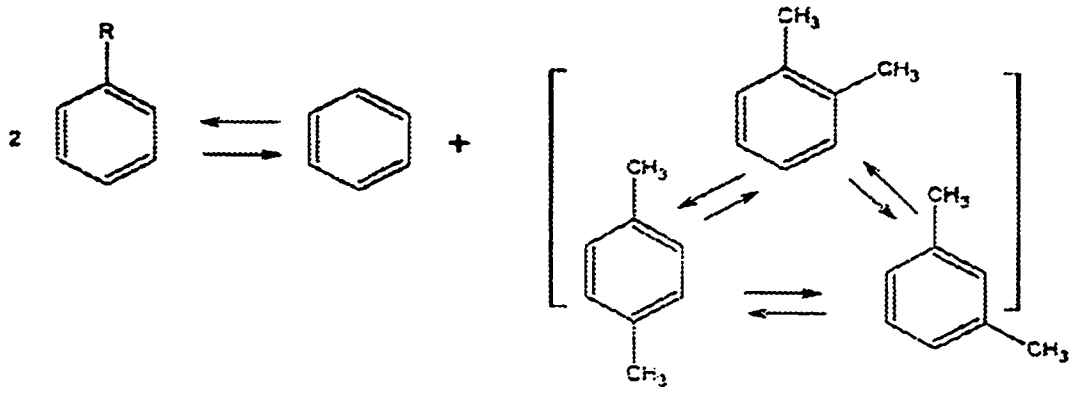

Disproportionation

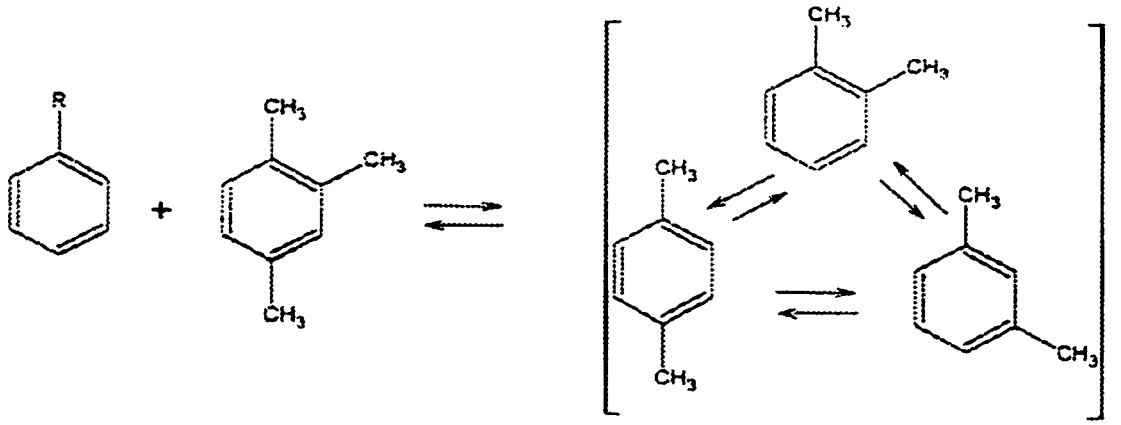

Transalkylation

Fig. 2.17 The Process of disproportionation and transalkylation

Chapter 3

Experimental

3.1 Source of Materials

Chemicals	Supplier
Na-ZSM-5	Chemie Uetikon AG
Hydrogen Chloride (12M)	BDH
Sulfuric Acid (18M)	BDH
Lithium Tetraborate	Aldrich Chemicals inc.
Potassium Carbonate	Aldrich Chemicals inc
Sodium Hydroxide (19.4N)	Aldrich Chemicals inc
Ammonium Chloride	ACP Chemicals inc.
(Si-O) species #1	In our Laboratory
(Si-O) species #2	Strem Chemicals
KBr (FT-IR) grade	Aldrich Chemicals inc
CsI (FT-IR) grade	Aldrich Chemicals inc
Sodium Standard (1000 ppm)	Fischer Scientific
Aluminum Standard (1000 ppm)	Fischer Scientific
Hydrogen Peroxide (30%)	ACP Chemicals inc.
Amberlyst 15 ion-exchange resin	Rohm and Hass *co.*
n-Hexane and 3-Methyl pentane	Aldrich Chemicals inc.
n-Heptane and 3-Methyl hexane	Aldrich Chemical inc.

3.2 Introduction

In this chapter, we will be discussing the development and optimization of the Desilication Reinsertion and Stabilization (DRS) procedure. The process for the removal of silicon is called desilication. It was developed as a way to generate materials which have an improved catalytic activity due to higher density of proton sites. We define desilication as a selective removal of silicon from a highly siliceous material using a mildly alkaline solution. This has the effect of decreasing the Si/Al ratio in a controlled and systematic manner. It is a direct means of increasing the cation exchange capacity of the solids.[121] The desilication conditions using sodium carbonate have been optimized so that we do not have a partial or full collapse of our zeolite network.

The next step was to find a procedure to impregnate the sodium orthosilicate or orthosilicic acid onto the desilicated sample and these conditions will be described in full within this section. All these steps bring about a decrease in the medium pore size of the micropores, while maintaining the surface area and catalytic activity as high as what was reached with the desilicated zeolite. A very important application of the DRS method is in shape-selectivity, where products of a larger size may not exit as such, they are broken down into smaller entities before they can leave the zeolite pores. The large molecules that do not reduce their size eventually grow bigger, forming large polyaromatic compounds. This is known as coke, and it will be discussed in greater detail within this section.

3.3 Various Treatments Applied to the ZSM-5 Zeolite

3.3.1 Desilication

The application of a strongly alkaline solution medium on the one hand represents the conditions for the zeolite synthesis, but on the other hand silicates can be dissolved in an alkaline solution. [122] The removal of silicon atoms from highly siliceous zeolites using hot alkaline solution of sodium carbonate which hydrolyzes to sodium hydroxide, or sodium hydroxide directly, results in severe structural collapse.[123,124] In addition there is the possibility of other species recrystallizing from the solution especially during the treatment of zeolites with high aluminum content. [125]

Le Van Mao et al. [126] have developed a technique whereby silicalite and other silica rich zeolites such a Na-ZSM-5 and some with a lower Si/Al ratio, treated with mildly alkaline solution of sodium carbonate in such a way to effect the selective removal of silicon atoms from these structures.[127]

3.3.2 Experimental

3.3.2.1 Sample Preparation

The Na-ZSM-5 zeolite was purchased from Chemie Uetikon AG. It was in the powder form and dried at 120°C overnight prior to treatment.

3.3.2.2 Desilication

The commercial Na-ZSM-5 zeolite was treated with sodium carbonate as follows: 20.0 g of Na-ZSM-5 zeolite was placed in a polypropylene bottle containing 200 ml of 0.8 mol/L of sodium carbonate solution. The bottles were then placed in a hot bath (Fischer Scientific Versa bath Model 206), where the mixing period of the liquid sample lasted 4 hours at a temperature of 80°C and mixed at a rate of 60 Rotation Per Minute (RPM). The suspension was allowed to cool and settle before the filtration step.

The solid-liquid mixture was filtered and the filtrate was removed and kept for the later evaporation step that gave us a solid compound which was found to be sodium orthosilicate. This will be discussed in greater detail in section 3.3.2.4. The solid sample was washed with 2.0-2.5 liters of hot distilled water, filtered and dried overnight in air at 120°C.

The next step was to wash the desilicated solid as follows. In a beaker, 20.0 g of desilicated catalyst was added to 200 ml of water. The suspension was heated at 80°C under mild stirring for a period of 2 hours this will remove the loosely bound silicate species and the sodium that came from the desilication step. The solid material was then recovered by filtration, washed with some distilled water and finally dried overnight at 120 °C. The resulting solid, which was used for the preparation of the DRS sample, is herein referred to as Na-DZ (1).

Another solid material, which was used for the preparation of the desilicated sample with the largest pore size, was obtained using the same desilication procedure. The treatment with the sodium carbonate solution as previously reported, was repeated two more times for a total of 12 hours. The solid was then filtered and washed with 2.0-2.5 liters of water for the same reasons as previously mentioned, and the solid was dried in the oven at 120°C. In a beaker, 20.0 g of a solid desilicated for 12 hours, where 200 ml of distilled water was added and heated to 80°C under mild stirring for a period of 2 hours. The resulting solid is herein referred to as Na-DZ (3).

3.3.2.3 The Formation of The Acidic Form ZSM-5 and Desilicated Zeolites

The ammonium form of the ZSM-5 zeolite was prepared by repeated ion-exchange of the sodium form with a 5 wt.% solution of ammonium chloride at 80°C under mild stirring (1.0 g of solid for 10 ml of solution). Each treatment lasted 2 hours, after which the used solution was decanted and fresh solution was added. This procedure was repeated two more times for a total of three times. The resulting solid was then filtered out, washed with water and dried overnight in air at 120°C. The acid forms were generated by activating the sample in air at 500°C overnight. They are herein referred to as HZ (parent H-ZSM-5) and HDZ (prepared from the Na-DZ(3)).

3.3.2.4 The DRS Sample Produced Using Sodium Orthosilicate

The orthosilicate species used in the reinsertion process, was obtained by evaporation to dryness of the liquid filtrate (treatment with the sodium carbonate to prepare the Na-DZ(1)), and then drying in air at 120°C overnight. The resulting solid was identified by x-ray powder diffraction using the Joint Committee for Powder Diffraction Standards (JCPDS) database and the Micro-Powder Diffraction Search-Match of Fein Marquat (μPDSM) software.

The impregnation of the sodium orthosilicate (5.0 wt.%) into the NH_4-DZ(1) was carried out as follows: 0.15g of sodium orthosilicate was dissolved in 13.0 ml of water by heating at 80°C for a period of 30 minutes. An amount of 3.00g of H-DZ(1) was added to the previous solution and stirred for several minutes to make sure we have a highly homogeneous solution. The suspension was then evaporated quickly to dryness on a hot plate. The resulting solid was first heated overnight in air at 120°C, and then activated in a stepwise manner. The zeolite was heated at a base temperature which in our case is 300°C for a period of one hour. The temperature was then raised by 50°C/h until the final activation temperature of 700°C is reached. This last temperature was maintained for a period of 16-18 hours.

3.3.2.5 The DRS Sample Produced using Orthosilicic Acid

The sodium orthosilicate which was extracted from the desilication step (as previously explained) was used. An amount of 0.40 g of sodium orthosilicate was dissolved in a 10 ml volume of distilled water to make an 8 wt.% solution. The solution was passed through a column that contains a packed resin in the acid form. Water was being used to push the solution down the column and the resulting solution accumulated was known as orthosilicic acid . A volume of 40-45 ml was obtained during this process and our next step was to concentrate the orthosilicic solution. This is done by evaporating the liquid in a rotovap set up. The water bath is being heated to 70°C and under vacuum. The process is stopped when the solution has been reduced from (40-45) ml to between 6-8 ml. Its color has changed from transparent to a light yellow tint. It will be referred to as a concentrated orthosilicic acid solution.

In the next step, we inserted 5.0 g of ammonium form desilicated ZSM-5 zeolite (NH_4DZ) into the concentrated orthosilicic acid and passing the mix through the rotovap in the same way as mentioned above until complete dryness. The DRS that was impregnated with 8% of orthosilicic acid (DRS (8 wt.%)) sample was then put in the oven overnight at 120°C so that it is completely dry. In the next step, we activated the sample in a stepwise manner by increasing the temperature by 50°C/hour, until reaching a temperature of 700°C and this is done for a period of 16-18 hours.

The DRS (8%) sample that has been activated stepwise to 700°C, 5.0 g was spread out on a filter paper in a buchner funnel. This funnel had a diameter of 8.5 cm and a depth of 3.5 cm. A volume of 350 ml of hot water was passed through the spread out catalyst. This all lasts no more than 10 minutes with applied vacuum. The sample was then dried at 120°C overnight and then reactivated to 700°C stepwise for a period of 16-18 hours.

3.4 Conditions for the MTG/MTO Reaction

Three zeolites were tested in the methanol to gasoline and in the methanol to olefin reaction. The catalysts used for these tests over the course of this project were: H-ZSM-5 (HZ) , H-DZSM-5 (HDZ), DRS (5 wt.%) and DRS (8 wt.%). They were extruded with bentonite clay (20 wt.%) which was used as a binder. The catalyst was then dried at 120°C overnight and finally activated in air at 500°C for 3 hours.

Catalytic runs were performed by injecting methanol, using an injection syringe on an infusion pump into an alcohol vaporizer-gas mixer. The vaporized methanol feed was then carried by the carrier gas (nitrogen) through a catalyst bed set in a tubular quartz reactor container, inside a furnace which was thermoregulated. A chromel-alumel thermocouple was placed in the catalyst bed and was used in conjunction with a digital thermometer unit to monitor the reaction temperature. The gaseous mixture flowing out of the reactor ran through a series of condensers maintained at 5-10°C, to a liquid collector immersed in an ice bath followed by a dynamic gas sampling bulb from which gas sampling was carried out. The configuration and size of the tubular reactor used in the present work has been described in a publication of Le Van Mao et al.. [128]

During the reaction, while the liquids were being collected, the gases were analyzed periodically by gas chromatography using a 30 m long JW alumina column mounted on a Flame Ionization Detector (FID) Mini-3 Shimazu GC apparatus equipped with a HP 3392 A integrator. Liquid fractions were then analyzed using a capillary column (50 m PONA type fused silica coated with cross linked polymer) mounted on a FID HP 5890 gas chromatograph.

The reaction conditions used in the experiments were as follows:

temperature = 375-550°C; catalyst weight = 2 g ; total pressure = 1 atm ;

weight hourly space velocity (WHSV)= 2.4 h^{-1}; duration = 3h.

The total conversion (C atom %) is expressed as follows :

$$\text{Conversion} = 100 \times NC_{prod}./ NC_{feed}$$

where NC_{prod} and NC_{feed} are the number of C atoms in the product and the feed streams, respectively. The selectivity in the product *i* is expressed as follows:

$$S_i = 100 \times Nc/NC_{prod}$$

where Nc, is the number of C atoms of product *i* in the product stream.

3.5 Qualitative Study of the Molecular Sieving Effect using the GC technique for Separation of BTX Aromatics.

The objective of this study is to assess the sieving effect of the zeolite materials with respect to BTX aromatics (benzene, toluene and the three xylene isomers). To that purpose, very thick zeolite containing membranes (called disks because of their thickness of ca. 1.5 cm) were prepared using fibrous sepiolite clay as matrix.[129] The percentage of zeolite component in these zeolite/sepiolite disks was 50 %. This composite material contained a percentage of undesirable pinholes (large transecting pores due to the presence of the clay) of less than 5% owing to the different speed of settlement of the zeolite particles (when compared to the fibrous sepiolite) in the preparation suspension. The zeolite disks were loaded in a stainless steel disk holder which was placed in the oven of a HP 5890A gas chromatograph equipped with a flame ionization detector. A mixture of BTX aromatics was first injected into the injection port of the GC and the vapors of these hydrocarbons, carried by a nitrogen flow, went through the disk which was maintained at 150°C Two distinctive peaks were observed: Peak I, quite sharp, corresponded to the non-adsorbed hydrocarbons which were thus immediately released to the main gas stream, while Peak II (very broad) was associated with the hydrocarbons adsorbed by the zeolite particles and the outward diffusion which was significantly delayed by constraints from the zeolite pores. In some cases, the hydrocarbon could be present in both peaks owing to the nearness of the sizes of adsorbate and adsorbent. The reason for the use of BTX aromatics stems from their molecular size, and more specifically, their kinetic diameter [130] (table 4.15) in the range of the ZSM-5 zeolite pore size. This allows the prediction of their diffusion through the ZSM-5 zeolite micropores and

the same molecular sieving effect.

3.5.1 Selective Absorption of n-heptane and Isooctane..

The disks were produced in the same way that was explained above. We used a proportion of 50% zeolite and 50% sepiolite. Three zeolite disks were then loaded in a stainless steel disk holder which was placed in the oven of a HP 5890A gas chromatograph equipped with a flame ionization detector.

An equimolar mixture of n-heptane and isooctane was then prepared and 0.05µl portions of it was then injected into the gas chromatograph. The GC conditions were the following:

- Oven: 110°C for 20 minutes, then ramping 50°C/min. to 300°C for 40 minutes.
- Injector: 200°C
- Detector : 300°C

The optimal integrator parameters for all the runs were kept constant for comparison purposes and determined to be:

For the first 16 minutes of the run:

- Attenuation : 9
- Chart speed : 0.3
- Thresh hold : 7
- Peak width : 0.16
- Area rejection : 200 000

Past 16 minutes the parameters changed to:

- Attenuation : 7
- Chart speed : 0.3
- Thresh hold : 5
- Peak width : 0.16
- Area rejection : 200 000

3.6. Characterization of Catalysts

In heterogeneous catalysis, characterization techniques are one of the most important tools to better understand the catalyst before and after the different chemical or thermal treatments which could be applied to the zeolite catalyst.

Some of these characterization techniques include:

- Atomic Absorption Spectrometry (A.A.S.)
- Determination of the BET surface area and pore size distribution
- X-ray powder Diffraction (XRD)
- Ammonia Temperature Programmed Desorption (TPD) and Titration
- Diffuse Reflective Infrared Fourier Transform Spectroscopy (DRIFTS)
- Differential Scanning Calorimetry and Thermal Gravimetric Analysis (DSC/TGA)
- Constraint Index (CI)

3.6.1 Atomic Absorption Spectroscopy (A.A.S.)

This technique was used for the analysis of the chemical composition of the different zeolite samples which have been used over the course of this research. The method involved weighing out accurately between 0.1100 g and 0.1300 g of our zeolite sample in each platinum crucible for a total of three. The crucibles were then placed in an oven at 800°C for a period of 2 hours. They were then cooled and reweighed to obtain the weight without any trace of water. To these crucibles, 0.9g of fusion mixture (potassium carbonate and lithium tetraborate in a ratio of 2:1) was added to the zeolite material, it was mixed and ashed in the furnace for another 2 hours at 800°C. This last step helps complete the decomposition of the zeolite so we could analyze its composition. The resulting mixtures were transferred to three separate 150 ml beaker and digested with a strong mineral acid mixture of 5 ml of HCl (12M) and 10 ml H_2SO_4 (10%) solution. The beakers were then covered with a watch glass to avoid any sample loss. Each mixture was then heated on low, on separate hotplates for a period of 30 minutes. Then 4 ml of 30% hydrogen peroxide was added to each of the beakers and the dissolution mixture was further digested for a few minutes until effervescence stopped. The final mixtures were placed on a hotplate and heated on low overnight. The next morning, the solutions were cooled and transferred to a 100 ml volumetric flasks They were then diluted to the mark with distilled water. Appropriate dilute solutions were prepared from this stock solution. The standard solutions were prepared from 1000 ± 0.2 ppm metal (such as Na or Al). These solutions were made every few months to assure a good standard curve.

The analysis of the different solutions was performed on a Perkin-Elmer model 503 instrument. For the analysis of aluminum for example, five standard solutions which ranged from 10 ppm to 50 ppm were prepared. Finding the absorbance of these solutions enabled us to draw a standard curve, and from this curve we were able to find the concentration of solutions to be analyzed, knowing their absorbance. The wt.% oxides of aluminum, sodium and silicon was used because it is the convention in catalysis.

The % of oxide present was determined using the following equation:

$$\% \text{ Element} = R_a/R_{std}\,(C_{std}/W_a)(V_a)(M/F)(D.F) \times 100$$

R_a = reading obtained from the sample solution

R_{std} = reading obtained from the standard solution

C_{std} = concentration of standard solution (ppm)

W_a = weight of the dried sample (g)

V_a = volume of original sample solution used (ml)

M = molecular weight of element in the oxide form (g/mole)

F = formula weight of element (g/mole)

D.F = dilution factor

We could define the dilution factor using the following equation:

$$D.F = V_{ds}/V_{ad}$$

Where:

V_{ds} = volume of the diluted sample solution (ml)

V_{ad} = volume of aliquot taken from the dilution (ml)

To determine the Si/Al ratio, we used the following equation:

$$Si/Al = 0.5\ [(W.SiO_2)/(W.Al_2O_3)]\ x\ [(MW.Al_2O_3)/(MW.\ SiO_2)]$$

Where:

W. = weight percent

MW. = molecular weight

3.6.2 B.E.T Analysis (Brunnauer, Emmet and Teller)

In our laboratory, we are very privileged to have two pore dimension and surface area measurement instruments B.E.T instruments, for the analysis of our samples. This could be done by two methods, they are : 1) nitrogen to determine if we have micropores and 2) argon to determine the Horvath-Kawazoe pore size distribution and the median pore diameter of our micropores, which is at the very core of our research.

The procedure for both analysis technique starts with the cleaning of the B.E.T tube with distilled water, then with acetone and finally placing it in a drying oven set to 120°C overnight. After this time, the tube was degassed on the ASAP 2000 instrument down to less than 10μm Hg pressure. The tube was weighed empty, the sample was kept under vacuum while keeping the sample at 220°C for a period of 4 hours in the case of nitrogen analysis and for at least 24 hours in the case of the argon analysis. After cooling the tube down to room temperature, the weight was recorded and it was inserted with other run parameters (such as # of adsorption points) in the ASAP 2000 program. The full analysis was performed in about 4-6 hours for nitrogen analysis and 22-26 hours for the argon analysis of various zeolites such as ZSM-5, Na-X and Na-Y. The ASAP instruments give reproducible results within a range of ± 7%. [131]

3.6.3 X-Ray Powder Diffraction

3.6.3.1 XRD Analysis of Zeolite samples

All of the samples were pre-heated at 550°C overnight and left in the oven at 120°C before the XRD analysis was performed. A solid reference is scanned to make sure that the instrument is well calibrated. We are looking for the characteristic peak of the silicium to be at the correct 2θ angle. When the desilicated and the reinserted samples were analyzed on a certain day, the parent zeolite heated in the same manner was also analyzed on that same day. This method of analysis insures that any fluctuation in the instrument's precision which sometimes changes from day to day, was taken into account. The samples were ground for a period of 10 minutes and placed into a plexiglass holder. Each sample was scanned in the region of $5° < 2\theta < 60°$ and the counts were recorded automatically at a scan speed of 0.5°/min. and a step size of 0.02°. The peak intensities were taken as the number of counts recorded by digital integration during a complete scan at constant angular velocity. The Relative Crystallinity (RC) of the sample was determined using the following equation:

$$RC\ (\%) = I_0/I\ (100)$$

Where: $I_0 = \sum$ peaks intensity for the sample

$I = \sum$ peaks intensity for the external standard

We used the established method (ASTM), which was to choose the five most intense peaks the XRD pattern of the ZSM-5 zeolite for the analysis in the range of 2θ between 22.5°- 25°. All measurements were done in duplicate and the % error on all measured values was within 5%.

3.6.3.2 XRD Analysis of the Extracted Silicate Species

The liquid filtrate from the desilication step was heated to evaporate the solution. Once this has been achieved a white powder remains on the bottom of the flask which is then heated in a drying oven to 120°C for a period of 24 hours (overnight). We knew that the compound extracted during the desilication process from the silicate family, but we wanted to determine if this compound was orthosilicate, pyrosilicate, a mixture of both or some totally other compound.

We obtained the XRD spectra of the solid sample, in the same way as was described in section 3.6.3.1. Once the spectrum of the product was established, we determined the composition of the compound using the Joint Committee for Powder Diffraction Standards (JCPDS) and the micro powder diffraction search-match of Fein Marquat (μPDSM), they were used for phase identification after the sample was analyzed. The search match software asked us what elements we may have in our compound, and it rejects all the ones we do not have. Then using this information and the diffraction pattern it will give us a series of names of possible compounds with a value indicating the similarity between the diffraction peaks of the compound in the software's database and the solid compound that we had just finished analyzing. We then knew with great certainty, the nature of the compound that was extracted.

3.6.4 Ammonia Temperature Programmed Desorption (TPD)

A 1.0 g of sample extrudates was weighed out and set up in a reactor tube made out of quartz that has an internal diameter of 1.5 cm and 30 cm in length. The sample was heated to 300°C for a period of 3 hours with as a carrier the flow of helium (20ml/min). The next step in the procedure was to drop the temperature to 100°C and stopping the flow of helium. The ammonia was passed through the catalyst bed for a period of 45 minutes at a flow rate of 20ml/min. After this time, the ammonia was switched for helium, while maintaining the temperature at 100°C for a period of 1.5 hours. When this period was over, the connector from the reactor to the Thermal Conductivity Detector (TCD) was installed and we were waiting for the signal on the gas chromatograph (model 5890 from Hewlett Packard) to stabilize.

Once the signal had stabilized itself, the reactor needs to be heated for 6 minutes at 100°C. Then it was ramped from 100°C to 600°C over a period of 20 minutes and then staying constant at this temperature until all the different types of acid sites had desorbed their chemisorbed ammonia.

We could then estimate the ratio of medium/strong acid sites versus the weak. A comparison could be made for the variations in the ratio for the different catalysts that have been treated differently.

3.6.4.1 Determination of the Acid site Density using Ammonia Desorption

A 1.0 g of sample was weighed out and placed in a reactor tube. Nitrogen was allowed to flow at a rate of 20 ml/min through the catalyst sample and it was heated according to a pre-determined program for a period of 4.5 hours to help desorb as much of the water as possible. Then the flow of nitrogen was stopped and ammonia was passed through the sample at the same rate as mentioned above for a period 45 minutes, while the reactor was kept at a constant temperature of 100°C. After this time had elapsed, the ammonia flow was stopped and nitrogen was flowed again through the catalyst while the reactor was maintained at 100°C for a period of 16 hours to remove any of the physisorbed ammonia which might remain. Once the time had elapsed, a volume of 60.0 ml of a known concentration of acid was pipetted to a graduated cylinder and with nitrogen bubbling through the solution, a new temperature program was set up for a period of 7 hours. During this temperature program, the maximum temperature reaches 580°C for a period of at least 5 hours.

In the next step, we stop the heating and nitrogen flow. A few drops of methyl red indicator was added to the solution and the color was yellow (acidic). It was then clear that the solution needs to be titrated with a base (NaOH) until an end-point is reached. Then the concentration of acid sites per gram of catalyst could easily be calculated using the following equations:

$$(1)\quad N_a V_a = N_b V_b$$

where: N_a = Concentration of hydrochloric acid (0.03021N)

V_a = Volume of hydrochloric acid (needs to be determined)

N_b = Concentration of sodium hydroxide base (0.1N)

V_b = Volume of the base titrant read of the buret

$$(2)\quad V_n = V_1 - V_a$$

where: V_n = volume used to determine the number of acid site

V_1 = volume of acid, initially pipetted into the graduated cylinder

V_a = volume of acid determined from equation (1)

$$(3)\quad N_{NH3} = V_n N_a$$

where: N_{NH3} = Concentration of ammonia chemisorbed (mmol/g)

V_n = Volume used to determine the number of acid sites (from equation (2))

N_a = Concentration of the acid (0.03021N)

$$(4)\quad A_C = N_{NH3} / Wt.$$

where: A_C = acid sites concentration per gram of catalyst

N_{NH3} = Concentration of ammonia chemisorbed (mmol)

Wt. = Weight of catalyst used for the acid site concentration (g)

3.6.5 Diffuse Reflectance Infrared Fourier Transform Spectroscopy (DRIFT)

A 2.0 wt.% sample was made from 0.01 g of zeolite and 0.49 g of cesium iodide. They were mixed thoroughly so that the sample would be as homogeneous as possible when it was analyzed by the FTIR. The sample was then dried in the oven at 120°C overnight, to remove as much of the humidity (water) that may have been adsorbed onto the zeolite before the sample was scanned.

Diffuse reflectance infra-red spectroscopy (DRIFTS) was performed with the Bomem MB 155S apparatus. The sample was scanned in the region of 700 to 900 cm^{-1} with a resolution of 8 cm^{-1} at 36 scans/min.

3.6.6 Differential Scanning Calorimetry and Gravimetric Analysis (DSC/TGA)

Differential Scanning analysis of the zeolites was performed on a Universal V3.3BTA instrument interfaced to an Dell computer. The Thermal Gravimetric Analysis was performed on a Q500 V3.1 Universal instrument. The flow rate of the nitrogen carrier gas was 20 ml/min and 7.0000 to 10.0000 mg of catalyst sample were used in each run. The linear heating rate of the system was programmed to 15°C/min. The aluminum crucibles were used for both the sample pans.

In general, the change in weight of a catalyst sample, as recorded in the thermogravimetric analysis curve (TGA), with the increasing temperature was used for the determination of the amount of species incorporated as well as the limit of thermal stability of the zeolite sample.[132]

3.6.7 Constraint Index

This constraint index (CI) test originally developed in the Mobil laboratories has been an extremely useful catalytic test for investigating the relative pore sizes and shape selective properties of acidic zeolites. The test was designed to allow discrimination between pores systems composed of 8-, 10- and 12-ring ports.

In our case, we decided to use this test to try and see if any differences exist between the pore narrowed, the large pore size and all the ZSM-5 zeolites in between that have been tested.

Catalytic runs were performed by injecting an equimolar mixture of n-hexane and 3-methyl pentane, using an injection syringe on an infusion pump into a vaporizer-gas mixer. The vaporized feed was then carried by the carrier gas (nitrogen) through a catalyst bed set in a tubular quartz reactor container, inside a furnace which was thermoregulated. A chromel-alumel thermocouple was placed in the catalyst bed and was used in conjunction with a digital thermometer unit to monitor the reaction temperature. The gaseous mixture flowing out of the reactor ran through a sample lock glass tube and the liquid fell in a collector tube which was heated with a lamp to decrease the production of liquid fractions.

During the reaction, while the liquids were being collected, the gases were analyzed at 20 minutes by gas chromatography using a 30 m long JW alumina column mounted on a FID Mini-3 Shimazu GC apparatus equipped with a HP 3392 A integrator. Liquid fractions were then analyzed using a capillary column (50 m PONA type fused silica coated with cross linked polymer) mounted on a FID HP 5890 gas chromatograph.

The reaction conditions used in the experiments were as follows:

temperature = 120°C; catalyst weight = 1.5 g ; total pressure = 1 atm ;duration= 0.37h; Liquid Hourly Space Velocity (LHSV)= 2.7 h^{-1}

An amount of 1.5 g of catalyst was used with nitrogen as the carrier gas at a flow rate of 11.0 ml/min with the reactor being heated to 120°C. We made an equimolar solution of n-hexane and 2-methyl pentane which was injected in the gas chromatograph containing the same column and in the same condition as in the case of the methanol to gasoline reaction. We determined with precision, the proportion of each component in the equimolar mixture The time of the reaction lasted only 20 minutes because any longer would bring about a deactivation of our catalyst and a very considerable decrease in the % conversion. Two flow rates were taken: the first at 10 minutes and the second just before the injection at 20 minutes. Once the gas sampling was analyzed by the gas chromatograph, the constraint index value was determined by the following equations:

(1) For Hexane : $dC_t/dt = C_t - C_o' / \Delta t$

where the terms are defined as the following:

C_t : concentration of n-hexane for the run (% area)

C_o': Concentration of n-hexane in the equimolar mixture (%area)

Δt: Time of the reaction in minutes

(2) For 2-methyl pentane: $dC_2/dt = C_2 - C_o'' / \Delta t$

where the terms are defined as the following:

C_2: concentration of 2-methyl pentane for the run (% area)

C_o'': Concentration of 2-methyl pentane in the equimolar mixture (%area)

Δt: Time of the reaction in minutes

Bringing together both equations, we get a simplified version for the Constraint Index (CI):

$$CI = C_1 - C_o'' / C_2 - C_o''$$

Chapter 4

Results and Discussion

4.1 Synopsis of Results Obtained During the M.Sc. Work

The pore size engineering project was started in September of 1996. Our main goal was to find a way to decrease the pore size of a MFI type zeolite. We started by taking the sodium form zeolite (Na-ZSM-5), which had a silicon/aluminum ratio (Si/Al) of about 20 and removed a portion of the silicon species (no more than 30%), using a process known as desilication. When this process was used in collaboration with thermal treatment, it was known to increase the pore size of the zeolite sample when compared to the untreated sample. From the desilication step, we evaporated the washing water solution and isolated a solid that was determined by x-ray diffraction (XRD) match scan to be in large proportion sodium orthosilicate and, in smaller amounts, its dimer sodium pyrosilicate. The isolated solid was then be reinserted on the desilicated sample, in a range of proportions from 1wt.% to 5 wt.%, using a technique called dry impregnation. We determined that for the DRS method, an amount of 2.5wt.% of sodium orthosilicate gave the best result for the median pore diameter. The pore size was measured using the B.E.T argon instrument to be 4.9Å reduced from 5.6Å for the desilicated sample. It was also shown that the pore volume, surface and micropore area all remained very similar to the parent (untreated) and the desilicated samples.

Performing x-ray diffraction tests, gave us very strong evidence that the removal of a portion of the silicon species and the reinsertion of a fraction of that same species (sodium orthosilicate), did not change the nature of the ZSM-5 zeolite structure. We concluded this by measuring the percent crystallinity which was determined to be about 85% for both the desilicated and reinserted zeolite materials, compared to the reference parent zeolite.

Silicon (^{29}Si) and aluminum(^{27}Al) Magic Angle Spinning Nuclear Magnetic Resonance (MAS-NMR) spectra were also ran on the desilicated and reinserted species (DRS). The aluminum MAS-NMR proved that desilication did not affect the aluminum sites in any way because if some aluminum was removed the octahedral signal would have increased. We noticed that the octahedral and tetrahedral signals remained the same when compared to the reference.

As for the silicon MAS-NMR, it was clearly determined that the number of aluminum atoms that were around a "central" silicon is one, for both the parent and desilicated samples. The only change was that the process of desilication brought about an increase in the proportion of one aluminum around the central silicon. This could be explained very simply by the fact that desilication removes silicon atoms from silicon rich zeolites. Their proportion in relation to the aluminum atoms has decreased, so the Si/Al ratio decreases.

In the case of the DRS method, we reinserted a much smaller amount of sodium orthosilicate than we initially removed. The reinserted silicate species incorporates initially into the zeolite pores, migrates to the external pore opening using thermal energy and water as a carrier. Using the ^{29}Si MAS-NMR, we determined that the R value (which is defined as the area ratio: Si(1Al)/ Si(0Al)) was close for the parent and the DRS samples.

This means that the actual removal of silicon from the framework during the desilication process did not modify the aluminum tetrahedral sites, while the reinsertion decreased the R value compared to the parent's value.

One of the highlights of the DRS study during my M.Sc. research project was that even though we obtained a decrease in the median pore diameter to 4.9Å, the major drawback was the very low success rate of the pore narrowing, it was close to 20%. This tells us that the physico-chemical process from which originates the pore narrowing is not performed in the most favorable conditions. It is important for any future research on this topic, to take this important point into account and find ways that would give us greater reproducibility.

It was postulated, that any future work on this topic would have to answer or at the very least shed some light on some of the following questions: a) what is the exact mechanism that results in the pore narrowing for the production of the DRS materials, b)what is the precise reaction temperature at which the reaction between the reinserted species and the zeolite occur, c)could pore reduction go even lower than 4.9Å, d) what kind of product shape-selectivity would these reduced pore size catalyst give when used in the methanol to gasoline (MTG) and methanol to olefin (MTO) reactions and, e) how would they perform when used as membrane disks with sepiolite clay as matrix, for the separation of benzene, toluene, xylene mixtures (BTX) and C_7 isomer mixtures.

The direction and the goals were thus set for the research to be conducted during the Ph.D years. The following chapter, will not only lay out the results that have been generated during the past 3 years, but also give the explanation of what they mean and the reasoning behind the work that was accomplished.

4.1.1 Objective of Pore Size Engineering

In this research, the first part was to establish a way starting from the H-ZSM-5 zeolite which has a medium pore size of 5.2Å, to form a sample that has a larger pore size (DS) and one that has a smaller size (DRS). These samples would maintain the same basic structure and characteristics of the ZSM-5 zeolite while differing in their pore opening.

The application of a desilication treatment using a basic medium, promoted the removal some of the structure's silicon and this had the effect of increasing the median pore size to 5.9Å.

Isolating some of the extracted silicon species from the desilication step and then reinserting it back into a sample that had been desilicated and stabilized to high temperature, gave us a decrease of the median pore size to 4.6Å or lower. This is termed DRS for Desilication, Stabilization and Reinsertion.

The second part of this work was to apply catalytic applications such as product shape selectivity in the methanol conversion and molecular sieving effect in the adsorption of the BTX aromatics, to the engineered pore size and H-ZSM-5 zeolites. It was important for us to see what type of products these different pore size zeolites would form when used in the different catalytic applications.

4.2 Desilication

Desilication could be defined as a process where the removal of silicon species from the zeolite's framework occurs. Desilication was an extremely important process in the DRS method. The desilicated zeolites are termed metastable structures because they could undergo some minor structural changes when some heat is applied, in order to stabilize their pore network and get a change of their pore size distribution compared to the pore network of the untreated sample.[133]

In the M.Sc. research, we performed the desilication on the Na-ZSM-5 zeolite with a solution of sodium carbonate and sodium hydroxide (0.8M/0.01M). We knew that this solution extracted silicon from the framework. In other terms, it created small and big holes within the structure. By adding sodium hydroxide to the solution, it would shift the equilibrium in equation (2) to the left which made the solution much more basic. The corrosive action was greater and this has the potential to remove bigger parts of silicon species from the framework which would create much larger holes, that were not wanted. Also such a corrosive action would increase the risk of provoking a collapse of some parts of the ZSM-5 structure.

(1) $Na_2CO_3 + H_2O \rightleftharpoons NaHCO_3 + NaOH$

(2) $NaHCO_3 + H_2O \rightleftharpoons H_2CO_3 + NaOH$

It was important in the desilication process to avoid a decrease of the Si/Al ratio of more than 30% because it had been determined that any greater change will cause an irreversible collapse of the structure and thus be of no use for any type of application. During this procedure, three variables were controlled, they were: 1) temperature of the water bath, 2) initial pH of the solution and 3) the period of time each desilication process lasts.

The pH of the alkaline solution was measured to be 11.8, and this is what promoted the breakage of the-[Si-O-Si]- bonds. The proposed mechanism for the desilication of the ZSM-5 zeolite was seen in figure 4.1. We can notice that the two products which are being extracted during the process are : a) Sodium orthosilicate (Na_4SiO_4) and smaller amounts of its dimer b) Sodium pyrosilicate ($Na_6Si_2O_7$).

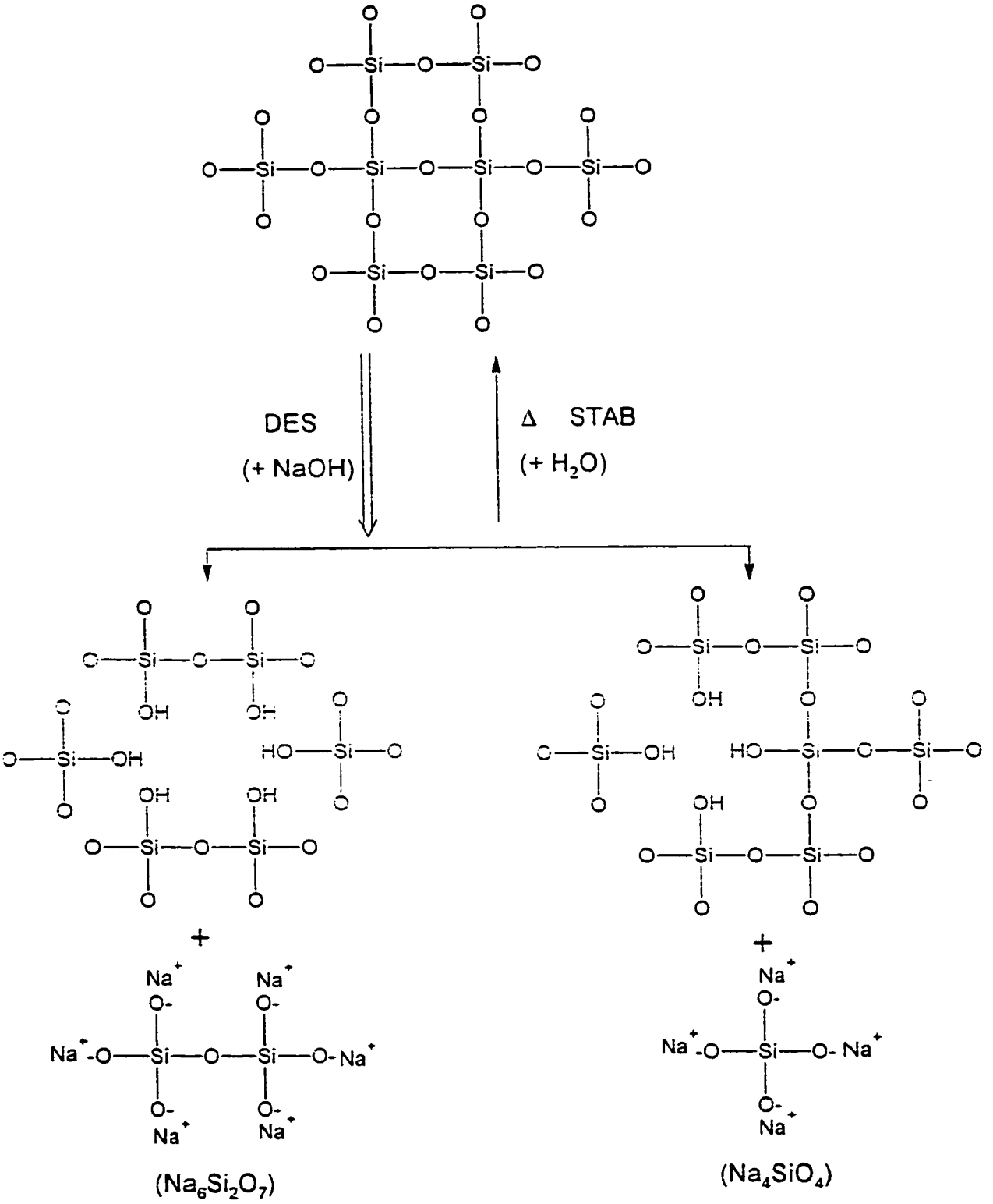

Figure 4.1 Mechanism of the ZSM-5 Desilication

Researchers from the Institute Fur Angewandte Chimie in Germany, had worked on a process that resembles the process of desilication, except that they promoted the removal of aluminum instead of silicon. Their aim was to determine the structural and catalytic effects of a post-synthetic sodium hydroxide treatment on the H-ZSM-5 zeolite. The application of a strongly basic medium on the one hand represents the conditions of zeolite synthesis, but on the other hand, silicates can be dissolved by alkali. This approach consisted of a controlled de- and realumination in order to achieve a catalytic modification by a post-synthetic treatment.[134,135]

The first step which was performed during the Ph.D research, was to determine if using no sodium hydroxide would make our desilication process milder so as to remove a larger quantity of smaller orthosilicate building blocks at the expense of larger pieces such as sodium pyrosilicate. We wanted to determine how using different desilication solutions would change the chemical composition of the treated samples. We also attempted to increase the duration of the desilication process using different periods of time: 4, 8 and 12 hours to see how this would change the results of the zeolite's composition.

We have recorded in the following tables, the chemical composition and textural properties results of the zeolites treated under different conditions. This was used in collaboration with the XRD match scan, to determine what was being removed and the best recipe for the desilication procedure.

Table 4.1 Chemical Composition of the Different Na-DZSM-5 .

Sample	% SiO_2	% Na_2O	% Al_2O_3	Si/Al	Na/Al
NaZSM-5	94.1	2.10	3.80	21.1	0.90
NaDZSM-5 0.8M/0.01M (4 hours)	93.0	2.40	4.60	17.1	0.80
NaDZSM-5 0.8M (4 hours)	93.3	2.80	4.00	20.2	1.20
NaDZSM-5 0.8M (8 hours)	90.3	5.46	4.27	17.9	2.10
NaDZSM-5 0.8M (12 hours)	92.4	2.92	4.70	16.7	1.02
NaDZSM-5 0.6M (4 hours)	92.6	3.63	3.81	20.6	1.57
NaDZSM-5 0.6M (8 hours)	92.3	3.13	4.60	17.0	1.12

In table 4.1, we can see that the parent zeolite that is treated with various desilicating solutions, has a decreased Si/Al ratio. If we compare the parent to the sample treated with 0.8M of sodium carbonate for different periods of time, we can see a clear trend that the longer the desilication period, the lower the Si/Al ratio.

The same trend was determined for the 0.6M sodium carbonate solution. When we used a more corrosive solution containing sodium carbonate and sodium hydroxide

(0.8M/0.01M), these results were very comparable to the results obtained for the sample desilicated with 0.8M sodium carbonate for a period of 8 hours.

In the liquid filtrate of the desilication step, we found the removed silicate species. It was evaporated, and the resulting solid was analyzed for its composition using X-Ray Diffraction (XRD) match scan. The first washing (filtrate #1) for the 0.8N solution of sodium carbonate was found to contain large amounts of sodium orthosilicate and smaller amounts of sodium pyrosilicate. We performed a second and third washing by passing 2.0 liters of warm water over the desilicated ZSM-5.We will refer to them as filtrate #2 and #3. On the XRD match scan results we determined that washings #2 and #3 contained at best very little of orthosilicate. It is known that using only sodium carbonate as a desilicating agent for a period of 4 hours in a water bath heated to 80°C, gave us a better desilication.

The 1st filtrate for the sample desilicated with a 0.6M solution of sodium carbonate, contained a very small amount of sodium orthosilicate. When we washed the sample with 2.0 liters of warm water and collected the 2nd and 3rd filtrates, we determined that they both contained no sodium orthosilicate.

When a solution of sodium carbonate and sodium hydroxide was used, a larger quantity of sodium pyrosilicate and a smaller quantity of sodium orthosilicate was removed in addition to some aluminosilicates. We defined this action was an irregular desilication and not ideal for our DRS process. The fact that some aluminosilicate was being removed was not acceptable because it would render the structure more fragile due to the simultaneous loss of silicate and aluminosilicate species. Even though this was the procedure used for my M.Sc., it was decided that, to improve the rate of success and pore reduction, we would stop using

sodium hydroxide in the desilicating solution.

Table 4.2 Textural Properties for Different ZSM-5 Zeolites Heated at 600°C.

Sample	Total Surface Area (Sq·m/g)	Micropore Area (Sq·m/g)	External Surface Area (Sq·m/g)	Micropore Volume (cc/g)
NaZSM-5	360.1	247.5	112.6	0.100
NaDZSM-5 0.8M/0.01M (4 hours)	388.4	281.6	106.8	0.114
NaDZSM-5 0.8M (4 hours)	338.9	232.7	106.3	0.094
NaDZSM-5 0.8M (8 hours)	373.8	258.2	115.6	0.105
NaDZSM-5 0.8M (12 hours)	396.5	274.1	122.4	0.111
NaDZSM-5 0.6M (4 hours)	461.0	340.1	120.9	0.137
NaDZSM-5 0.6M (8 hours)	443.0	319.0	123.19	0.100

In table 4.2, the textural properties of the desilicated ZSM-5 zeolite with different desilicating solutions, shows very clearly that none of these treatments had destroyed the catalyst. The results of all the treated samples were comparable to one another with no major variations. The results of the 0.8M and 0.6M sodium carbonate solutions for different periods of time, did not change very much, we considered the samples that were desilicated for a period of 4 hours for both sodium carbonate solutions. We thought they were the best compromise for the length of time of the process and the results achieved.

Using the XRD results for the analyzed samples, we were able to determine the Relative Crystallinity (%RC). The samples were found to have values above 85%, when compared to the parent reference sample. This indicates very clearly that the structure was not altered to the point that it would significantly change, when compared to the starting material. Even though the results for textural properties, chemical composition and percent relative crystallinity were very similar for all the samples, we decided to reject the sample desilicated with sodium carbonate and sodium hydroxide because the silicate species extracted was not what we believed would help us achieve the best conditions for a successful DRS process.

The next step in the process was to determine which of the 0.6M or 0.8M sodium carbonate solutions had the best desilication condition to improve and optimize the DRS process.

4.3 Reinsertion of Sodium Orthosilicate onto the Desilicated ZSM-5

Having narrowed it down to two desilication treatments: 1) 0.6M and 2) 0.8M, the next step was to determine which of the desilication solutions would give us optimal results in our DRS process. In past results, 2.5 wt.% of sodium orthosilicate (herein referred to as DRS(2.5%)), was the amount that gave us the greatest pore size reduction to 4.9Å .

In table 4.3, we summarized the results of investigation for desilication with 0.6M and 0.8M, using textural properties of the samples that have had a reinsertion of 2.5 wt.% of sodium orthosilicate applied onto them.

Table 4.3 Textural Properties of DRS (2.5%) for the 0.6M and 0.8M Desilicated Samples all activated to 700°C

Sample	Surface Area (sq·m/g)	Maximum Pore Volume (cc/g)	Median Pore Diameter (Å)
0.6M NaDZSM-5	371.52	0.1155	5.3
0.6MDRS (2.5%)	265.69	0.0832	5.7
0.8M NaDZSM-5	291.19	0.0914	5.3
0.8M DRS (2.5%)	285.81	0.0875	4.9

From the data in table 4.3, we could see very clearly that only a 0.8Mol/L solution of sodium carbonate used for the desilication, produced a pore narrowing to 4.9Å with values for the surface area and maximum pore volume very close between the desilicated and the reinserted samples. For the sample treated with 0.6M of sodium carbonate, the surface area of the DRS (2.5%) has decreased by 28.5%. It is also important to note that the maximum pore volume was smaller by 28.0% while the median pore diameter increased by 0.4Å. Another evidence that the 0.6M solution would not be suitable for our DRS stems from the fact that when we analyzed the extracted species from the 1st washing using the XRD match scan, it contained only a very small amount of sodium orthosilicate when compared to the filtrate of the 0.8M sodium carbonate solution. This gave us a very good indication to understand why pore reduction did not work for the sample desilicated with 0.6 Mol/L of sodium carbonate.

The next step in our procedure was not obvious at the time, but it was a move that totally changed and revolutionized our DRS process including the rate of success. Our goals during the Ph.D work was very simple and driven by the following points: 1) the need to increase the success rate of pore reduction, 2) decreasing the pore size to values below the 4.9Å and 3) understanding the mechanism, and determining the temperature of activation to achieve pore reduction.

In the following step, we based ourselves on the principles elaborated by two great scientists in the field of catalysis. E.F Vansant [136] elaborated a principle that would bring about the reduction of the pore size. This was accomplished by a reaction that promotes

siloxane bond formation. We also based ourselves on Breck's [137] observation, about the importance of silanol groups that react together to give these siloxane bonds that are at the very fabric of pore size reduction. We transposed their general observations onto our project and we decided to perform ion-exchange on the sodium form zeolite. The thinking was that the sodium form of the zeolite and of the orthosilicate, coming together during the reaction may make it very difficult to get siloxane, bonds which give us pore reduction consistently. Using ammonium chloride (5 wt%) we performed ion-exchange on our Na-ZSM-5 to give us NH_4-DZSM-5. We were hoping that this would make the reaction between the silanols and the sodium orthosilicate more favorable and improve the reinsertion process and its success rate.

The sodium orthosilicate is impregnated onto the ammonium form desilicated zeolite. When the sample is activated in a stepwise manner to 700°C, a migration of the sodium orthosilicate towards the pore opening occurs. The silicate species that has migrated, was spread out as a thick layer next to the pore mouth and at this point we had a reaction between the silanol group of the zeolite and the sodium orthosilicate to give a siloxane bond and a reduction of the medium pore size. We believe that this step would facilitate the reaction between the O-H group of the zeolite and the O-Na of the sodium orthosilicate.(see figure 4.2)

On the sample, we decided to reinsert a certain amount of sodium orthosilicate to see how the median pore diameter would vary with the deposition on both of these samples. Four different paths were envisioned to see in what order the heating, the reinsertion and the ion-exchange should be applied to give optimal results. In the following reactions, we are

going to elaborate four different methods and we will analyze their results.

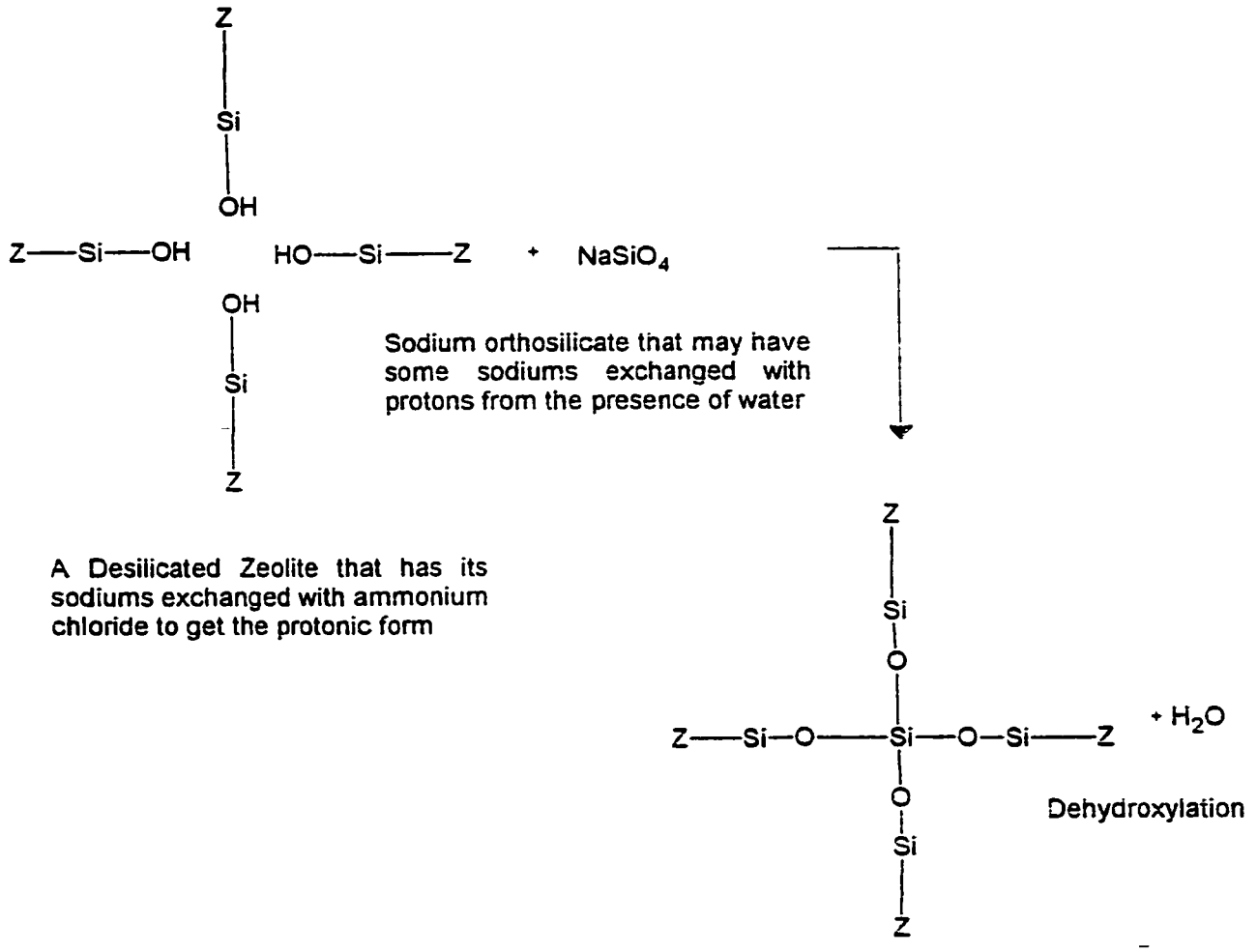

Figure 4.2 The Reaction of the Desilicated ZSM-5 with Sodium Orthosilicate.

Method A

- Do a 5 wt.% ion-exchange using ammonium chloride for a period of 2 hours, repeated three times.
- Heat the ammonium form exchanged sample in a drying oven at 120°C overnight.
- Perform the reinsertion of sodium orthosilicate (DR)
- Heat in a drying oven to 120°C overnight.
- Activate the sample in a stepwise manner to 700°C for a period of 16-18 hours (DRS)

* Comment: In order to see the reactivity of NH_4-DZSM-5 with sodium orthosilicate.

Method B

- Perform a 5 wt.% ion-exchange using ammonium chloride for a period of 2 hours, repeated three times.
- Heat the sample at 600°C for a period of 16 hours.
- Perform the reinsertion of sodium orthosilicate (DR)
- Activate the sample in a stepwise manner to 700°C for a period of 16-18 hours (DRS)

* Comment: In order to see the reactivity of H-DZSM-5 (DS material) with sodium orthosilicate.

Method C

- Heat the sodium form desilicated zeolite to 700°C for a period of 16-18 hours.
- Perform the reinsertion of sodium orthosilicate (DR).
- Perform a 5 wt.% ion-exchange using ammonium chloride for a period of 2 hours, repeated three times.
- Activate the sample in a stepwise manner to 700°C for a period of 16-18 hours (DRS).

* Comment: Na-DZSM-5 loaded with sodium orthosilicate, then ion-exchanged with NH_4^+ and activation.

Method D

- On the sodium form desilicated zeolite, perform the reinsertion of sodium orthosilicate (DR)
- Perform a 5 wt.% ion-exchange using ammonium chloride for a period of 2 hours, repeated three times.
- Activate the sample in a stepwise manner to 700°C for a period of 16-18 hours (DRS).

* Comment: Na-DZSM-5 (without activation) loaded with sodium orthosilicate, then ion-exchanged with NH_4^+ and activation.

Table 4.4 Textural Properties of the DRS Procedure Prepared by Method A.

Sample	Surface Area (sq·m/g)	Maximum Pore Volume (cc/g)	Median Pore Diameter (Å)
0.8M DRS (2.5%)	379	0.12	5.1
0.8M DRS (3.0%)	368	0.12	5.2
0.8M DRS (4.0%)	377	0.12	5.5
0.8M DRS (5.0%)	342	0.12	4.6
0.8M DRS (6.0%)	294	0.09	5.0
0.8M DRS (7.0%)	240	0.08	5.1
0.8M DRS (8.0%)	75	0.02	5.5
0.8M DRS (9.0%)	31	0.01	6.1
0.8MDRS (10.0%)	20	0.00	8.0

In the above table, we performed the DRS technique using the steps from method A. The amounts of sodium orthosilicate were chosen between 2.5 wt.% and 10.0 wt%.We wanted to know how the median pore diameter trend would change with the addition of sodium orthosilicate. Another important aspect was to see how the textural properties would change with each addition. The surface areas were very similar from 2.5 wt% to 7.0 wt.% of sodium orthosilicate. Any additions above 7.0 wt.% of sodium orthosilicate brought about a large decrease in the surface area reaching a minimum value for 10 wt.%. The reason for this is very simple, the addition of excess amounts of sodium orthosilicate tends to fill the pores, preventing the analysis gas from entering and measuring the internal surface area. The values measured are probably of the external surface area which are known to be only a fraction of the internal surface area.

The second column informed us on the maximum pore volume. The trend followed the same trend as the surface area. From 2.5 wt%-5.0 wt%, the value remained about the same. But for 6 wt.% of sodium orthosilicate and more, it had the effect of decreasing the pore volume to a large extent, with the value reaching a minimum for 10 wt.%. This information on the surface area and pore volume measurements clearly show that adding too much sodium orthosilicate may saturate the pores and prevent the analysis gas from penetrating inside of them. We could then conclude that the pore system is closed because of a blockage caused by too much sodium orthosilicate deposition.[138]

For this series, the smallest pore diameter was found to be at 4.6Å for a 5.0 wt.% reinsertion. When a higher portion of reinserted species was added, the median pore diameter increased considerably, reaching 8.0Å for a reinsertion of 10 wt.%. This meant probably a greater proportion of orthosilicate remained at the external surface of the zeolite particle, so that the mean diameter reported corresponded partially to the effect of the externally deposited orthosilicate.

The most important realization that we could take from method A, is the ion-exchange step that exchanges our sodium form zeolite with ammonium chloride to give the protonic form. By using this step, it promoted better conditions for our dehydroxylation reaction which gives the lowest pore reduction, reaching 4.6Å. The success rate of this method was determined to be 80% which is up from the 20% reached during the M.Sc. project. We saw a significant improvement on two fronts: a) the method's success improved from 20% to 80% and b) a further reduction of the median pore size from 4.9Å to 4.6Å. We decided based on these promising results, that the protonic form was probably more active

than the sodium form. This seems to be a very important factor that may be responsible for the better reproducibility of the DRS method, while giving smaller pore sizes.

Table 4.5 Textural Properties of the DRS procedure prepared by Method B.

Sample	Surface Area (sq·m/g)	Maximum Pore Volume (cc/g)	Median Pore Diameter (Å)
0.8M DRS (2.5%)	272	0.09	5.7
0.8M DRS (5.0%)	340	0.11	5.5
0.8M DRS (6.0%)	266	0.09	5.6
0.8M DRS (7.0%)	138	0.04	5.7

In the above table (4.5), we could see the same sort of trend for the decrease of the surface area and maximum pore volume with the addition of various amounts of sodium orthosilicate, up to 6 wt.% reinsertion. If we had continued adding sodium orthosilicate passed 7.0 wt.%, we would have had seen a continued decrease of the surface area and maximum pore volume similar to what was seen in method A. We found for a 5.0 wt% addition using method B, a median pore diameter of 5.5Å. The reason that we did not get good pore size reduction as in method A, lies with the fact that in method B, the second step of the protocol calls for heating the ammonium exchanged zeolite to 600°C before adding the sodium orthosilicate. At this point the structure passed from a metastable state to a thermally more stable state. By adding any amount of orthosilicate species, this will not act on the zeolite's structure to reduce its pore opening. There is very little or even no reaction between the sodium orthosilicate and the zeolite's silanol group, so the median pore size

remains almost the same as in the case of the desilicated zeolite.

Table 4.6 Textural Properties of the DRS procedure prepared by Method C.

Sample	Surface Area (sq·m/g)	Maximum Pore Volume (cc/g)	Median Pore Diameter (Å)
0.8M DRS (2.5%)	319	0.11	5.6
0.8M DRS (5.0%)	395	0.13	5.7
0.8M DRS (6.0%)	267	0.08	5.8

In the above table (4.6), we attempted to see in method C, if heating the desilicated sample to 700°C before the steps of reinsertion and ammonium exchange would give us better results. We did trials for three reinserted weights just to get an idea of the trend of the results that this method would give. The median pore diameter increased slightly with larger additions. It is believed that activating the structure before performing the reinsertion causes the zeolite micropores to enlarge too much and prevent any further modification. This has the effect to make the reaction more difficult between the sodium orthosilicate and the zeolite's silanol groups and would affect the siloxane bond formation causing no pore size reduction. The trend would indicate like in the case of method A and B, that adding more than 6 wt.% sodium orthosilicate would bring a large decrease in both the surface area and micropore volume, while the median pore diameter was larger than 5.8Å.

Table 4.7 Textural Properties of the DRS procedure prepared by Method D.

Sample	Surface Area (sq·m/g)	Maximum Pore Volume (cc/g)	Median Pore Diameter (Å)
0.8M DRS (2.5%)	320	0.12	5.8
0.8M DRS (5.0%)	254	0.08	5.8
0.8M DRS (6.0%)	242	0.07	5.9

The textural property results achieved using method D are as shown in table 4.7. The first step of this method was to perform the reinsertion of the silicate species on the desilicated zeolite. The next step was to perform the ion-exchange using a 5 wt.% solution of ammonium chloride. The results clearly indicate that both the surface area and pore volume decreased with addition of sodium orthosilicate. The median pore diameter remains in the region of 5.8-5.9 Å for the three reinsertions that were performed. We could hypothesize that the reinsertion process in the case of this method does not occur in the same way as for method A. The presence of large pore diameter values would indicate that the reaction between the silanol and the sodium orthosilicate does not happen. The ion-exchange which makes the zeolite's surface more acidic, causes, during the heating to 700°C, an increase of the micropores comparable to what is seen when a non-reinserted desilicated zeolite is ion-exchanged and then heated stepwise to a high temperature (700°C).

To summarize on the results of these four methods, method A seemed to be the most efficient method because the order of the steps help the sodium orthosilicate species react with the zeolite's silanols at the pore opening. This gave us a "considerable" pore reduction, when compared to the desilicated zeolite in the protonic form. Changing the order of just one

of these steps prevents pore reduction from occurring. This shows very clearly that for this technique to be effective, the ion-exchange with ammonium chloride needs to be done before the reinsertion of sodium orthosilicate. The last step required for pore size reduction to occur is the heating to 700°C. The energy was necessary for : a) the migration of the sodium orthosilicate from inside the pores to the pore opening and b) for the formation of the siloxane bonds. All the steps in method A are required but an even more important condition is that the order of these steps needs to be respected.

4.3.1 Chemical Composition of three Zeolite Materials studied in this Section

In table 4.8, we established the chemical composition of various zeolites that were studied in section 4.3. They included: Na-ZSM-5 (parent), Na-DZSM-5(1)(4 hour desilication), Na-DZSM-5(3) (12 hour desilication), H-ZSM-5, H-DZSM-5(3) (12 hours) and DRS (5 wt.%). All of these samples were treated as prescribed in the experimental section. They were analyzed by atomic absorption spectrometry to determine the concentrations of aluminum (Al_2O_3) , sodium (Na_2O) and by deduction the amount of silica (SiO_2). This technique was further discussed in the appendix section of this thesis.

Table 4.8 Chemical Composition of Various Zeolite Materials Studied

Sample	Activation Temp. (°C)	Si/Al atom ratio	Na_2O content (wt.%)
Na-ZSM-5	700	21.1	2.1
Na-DZSM-5 (1)	700	20.0	2.6
Na-DZSM-5 (3)	700	14.7	3.6
H-ZSM-5	600	19.5	0.9
H-DZSM-5 (1)	700	18.3	0.5
H-DZSM-5(3)	700	13.5	0.5
DRS (5wt.%)	700	18.9	0.6

In the above table, we can see that desilicating the parent Na-ZSM-5 that has a Si/Al ratio of 21.1, will decrease the Si/Al ratio of the desilicated Na-DZSM-5 that is formed. The longer the desilication time, the lower goes the Si/Al ratio. The sample that was desilicated for 4 hours had a Si/Al of 20.0, while the one that spent 12 hours in the basic medium, had a much lower Si/Al ratio at 14.4. From this, we can conclude that the longer the contact between the zeolite and the desilication solution, the lower the Si/Al ratio will reach.

These sodium carbonate treatments will have the effect to increase the sodium oxide content because some of the sodium may remain stuck within the structure. Therefore a contact between the desilicating solution and the solid, as in the case of the Na-DZSM-5 (12 hours), will create an increase of Na_2O that reaches 3.6 wt.% compared to 2.6 wt.% measured for the Na-DZSM-5 (4 hours).

We compared the effects of the ion-exchange (5 wt.%) with ammonium chloride on the parent and both of the desilicated samples to see how their Si/Al ratios would vary. The Si/Al ratios of the protonic form, was found to be slightly lower, when compared to the sodium form. We noticed that the sodium oxide content decreases considerably by the action of ion-exchange. This is normal because all the exchangeable sodium is being replaced.

The DRS procedure produces samples that have had desilication for a period of four hours and then an ion-exchange treatment for a total of 6 hours. For this sample, the Si/Al ratio was found to be 18.9 slightly below the 18.3 which was determined for the H-DZSM-5 (1) sample. The fact that the sample is ion-exchanged, causes a decrease of the sodium oxide content to very low levels.

Using the values from table 4.8, we were able to quantify the effect of the process of desilication to different samples and their alterations. This allowed us to understand the changes related to this treatment for all the important Si/Al ratio as well as the sodium oxide content. Desilication results in the occlusion of some Na_2O which is not ion-exchangeable unlike the original sodium sites of the zeolite.[139]

4.3.2 Textural Properties of Zeolite Materials studied in this Section

Table 4.9, shows the results that we obtained using the argon B.E.T. instrument. This method is explained in more detail in the appendix section of this thesis. This characterization instrument helped us determine the surface and micropore areas as well as the median pore diameter. It is important to note how these textural properties changed with the various treatments applied.

Table 4.9 Textural and Pore Characteristics of ZSM-5 Samples

Sample	Activation Temperature (°C)	Total surface area (m^2/g)	Micropore area (m^2/g)	Median Pore diameter (Å)
Na-ZSM-5	700	343	227	5.3
Na-DZSM-5 (1)	700	338	244	5.2
Na-DZSM-5 (3)	700	304	211	5.6
H-ZSM-5	600	423	261	5.2
H-DZSM-5 (3)	600	431	216	5.9
DRS (5wt.%)	700	368	220	4.6

Comparing the surface and micropore areas of the parent and desilicated ZSM-5 zeolites, we can clearly see that the desilicating action on the sodium form ZSM-5 zeolite has the effect of decreasing slightly the surface area compared to the parent sample. Desilication removes some of the silicate species, which creates some holes and this action is what reduces some of the micropore area from the protonic form of the desilicated ZSM-5, when compared to the parent (H-ZSM-5).

The median pore diameter of the sodium sample, desilicated for 12 hours, was the largest at 5.6Å compared to 5.2Å for the sample desilicated for only 4 hours.

Comparing the ion-exchanged samples, we could see that the surface area of the parent and the one of the desilicated sample are very close. The micropore area of the parent was greater than that for the desilicated sample. This may be explained by the fact that heating and desilicating a protonic form zeolite would decrease the micropore area. At the same time, it will increase its median pore diameter, by the greater corrosive action of an H-form zeolite which is heated to higher temperatures. The median pore diameter of the desilicated zeolite increases by a value of 0.7Å, when compared to the parent in the protonic form.

The DRS sample had a lower surface area than the H-ZSM-5 or the desilicated form. This indicated that the desilication and the reinsertion have had some effect on its value. By comparing the H-DZSM-5 and the DRS, the only difference is the extra reinsertion step in the latter sample. It is believed that this step is responsible for the large surface area decrease. Comparing both of their micropore areas, we could see that not much difference exists. The major change comes from the median pore diameter of the DRS, which lies at 4.6Å, while the H-DZSM-5 has a value of 5.9Å because it was desilicated for a longer period of time, 12 hours. The reinsertion of a small amount of sodium orthosilicate back into the structure is responsible for the considerable decrease in the medium pore size.

To summarize these results, we are now able to create two samples in opposite directions of the pore size scale. If we need a zeolite that has the ZSM-5 characteristics but demands a larger pore size than the 5.5Å usually found, it would be possible to perform a 12 hour desilication and an ion-exchange to get a median pore size of 5.9Å. While if the

catalyst is used for an application that requires a smaller pore size in the region of 4.6Å, then we just need to perform the DRS procedure for the reinsertion of 5 wt.% of sodium orthosilicate. The difference between these two extremes is fairly considerable at 1.3Å. This could play a major role in shape-selective reactions such as in the case of the MTG/MTO reactions or in the case of the molecule sieving process where membrane disks are made from one part zeolite and one part sepiolite matrix.

4.3.3 Acid Density

Table 4.10 Concentration and Strength of Acid Sites for Different ZSM-5 Zeolites

ZSM-5 Sample	Concentration of Acid Sites (mmol/g)	Ratio of (Strong + Medium) to Weak
Na-ZSM-5 (parent)	0	N/A
H-ZSM-5	1.10	1.25
H-DZSM-5	1.07	0.64
DRS (5 wt.%)	1.09	0.72

It was not possible to differentiate between Lewis and Bronsted acid sites when using ammonia as the probe molecule when determining the acid site density. This characterization technique like all others is explained in the appendix section at the end of the thesis.

We determined the order of the acid sites concentration to be the following:

HZ>DRS>H-DZSM-5>Na-ZSM-5

The results in table 4.10 indicate that the sum of the weak, medium and strong acid sites for three of the four samples are almost identical. As expected, the DRS lies between the H-ZSM-5 and the value of the H-DZSM-5, and the sodium form ZSM-5 does not possess any acid sites.

Comparing the H-ZSM-5 with the H-DZSM-5 which was obtained by a quite extensive desilication operation, we could see that it contains almost the same amount of acid sites per gram of catalyst as the H-ZSM-5. However the strength of these acid sites,

investigated by solid state proton NMR, is significantly lower than the parent zeolite.[140]

The DRS sample has undergone two sequential operations: i) very mild desilication and ii) controlled reinsertion of silicate. In practice, this resulted in a same acid site density and slightly weaker acid sites when compared to the parent zeolite, H-ZSM-5.[141]

As for the proportion of strong and medium strength acid sites versus the weak, the table 4.10 clearly shows that the parent ZSM-5 has the largest ratio compared to the desilicated or the DRS sample. It is what we expected because the latter two samples have had desilication applied to them, so the removing silicon will have the effect of decreasing the medium and strong acid sites. The DRS procedure has the effect to putting back some silicon within the framework, so this will slightly increase the ratio but it will still be weaker than the parent sample.

4.3.4 Fourier Transform Infra-Red Spectroscopy

This technique can help us understand the reaction of the sodium orthosilicate and the silanol. As we mentioned earlier, this reaction gives us a siloxane bond. It is characterized by a well-defined band in the region of 850-910 cm^{-1}.

This band will increase, when a greater number of siloxane bonds are being formed as in the case of the DRS sample.

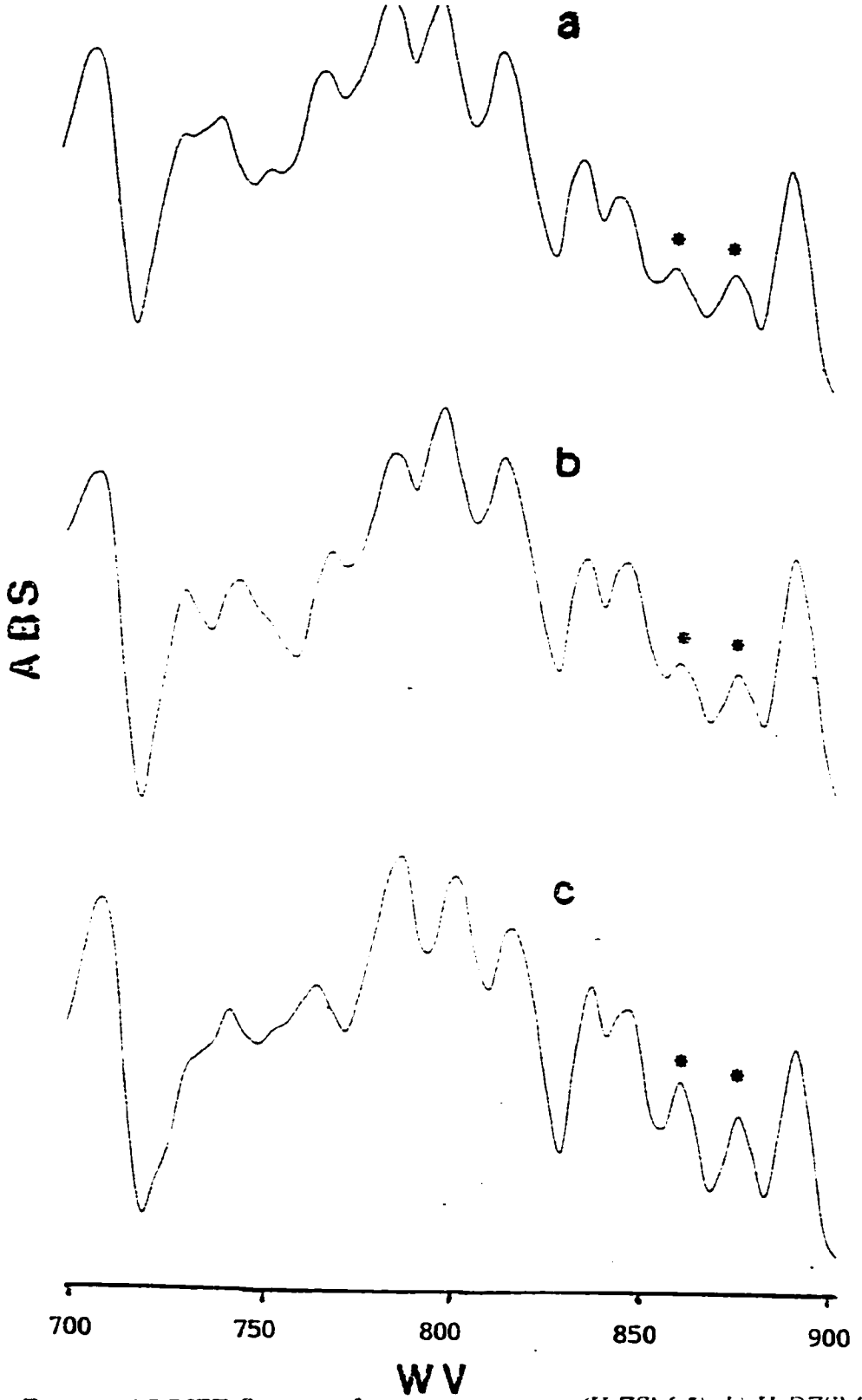

Figure 4.3 DRIFT *Spectra of : a) parent zeolite (H-ZSM-5), b) H-DZSM-5 and c) DRS(5 wt.%)Conditions were the following: resolution of 8 cm-1, 36 scans/min, 64 scans.*

The parent zeolite, H-ZSM-5 and the desilicated H-DZSM-5, exhibited two relatively weak bands in this region. This is understandable because the H-DZSM-5 which lost some silicon atoms during the desilication phase, experienced some healing with formation of some new surface siloxane bonds. However, the newly formed siloxanes were not numerous enough to give significantly different FT-IR bands when compared to the parent zeolite, H-ZSM-5. The DRS sample showed instead, two significantly stronger bands as shown in figure 4.3, thus indicating that the orthosilicate species incorporated had actually formed new siloxane bonds by reaction with the silanol groups of the zeolite surface during the activation (stabilization) phase, as previously hypothesized [142,143,144] However, since the newly formed siloxane groups were mainly located in the region of the pore mouth of the DRS sample, there was a pore narrowing owing to these anchored groups.

4.4 Steps Involved in the DRS Method

Pore size reduction occurs via four successive sets of events as shown in table 4.3. Individually each step, in a specific order, is crucial to the elaboration of a successful pore reduction process. The first event involves the incorporation of the orthosilicate species into the ammonium-desilicated zeolite being done at room temperature. The next step is the heating from the room temperature to the reaction temperature (T_r). This results in the migration of the orthosilicate species and water to the pore mouth as well as the decomposition of ammonium ions (550°C) yielding silanol groups (acidic) of the zeolite, as also observed by other researchers.[145] There would be a slow migration of the sodium orthosilicate species, that is deposited on the internal surface of the zeolite.This migration would be driven by the evacuation of adsorbed water which moves towards the pore mouths under the effect of the high activation temperature. The great solubility in water of the orthosilicate species is of great help to its migration from inside the pore towards the pore mouth. This results in having the internal surface area of the DRS material not significantly different from those of the desilicated zeolite (Na-DZSM-5) used as primary precursor.

The last events, involve the reaction of the orthosilicate species with the zeolite silanol groups in accordance with the reaction mechanism proposed in one of our previous papers.[146] It requires the recombination of surface silanol groups of high surface area silicas at elevated temperature.

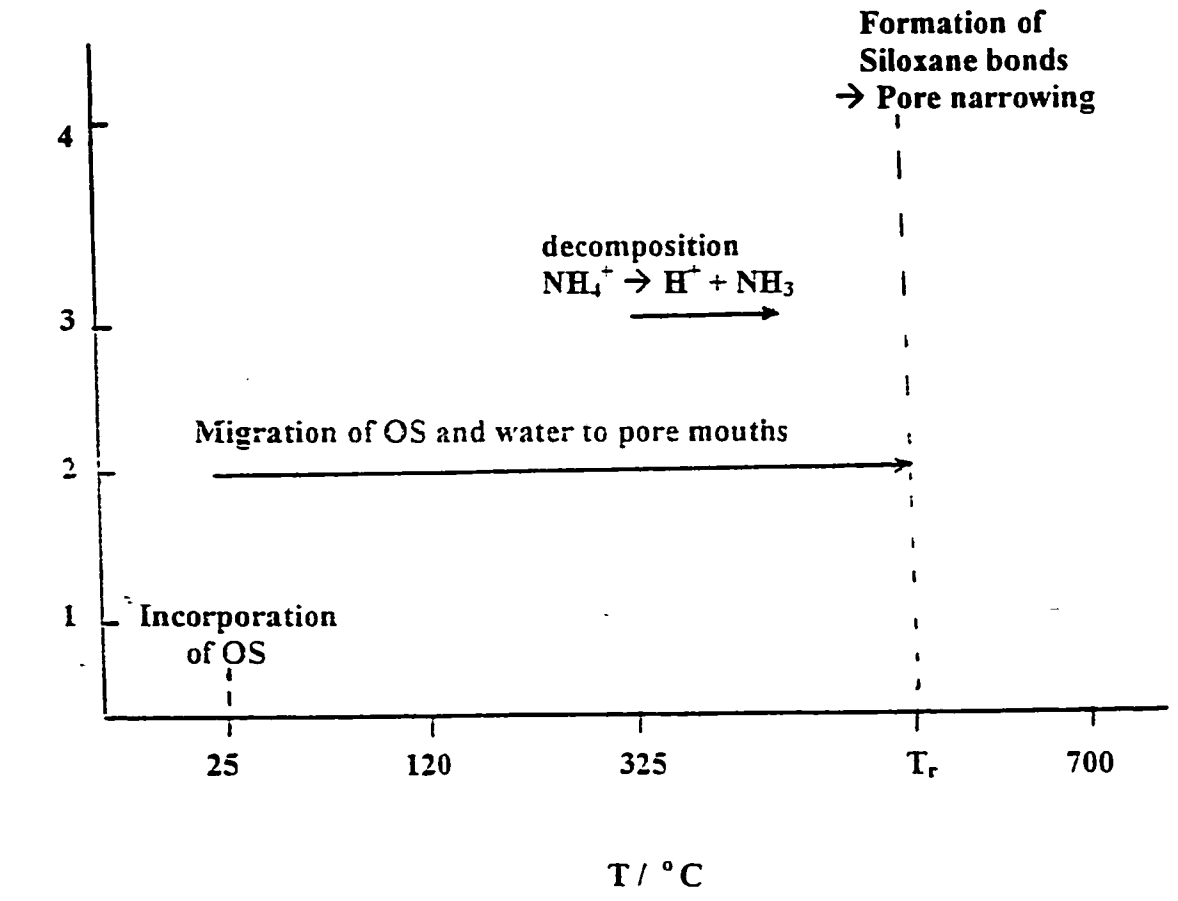

Figure 4.4 Suggested sequence of events occurring with the DRS method

(OS: orthosilicate species, T: temperature of activation)

4.5 Catalytic Applications of the Zeolites Pore Engineered with Sodium Orthosilicate

The objective of zeolite pore size engineering, is to get larger or narrower pore sizes compared to the parent zeolite and using the resulting zeolites for different industrial applications, and seeing how the product selectivity varies..

The first application was the methanol to gasoline (MTG) or methanol to olefin (MTO) reaction. Using this catalytic reaction, we could test for the product shape selectivity that was achieved using a smaller pore zeolite 4.6Å. For comparison purposes, we used the parent zeolite that had a medium pore size (parent) of 5.2 Å and the desilicated sample that had the largest pore size at 5.9Å.

The second application was to assess the sieving effect of these same three zeolites (DRS (narrower), parent and DS (larger) pore size) with respect to benzene, toluene and the three xylene isomers (BTX aromatics).[145]

4.5.1 Product Shape Selectivity in the Methanol Conversion

In the following table, is the distribution of olefins and product aromatics in the MTG reaction for three catalysts of different pore sizes. The one with the medium pore size is H-ZSM-5 (HZ), the one with largest pore size is H-DZSM-5 (HDZ) and the one with the smallest pore size is DRS. The temperature was varied between 375°C and 475°C to follow how the change in pore size and acidity would vary the selectivity of the olefins and aromatics.

Table 4.11 Distribution of Product Aromatics in the MTG Reaction

Selectivity (Catom %)				Distribution of product aromatics (Catom%)					
Zeolite	Rxn. Temp. (°C)	C_2-C_4 Olefins	Arom.	Benz.	Toluene	m-&p-Xylene	o-Xylene	C_9	C_{10}^+
HZ	375	2.10	3.49	2.23	14.6	83.1	0	0	0
HDZ	375	0.10	0.1	100	0	0	0	0	0
DRS	375	0	0.4	27.1	72.9	0	0	0	0
HZ	400	14.9	51.6	33.7	21.1	0	0	43	2
HDZ	400	4.30	0.2	93	7	0	0	0	0
DRS	400	0.02	5.8	100	0	0	0	0	0
HZ	425	17.7	41.9	21.9	0.91	0	31.5	41	5
HDZ	425	5.78	6.6	31.4	4.27	0	25.3	39	0
DRS	425	0.01	4.12	100	0	0	0	0	0
HZ	450	27.7	25.1	34.7	1.31	0	29.6	32	3
HDZ	450	19.8	8.03	1.87	2.86	28.6	0	53	14
DRS	450	0.07	5.19	99.2	0.76	0	0	0	0
HZ	475	23.6	14.1	0.64	22.9	35.1	0	39	3
HDZ	475	25.7	11.4	1.76	8.19	48.8	4.4	32	5
DRS	475	28.9	13.6	5.87	0.95	60.1	0	33	0

Table 4.11 shows the influence of shape selectivity in the MTG reactions for the aromatic product distribution and particularly in the production of C_9-C_{10} alkylaromatic fraction, since normally ZSM-5 zeolite does not produce any C_{10}^+ hydrocarbons.[147] Although the C_9 that are produced, are mostly the thermodynamically favored 1,3,5-trimethylbenzene, some 1,2,4-trimethylbenzene is also produced at lower temperature because of its smaller size. However, at 450°C, thermodynamics prevails so that 1,3,5- trimethylbenzene is produced.

It is worth noting that with the parent HZ zeolite catalyst, the aromatic selectivity goes through a maximum at 400°C. At that temperature, some C_{10}^+ aromatics are found in the product spectrum because they are formed on the unselective external surfaces of the zeolite particles. At higher reaction temperatures, the decreasing aromatic production corresponds to the increasing formation of light olefins, the later being thermodynamically more stable.

The HDZ sample, obtained by a quite extensive desilication operation, contains almost the same number of acid sites per gram of catalyst, when compared to the parent HZ zeolite as seen in table 4.10. However the strength of these acid sites, investigated by solid state proton NMR is significantly lower than in the case of the parent.[148] This is likely the cause of extremely low production of aromatics at low reaction temperatures (375°C-400°C) whose formation is associated with strong acid sites. However, at 450°C, the production of aromatics of the HDZ is almost equal to that of the parent. With the HDZ a very significant amount of C_{10}^+aromatics is produced, whereas only a trace amount of these very bulky alkylaromatics, is detected using the HZ zeolite.

This suggests that the pore size of the HDZ is significantly larger than that of the parent zeolite.The DRS sample has undergone two sequential operations (very mild desilication and controlled reinsertion of silicate) which in practice resulted in the same acid site density (table 4.10) and a slightly lower acid strength ratio, when compared to the parent zeolite.[149] Therefore, at lower reaction temperatures, the production of aromatics of the DRS sample is significantly lower than that of the HZ sample. However, at all the reaction temperatures investigated, the DRS sample produces less bulky alkylaromatics, even at 475°C at which the selectivities to aromatics are almost equal to each other. This unusual behavior of the DRS may be ascribed to a smaller pore size which prevents the formation and/or the outward diffusion of the bulky products. On the other hand, at higher reaction temperatures at which product light olefins are thermodynamically favored, the production of these olefins by the DRS is significantly higher than for the parent. Thus, these significant changes of selectivity in light olefins may be ascribed to the pore narrowing upon the DRS treatment. One of the most surprising catalytic properties of the DRS sample is that between 375-450°C, there are almost no light olefins produced while the aromatics yield is quite significant.[150]

Table 4.12 Production of Light Olefins at Higher Reaction Temperatures

Selectivity (Catom %)				Distribution of product olefins (Catom%)		
Zeolite	Rxn. Temp. (°C)	C_2-C_4 Olefins	Arom.	Ethyl.	Propyl.	Butenes
HZ	475	23.6	14.1	16.0	45.2	33.9
	500	29.4	11.4	13.4	42.6	44.0
	525	33.5	8.2	16.8	49.2	34.1
	550	40.9	13.2	16.1	43.7	40.2
DRS	475	28.9	13.6	14.0	51.5	34.5
	500	36.8	9.9	10.4	48.8	40.8
	525	47.6	14.9	11.1	53.9	35.0
	550	49.3	11.0	14.0	57.6	28.4

The above table (4.12), indicates that at higher reaction temperatures product light olefins are thermodynamically favored. The production of these olefins by the DRS zeolite is greater than in the case of HZ, with a marked preference for the propylene. Thus, these significant changes of selectivity in light olefins may be due to the pore narrowing upon the DRS treatment. Nevertheless, the selectivity to light olefins obtained with the HZ and the

DRS are much lower than another type of zeolite SAPO-34, probably because of the stronger acidity of the ZSM-5 zeolite.

For both catalysts studied in table 4.12, we could see that the aromatic production at temperatures of (475°C-550°C) does not vary very much. It reaches a maximum of 14.9% for the DRS sample 525°C. The parent HZ catalyst for a temperature of 475°C, reaches a maximum aromatic production of 14.1%. The parent sample possesses stronger acid sites than for the DRS, which could explain why a larger amount of aromatics are produced at 475°C compared to the DRS sample at the same temperature.

Table 4.13 Production of Liquid Hydrocarbons at Various Reaction Temperatures

Reaction Temp. (°C)	Sample	Yield (wt.%)		Liquid hydrocarbon	
		C_5^+ aliph.	Aromatics	Yield (wt.%)	Aromatics content (wt.%)
375	HZ	94.0	3.5	99.5	3.6
	DRS	99.0	0.4	99.6	0.4
400	HZ	36.7	51.6	41.6	58.4
	DRS	94.2	5.8	94.2	5.8
425	HZ	40.4	40.4	50	50.0
	DRS	95.9	4.1	95.9	4.1
450	HZ	47.2	25.1	65.3	34.7
	DRS	94.7	5.2	94.8	5.2
475	HZ	62.3	14.1	81.5	18.5
	DRS	57.5	13.6	80.9	19.1

The results from table 4.13, indicate that an unusually large quantity of aliphatic C_5 and C_6 hydrocarbons are produced over a quite broad temperature range for the DRS catalyst. This suggests that the joint effect of the narrower pore system of the DRS sample and a slightly lower acid site strength, results in a compression of the product spectrum to the region of C_5-C_6 liquid hydrocarbons. Interestingly, the DRS catalyst yields between 375° and 450°C almost 100 wt.% of liquid hydrocarbons with a small amount of aromatics mostly benzene as shown in table 4.11. This may constitute a more environmentally friendly alternative to the aromatic-rich gasoline obtained with the traditional MTG process. Another

characteristic of the DRS is that the induction period (reaction time needed to reach the steady state) is extremely long (65 minutes at least) in comparison with that of the parent zeolite (a few minutes). This is, perhaps, experimental evidence of the formation of narrower pore system in the DRS sample, in which bulky product molecules are subjected to some diffusion constraints, thus negatively affecting the desorption of all the reaction products.

4.5.2 Molecular Sieving Effect in the Adsorption of the BTX Aromatics

We decided to make sepiolite/zeolite disks, with the objective to study and assess the sieving effect of the zeolite materials, with respect to the BTX aromatics (benzene, toluene, and the three isomers of xylene).

The following table (4.14) is used as source of reference for the boiling points, critical diameter and kinetic diameter of the BTX and the C_9 aromatics.

Table 4.14 Molecular Characteristics of the BTX Aromatics[150]

Aromatics	Boiling Point. (°C)	Critical Diameter r (nm)	Kinetic diameter σ ($r_{min.}=2^{1/6}\sigma$) (nm)
Benzene	80.1	0.66	0.58
Toluene	110.6	0.66	0.58
p-Xylene	138.3	0.66	0.58
m-Xylene	139.1	0.71	0.63
o-Xylene	144	0.74	0.63
1,2,3-TMB	176.1	0.78	0.69
1,2,4-TMB	169.3	0.75	0.67
1,3,5-TMB	164.7	0.84	0.75

In order to correlate the crystallographic aperture or pore size of a zeolite with the dimensional parameters of various adsorbate molecules, there must be the establishment of a scale of molecular dimension (critical diameter) as shown in the above table. In early experiments, the molecular size was based upon the equilibrium diameter of the adsorbate

molecule. [151,152]

This was obtained by a calculation using the known molecular shape, bond distances, bond angles, and the Van der Waals radii. [153] This approach was not very satisfactory since it was observed that certain molecules were freely adsorbed but were larger than the known aperture size of the zeolite crystal. In an improved treatment of this problem, Kington and Macleod decided to use the collision or kinetic diameter.[154]

The kinetic diameter or sometimes known as the collision diameter, is defined as the diameter of the cylinder which can circumscribe the molecule in its most favorable equilibrium conformation, the smallest distance between two molecules.[155]

Table 4.15 Adsorption Tests with BTX aromatics at 150°C

(Molecular Sieving Effect)

Zeolite	Adsorbate	Peak I (% area) (non-adsorption)	Peak II (% area) (Adsorption)
HDZ Pore Size = 5.9Å	Benzene	0	100
	Toluene	0	100
	p-xylene	0	100
	m-xylene	0	100
	o-xylene	0	100
HZ Pore Size = 5.2Å	Benzene	0	100
	Toluene	0	100
	p-xylene	0	100
	m-xylene	14	86
	o-xylene	10	90
DRS Pore Size = 4.6Å	Benzene	0	100
	Toluene	0	100
	p-xylene	0	100
	m-xylene	92	8
	o-xylene	89	11

Essentially, table 4.15 shows that with the parent ZSM-5 zeolite (HZ) and at a temperature of 150°C, adsorbates such as benzene, toluene and p-xylene were totally adsorbed while the bulkier meta- and ortho- xylenes were almost all adsorbed. With the desilicated (HDZ) sample which had a larger pore size, there was a complete adsorption of

these BTX aromatics.

The DRS sample, however, rejected almost totally the bulky meta- and ortho- xylenes, showing that there was a strong molecular sieving effect by the narrower DRS micropores. The results also show that the pore enlargement or narrowing resulting from the DS or the DRS treatment, is a three-dimensional process. In fact, the latter did not yield any slit-shaped pores which, otherwise, would adversely affect the adsorption of smaller molecules by the DRS sample.

It is known that in petroleum refineries, components of C_8 aromatics cuts are currently separated by distillation (o-xylene and ethylbenzene) and by crystallization or adsorption (p-xylene).[156] For meta- and para-xylenes separation, the DRS sample appears to be more efficient than the parent zeolite, HZ, under our testing condition.

4.6 Reinsertion of Orthosilicic Acid on the Desilicated ZSM-5

The orthosilicic acid was formed using the ion-exchange capability of the amberlyst resin, for exchange of its proton for the zeolites sodium ion. We knew from our results and the ones published by other researchers such as Mirth and Lercher [157], that pore reduction would occur because of the reaction between the silanol of the zeolite and the silanol of the reinserted species. This would give siloxane bonds that are responsible for pore size reduction. In the previous section, we explained how we exchanged the zeolite's sodium for a proton using ammonium chloride. So the zeolite's silanol helps trap the sodium by exchange with the proton and the siloxane bond is formed. This has the effect of forming the siloxane bond with more ease and to increase the success of the pore reduction process.

At this point, we hypothesized that if we were able to change the sodium ion in the sodium orthosilicate for a proton, this would give us orthosilicic acid. Reinserting this species, we should see a better rate of success for pore narrowing. The steps of reinsertion and stabilization are the same as mentioned in section 4.5. The result is that the medium pore size decreases to 4.6Å.

The resin used is called Amberlyst 15 ion-exchange resin and it is produced by Rohm and Hass. This resin is known to be very acidic, so there was no problem exchanging the sodium from the sodium orthosilicate for protons. We know that the sodium orthosilicate has four sodium atoms around the central silicon atom. The first question that comes to mind is how many sodiums would be exchanged with this procedure? We decided to try and answer this question by performing atomic absorption spectroscopy on the dissolved sodium orthosilicate solution to determine the sodium content. We performed the same test for the

orthosilicic acid solution exiting the column. The analysis indicated that the orthosilicic acid had two times less sodium than the sodium orthosilicate. From this result, we established that two out of the four sodium atoms were exchanged when passed through the resin.

We decided to investigate the textural properties of the ZSM-5 zeolites. For data in table 4.16, the DRS method was applied, using different amounts of orthosilicic acid which was made from the sodium orthosilicate passing through the amberlyst column.

4.16 Textural Properties of Various DRS Samples with Varying Amounts of Orthosilicic Acid

Sample	Total surface area (m^2/g)	Maximum Pore Volume (cc/g)	Median Pore diameter (Å)
DRS (2.5 wt.%)	253	0.13	5.6
DRS (5.0 wt.%)	284	0.13	5.4
DRS (6.0 wt.%)	301	0.13	4.8
DRS (7.0 wt.%)	288	0.12	5.0
DRS (8.0 wt.%)	336	0.12	4.4
DRS (9.0 wt.%)	296	0.13	5.2
DRS (10 wt.%)	286	0.12	5.5
DRS (11 wt.%)	266	0.12	5.4

The results found in table 4.16 indicate very clearly that the surface area and the pore volume did not vary very much for samples that had reinsertion of different amounts of orthosilicic acid. The most important change that was noticed, is in the median pore diameter.

At 2.5 wt.% reinsertion the pore size is at a maximum value (5.6Å). Addition of more orthosilicic acid decreases the pore size to a minimum value of 4.4 Å at 8.0 wt.% reinsertion. Adding more than 8.0 wt.% shows a trend that is increasing to another maximum value at about 5.5Å for 10 wt.%.

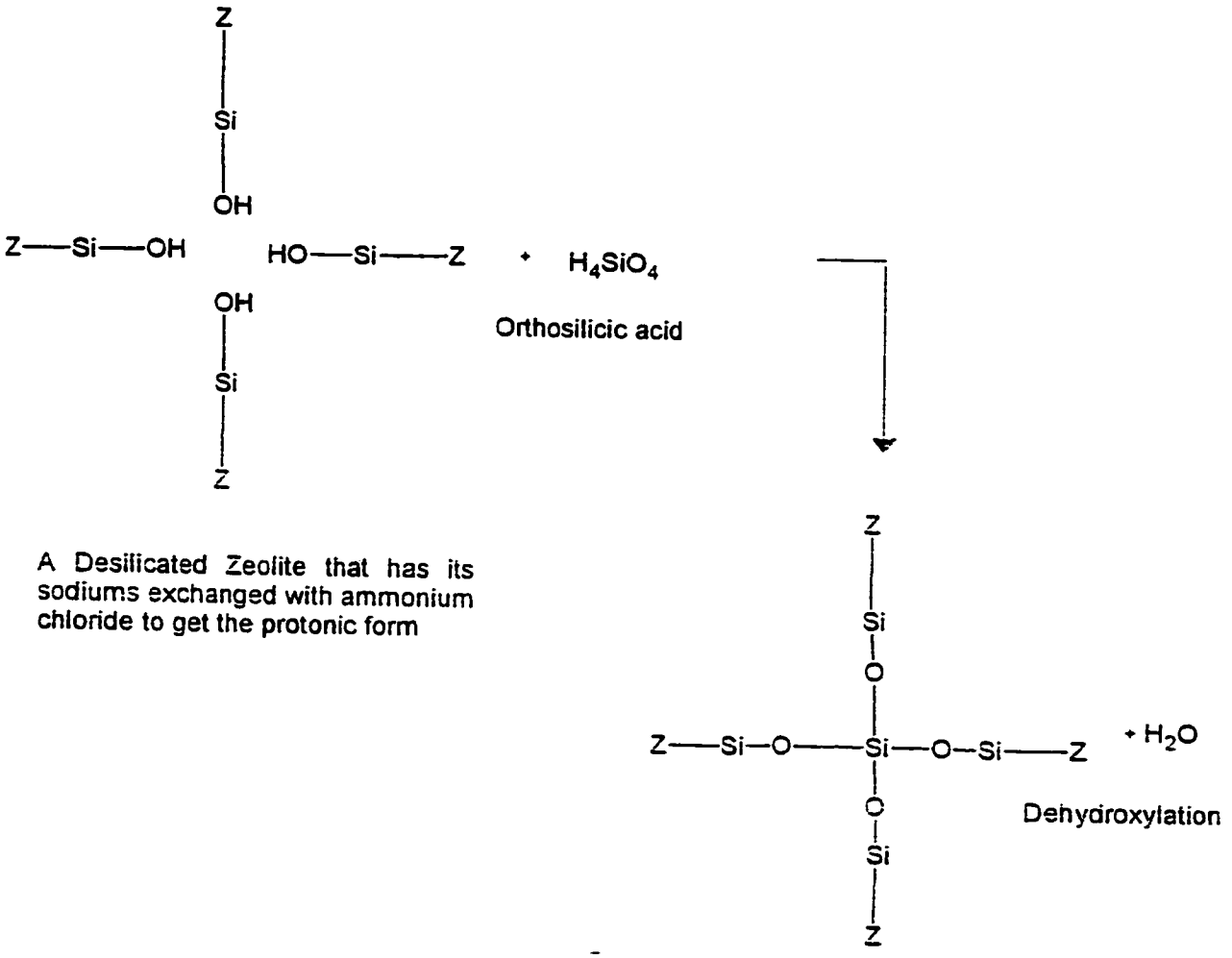

Figure 4.5 The Reaction of the Desilicated ZSM-5 with Orthosilicic acid.

It is our belief that the zeolite's silanol groups react with the orthosilicic acid to give a dehydroxylation which is favored by the silanol groups in the orthosilicic acid and on the zeolite surface.

Promoting ion-exchange of the zeolite with ammonium chloride helps keep the pH below 3 and avoids the dissociation of the zeolite's proton. We believe that the reinsertion process was much easier because the silanol groups of the zeolite are fully protonated and they react together with the partially ion-exchanged orthosilicate species to give siloxane bonds. We were able to reinsert a larger portion of sodium orthosilicate 5.0 wt.% which gave a median pore diameter of 4.6 Å.

Using a protonic zeolite helps maintain the pH below 3 Partial exchange of the sodiums on the sodium orthosilicate gives silanols that favor the formation of siloxane bonds more than what we have previously seen. The amount which was reinserted was higher at 8 wt.% and the pore reduction was measured to be the smallest at 4.4Å. More importantly the success rate for this method was the highest at 90%.

We determined (section 4.5), that when excess amounts of sodium orthosilicate were reinserted, the surface area and pore volume decreased greatly. While with the orthosilicic acid, adding more than 10 wt.% gave values that were still very high surface areas, comparable to all the others samples analyzed within the series. This is another indication that the reaction between the orthosilicic acid and the protonic form zeolite is more successful.

In 10% of the cases, the method gave a pore size between 5.5Å- 5.7Å.
We were able to establish a very simple treatment that would be applied to the sample that would reduce the zeolite's pore size close to what was realized in 90% of the time (4.4Å).

The sample has gone through all the normal steps in the DRS process. Once we determined by argon BET that the median pore size was for example 5.3Å, we then took the sample and spread it on a filter paper within a buchner funnel. An amount of 350 ml of distilled water is heated and used to wash the zeolite. The sample is then dried in the oven at 120°C overnight. The next step is to heat the sample to 700°C stepwise for 16-18 hours. It is then analyzed by the argon BET instrument. The median pore diameter was measured to be 4.5Å. This washing procedure probably works by removing some of the excess orthosilicic acid at the pore mouth. Also, the heating to high temperature creates a reaction between the zeolite's silanol and the ones of the orthosilicic acid to give siloxane bonds. It is the formation of these bonds that help the reduction of the pore diameter. The questions that may be asked is the following: Is the DRS sample with a 4.4Å median pore size, exactly the same as the sample that has a size of 4.5Å ? Do they give the same product spectrum in the MTG reaction

4.6.1 Using a Commercial Sodium Orthosilicate in the DRS Method

At the start of the Master's project, we tried to find a company that would be able to supply us with some sodium orthosilicate, but none was found. During the second year of the Ph.D project, we came across, an American company, that sold a product which they called sodium orthosilicate. This product from now on will be referred to as commercial sodium orthosilicate and we decided to use it in the same way. To avoid any confusion, from this point on, the one isolated from the desilicating step will be referred to as the non-commercial sample.

Various amounts (2.5 wt.%-10 wt.%) of the commercial sample were made and individually passed through the resin filled column, in the same way as for the non-commercial sample, the results are shown in table 4.17.

Table 4.17 Textural Properties of Various DRS Samples with Varying Amounts of a Commercial Orthosilicic Acid

Sample	Total surface area (m^2/g)	Maximum Pore Volume (cc/g)	Median Pore diameter (Å)
DRS (2.5 wt.%)	204	0.09	5.6
DRS (5.0 wt.%)	373	0.16	5.4
DRS (7.5 wt.%)	279	0.10	5.7
DRS (10 wt.%)	277	0.12	5.4

The results from the above table, indicate that the commercial sodium orthosilicate did not work in the same way as the non-commercial because its median pore diameter was not reduced. We decided to characterize the commercial orthosilicate using the XRD instrument and then performing a match scan to see if the composition is the same as the sodium orthosilicate that we extracted. The result gave a very clear indication that the commercial sodium orthosilicate was composed in great majority of sodium silicate which was determined by XRD match scan to be that is in the meta configuration (Na_2SiO_3) .

For having tried the reinsertion of the meta form of the silicate species in my M.Sc. project, we know that no pore reduction could be achieved.

4.6.2 The most Important Step in the DRS Procedure

The steps of the DRS procedure were discussed in great detail earlier in the thesis. We wanted to determine the best conditions that were responsible for the method to achieve or not achieve pore reduction. After looking over the different steps involved, it was determined that the stepwise heating was done in a way that was gentle to the zeolite and in the most controlled conditions possible. The volume of the solution, where the sodium orthosilicate was dissolved, just covered the solid product with a minimal amount. This would allow us to get the most concentrated solution possible going through the column containing the ion-exchange resin. The volume that was collected from the column was between 40-45 ml which ensures that all the orthosilicic acid will be used in the next step. The amount of solution collected past 45 ml, was analyzed by atomic absorption spectroscopy and was found to contain no sodium or silicate species.

In the next step, lies the crucial conditions for the method to work. It is when the solution is evaporated using the rotovap, and reduced to a volume between 6-8 ml of orthosilicic acid solution, that the pore size reduction occurs in 90% of trials.

In the following table, we are going to show what median pore diameter results were achieved for the impregnation of the same amount of orthosilicic acid. The volume of the active solution (~ 40 ml) was reduced to a volume range between 7-20 ml.

Table 4.18 Results of the DRS Pore Size for the Impregnation of Different Concentrations of Orthosilicic Acid

Sample Names	Dilution Volume (ml)	Median Pore Diameter (Å)
DRS (8%)	20	6.1
DRS (8%)	15	5.9
DRS (8%)	12	5.6
DRS (8%)	11	5.7
DRS (8%)	10	5.7
DRS (8%)	9	5.4
DRS (8%)	8	4.4
DRS (8%)	7	4.4

The reason why a larger impregnation volume does not give the necessary conditions for pore reduction, could be explained by the fact that we used 5.0 g of zeolite for the impregnation using a method which is referred to as " the incipient wetness technique". This technique could be defined as the addition of a sufficient amount of solution containing the orthosilicic acid to fill the pore volume.[158] Knowing that the ZSM-5 zeolite has an internal volume of 40%,comes out to 2.0 ml of internal volume. This volume provides the optimal condition for the incipient wetness impregnation technique. If for example, we take the ZSM-5 zeolite and we wanted to apply the process of impregnation, this would require a minimum volume of 5 ml to cover the solid sample. So when the orthosilicic acid solution has been reduced from 40 ml to between 5-10 ml, a portion of only 10-20% of the inserted species has

remained on the exterior portion of the pores. The majority of the orthosilicic acid has entered the pores and will play an active part in the pore reduction process. This explains why good results are obtained with volumes of 6-8 ml. Because a large amount of the reinserted species entered the pores, the formation of siloxane bond, which is responsible for the reduction of the median pore diameter is easier. Using a larger volume for the reinsertion, causes too much of the reinserted species to remain on the external surface and, in this position, they do not play a role in pore reduction.

4.6.3 X-Ray Diffraction

We decided to investigate if any structural changes were detected using the XRD instrument. The following samples were analyzed in duplicate tests:

1) DRS (8 wt.%) 4.4Å, DRS (8 wt.%) 4.5Å, DRS (8 wt.%) 4.5Å (washed for a second time), DR (8 wt.%) 120°C,H-DZSM-5 (120°C) and H-DZSM-5 (700°C).

All of these samples were compared to the desilicated zeolite (H-DZSM-5) which was used as a reference. We were able to compare the x-ray patterns and then measure the relative crystallinity (RC) by using the intensity value for the characteristic peaks in the 2θ range of 22.5° to 25° in accordance with the method of Kulkarni et al..[135]

Table 4.19 The Relative Crystallinity value of Different Zeolite Samples

Samples	Intensity from Trial #1	Intensity from Trial #2	Average Intensity	Relative Crystallinity (%)
H-DZSM-5 (Reference) 120°C	7960	7996	7978	Reference*
DR (8%) 120°C	6692	6880	6786	85.1
H-DZSM-5 (Reference) 700°C	8121	8071	8096	Reference**
DRS (8%) 4.4Å	6842	6750	6796	83.8
DRS (8%) 4.5Å	9665	9575	9620	119
DRS (8%) 4.5Å (washed)	7040	7084	7062	87.3

*The H-DZSM-5 zeolite heated to 120°C, was used as a reference for the DR (8%) 120°C

** The H-DZSM-5 zeolite heated to 700°C, was used as a reference for the DRS samples

There was two reasons that would explain why it was decided to use an external standard rather than an internal standard, as follows : 1) characteristic peaks of the ZSM-5 zeolite were known to fall in the range of 22-25°, so the use of internal standards like for example sodium chloride or potassium chloride, would have its own peaks fall in the same range and it would make it almost impossible to differentiate the intensity of the zeolite peaks from the ones of the internal standard, 2) for ZSM-5 with a high number of cationic sites (low Si/Al ratio), the grinding procedure used to prepare the solid "zeolite-internal standard" would bring a phenomena known as solid state exchange which would alter the intensity of some characteristic peaks of the x-ray pattern of the acidic zeolite. For these two reasons, the association of international zeolite researchers have accepted the use of external

standards, and advised the use of the relative crystallinity with respect to the parent zeolite rather than the degree of crystallinity. [123,135]

The results in table 4.19 illustrate that all the zeolites have maintained their relative crystallinity when compared to the reference sample with all the values being above 83%. We noticed that the results for both DRS samples: a) DRS (8%) 4.4Å and b) DRS (8%) 4.5Å were not identical even though their pore sizes are very close. It is important to point out the fact that their treatments were slightly different. The DRS(8%) 4.4Å had a relative crystallinity (RC) value of about 84%.This means simply that there was a slight change of the zeolite's crystal structure following the DRS procedure when it is compared to the reference. The DRS sample that had a median pore size of 4.5Å, has a relative crystallinity value of 119%, which means that there was something in the zeolite's crystal structure that increased the intensity of some peaks when compared to the reference. We attempted to see if the orthosilicate species was deposited on the external portion of the pore. We decided to wash the sample with some hot water and then having it dry at 120°C. The second step involved analyzing the sample by XRD, to see if there was a change in the relative crystalline (RC) value of the sample.

The conclusion of our findings were very clear; the RC value decreased from 119% to about 87%. This decrease is due to the movement of the reinserted species probably positioned at the pore mouth. It is the presence of this species that affects the RC value. When the sample was mixed in hot water (350 ml) for a period of 1hour, the sample showed an RC value similar to DR 120°C and DRS 4.4Å because the excess silicate species that is deposited, has been washed off and it would not have a very different effect that the

analyzing the sample by XRD, to see if there was a change in the relative crystalline (RC) value of the sample.

The conclusion of our findings were very clear; the RC value decreased from 119% to about 87%. This decrease is due to the movement of the reinserted species probably positioned at the pore mouth. It is the presence of this species that affects the RC value. When the sample was mixed in hot water (350 ml) for a period of 1hour, the sample showed an RC value similar to DR 120°C and DRS 4.4Å because the excess silicate species that is deposited, has been washed off and it would not have a very different effect that the desilicated sample on the crystalline structure.

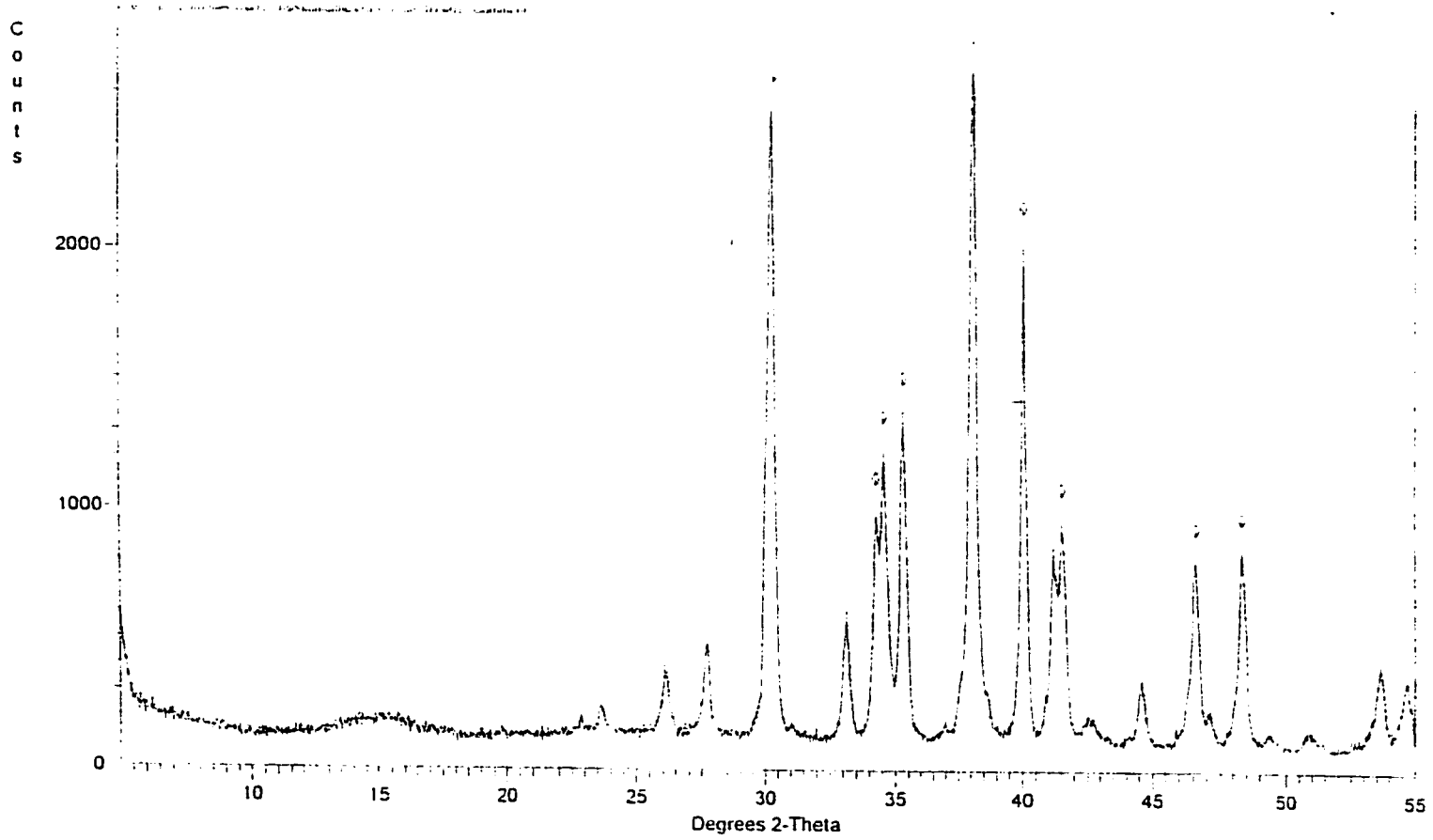

Figure 4.6 XRD Pattern of Sodium Orthosilicate

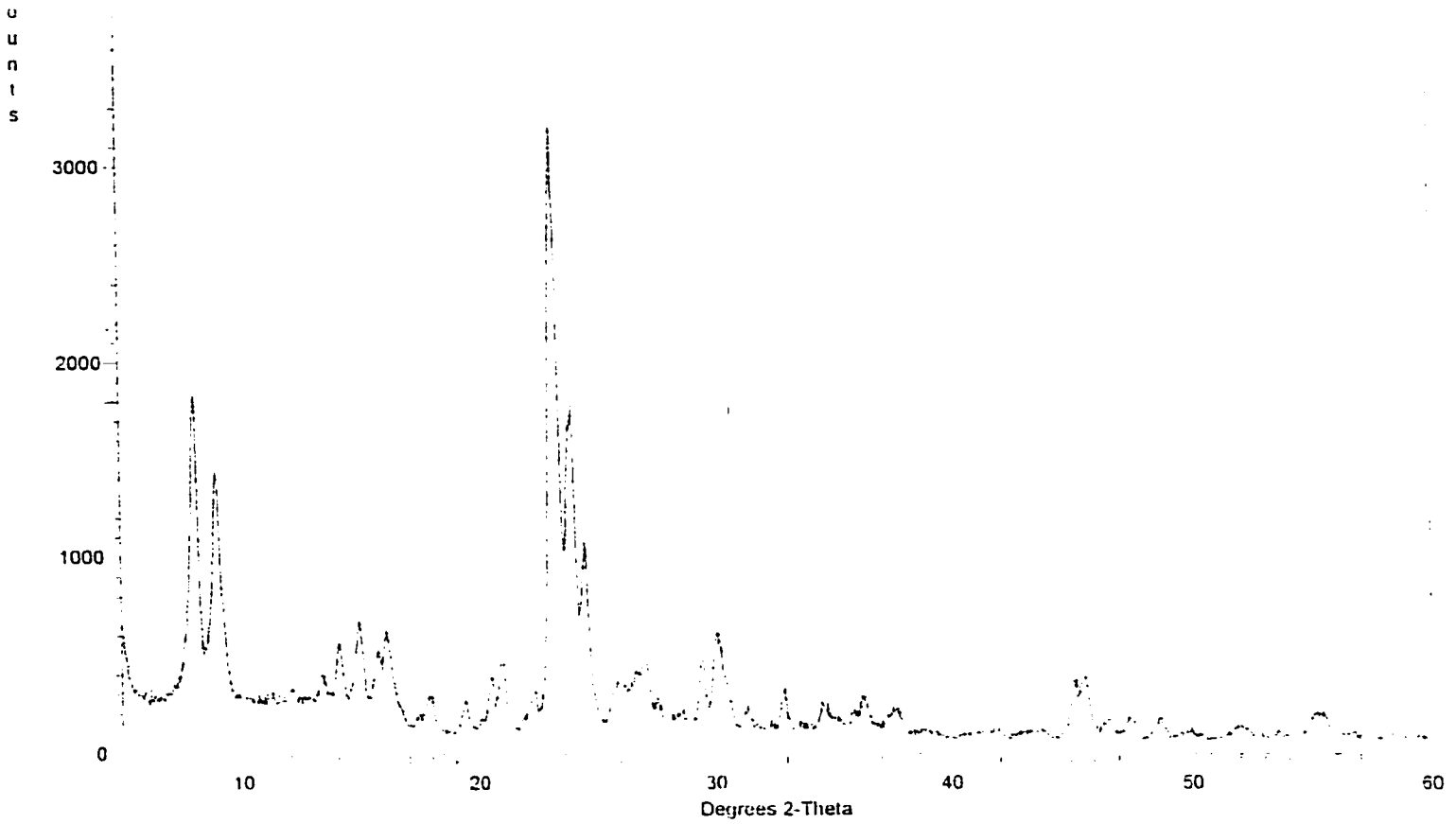

Figure 4.7 XRD Pattern of NH_4DZ (120 °C)

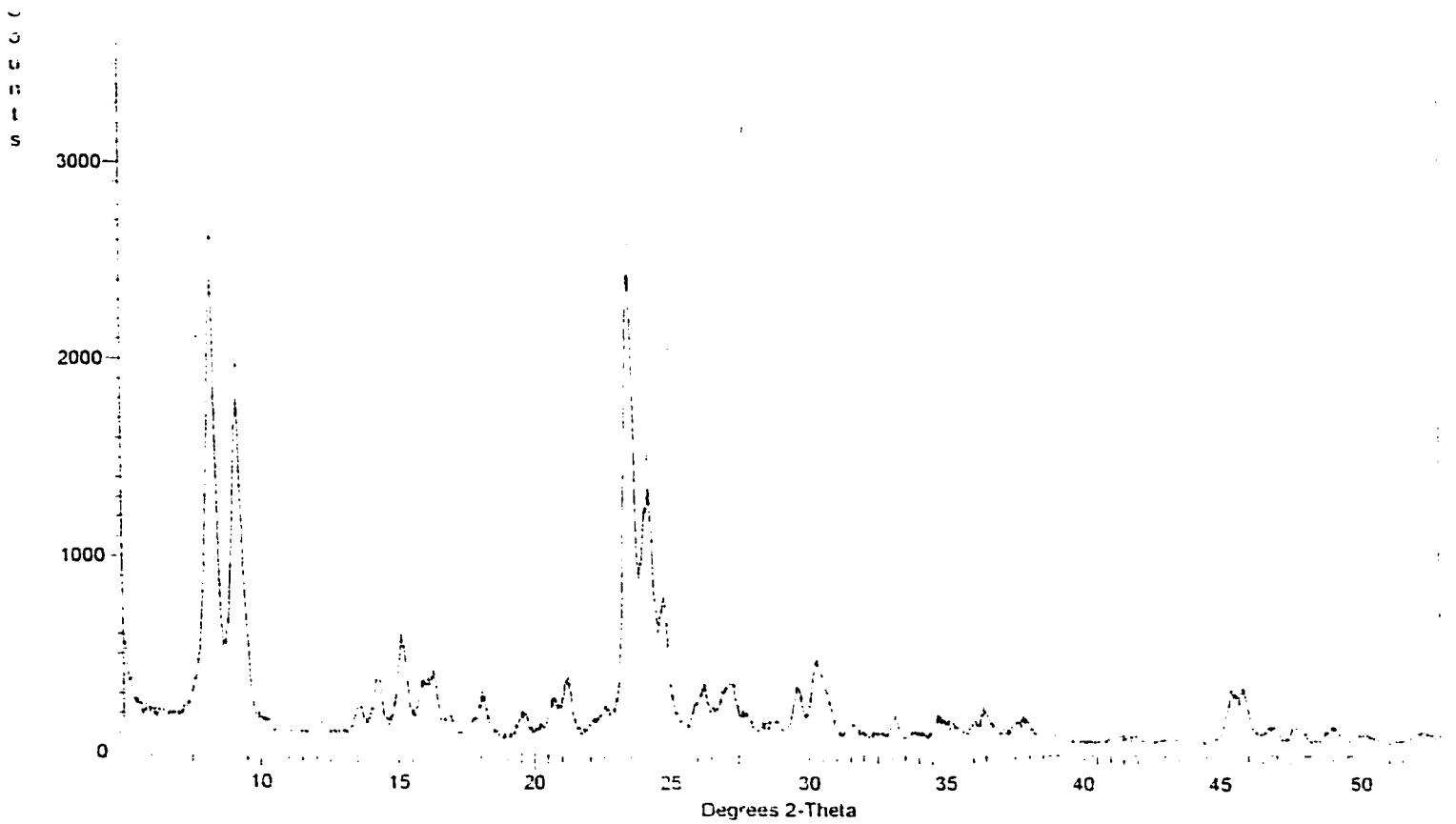

Figure 4.8 XRD Pattern of NH_4DZ (700 °C)

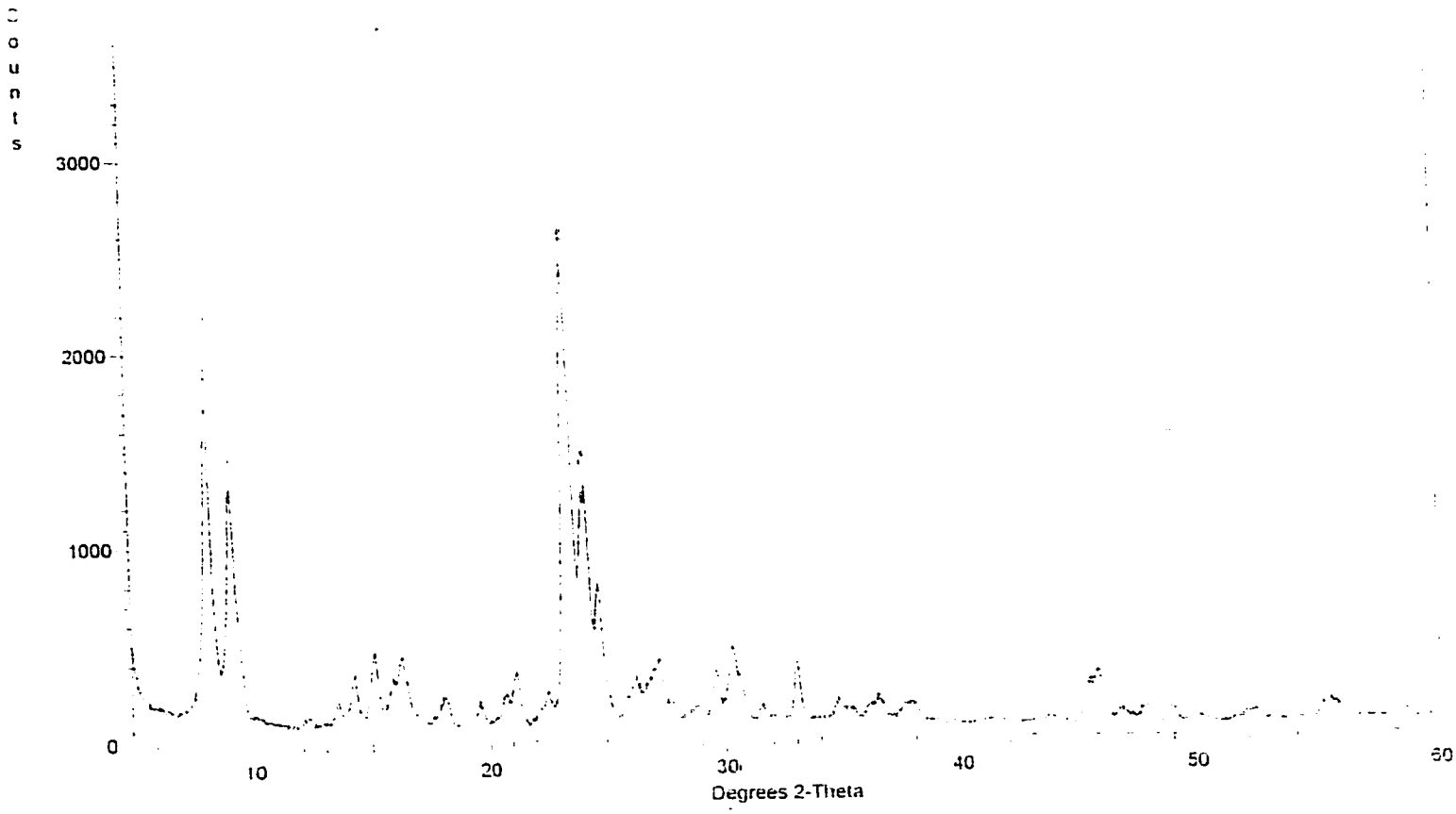

Figure 4.9 XRD Pattern of DRS (8wt.%) (120 °C)

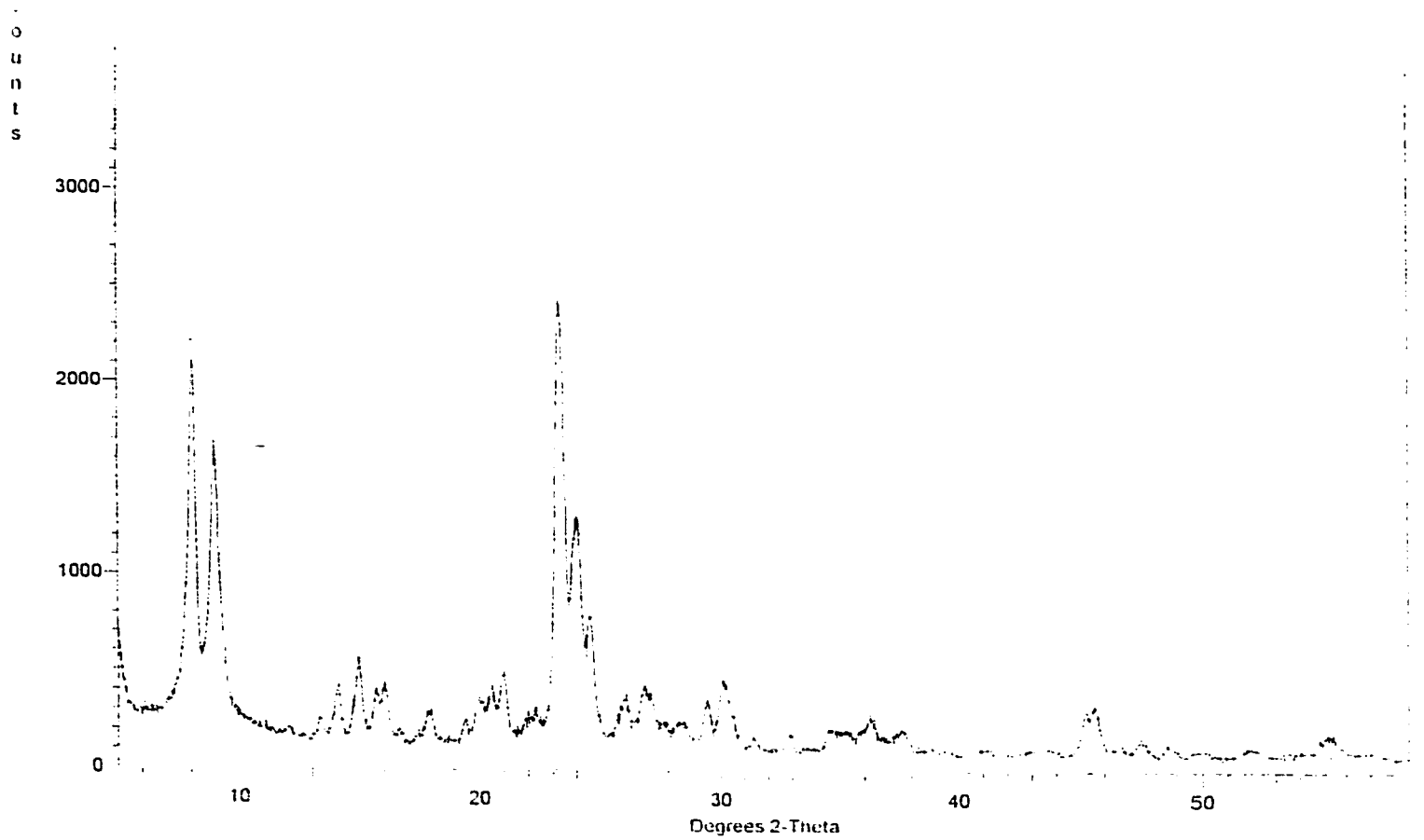

Figure 4.10 XRD Pattern of DRS (8 wt.%) 4.4Å (700 °C)

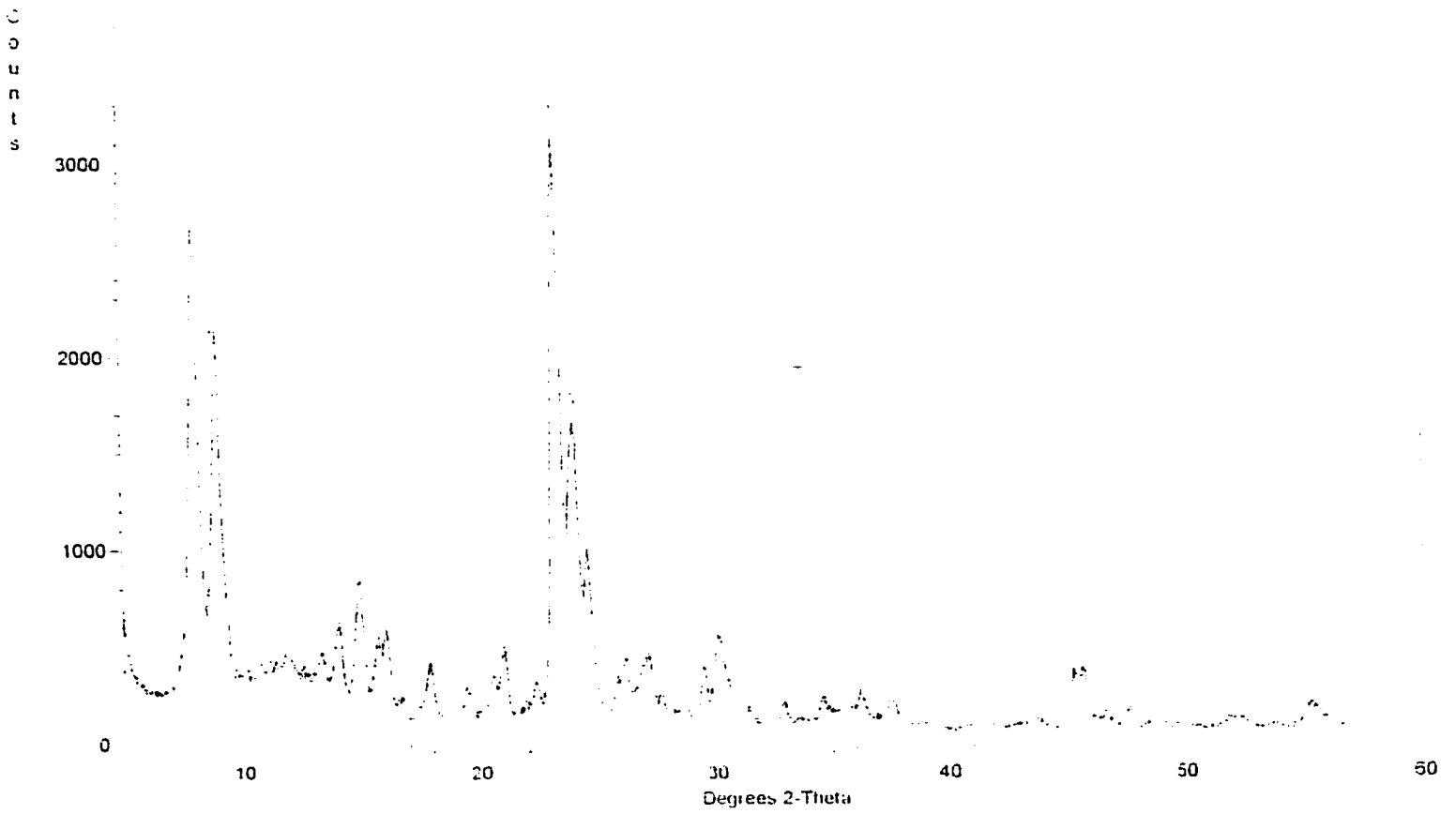

Figure 4.11 XRD Pattern of DRS (8 wt.%) 4.5Å (700 °C)

4.6.4 Ammonia Temperature Programmed Desorption (TPD)

This characterization methods very powerful for the determination of the proportion of strong, medium and weak acid sites. Most of the reactions under consideration are catalyzed by acid sites, this is why it is very important to have a good idea of the acidic nature of the catalyst.

Table 4.20 The Proportion of Strong and Medium Acid Sites Versus the Weak

Samples	Ratio of Strong + Medium / Weak
H-ZSM-5	1.25
H-DZSM-5	0.64
DRS (8 wt.%) 4.4Å	1.11
DRS (5 wt.%) 4.6Å	0.72

In the above table, the parent H-ZSM-5 had a ratio of 1.25 which is higher than the desilicated sample which had a value of 0.64. This is understandable because the process of desilication removes silicon from the framework and increases the proportion of aluminum and the weakest acid sites. The two samples, where pore reduction was achieved are the DRS (5 wt.%) 4.6Å using sodium orthosilicate and the DRS (8 wt.%) 4.4Å using orthosilicic acid.

The DRS(5 wt.%) 4.6Å sample had a ratio of 0.72 which is slightly higher than the desilicated sample. This is the case because it involves the reinsertion of a small amount of sodium orthosilicate which increases even slightly the silicon proportion within the framework and distances between the aluminum sites.

The DRS (8 wt.%) 4.4Å was determined to have a ratio which was situated closer to the parent at 1.11. The fact that a larger quantity of orthosilicic acid is reinserted within the structure, may be responsible for a value which is very close to what was determined for the parent because the orthosilicic acid is more acidic than the sodium orthosilicate, and this may explain why the 4.4Å has a stronger ratio than the sample with a 4.5Å median pore size.

4.6.5 Fourier Transform InfraRed Spectroscopy (FTIR)

Using the Diffuse Reflectance Infrared Spectroscopy (DRIFT), we wanted to investigate two regions:(1) the region of the orthosilicate species which is between 790-800 and (2) the siloxane bond region which is between 860-880 cm^{-1} would vary in the case of the DRS(8 wt.%) with a 4.4Å median pore diameter compared to the parent and desilicated spectrums.

We also analyzed using the DRIFT technique, the sodium orthosilicate that we isolated from the desilication procedure. It was important to determine where its characteristic peaks were, so that we may compare them to the spectra of the other three.

The figures of the Infrared spectra for the parent ZSM-5, the sodium orthosilicate, the desilicated and reinserted samples are all shown from figure 4.12-4.15. The samples were scanned in the region of 700-900cm^{-1}, with a resolution of 4 cm^{-1} and 64 scans.

Compare the region of 790-800 cm^{-1} for the H-ZSM-5 (fig.4.12) and the sodium orthosilicate (fig.4.15). We can see very clearly that the orthosilicate has a very large peak at about 800 cm^{-1} that the parent sample does not possess. The desilicated sample (fig.4.13) has the same peak at 800 cm^{-1} because during the desilication procedure some of the silicon species (sodium orthosilicate and others) may not have been totally removed by the washing with hot water. The fact that some of the silicate species is still weakly held to the structure gives us the peak that is characterized by the band at 800 cm^{-1}. The DRS (fig.4.14) sample, involves the reinsertion of a small amount of sodium orthosilicate (8 wt.%). We do observe a peak in the 800 cm^{-1} region which is explained very simply by the fact that a small amount of the orthosilicate has been reinserted into the framework.

In the region of 860-880 cm^{-1}, we do see a very small increase in the siloxane band of the reinserted sample when compared to the parent and desilicated samples. This increase is due to the reaction that occurs between the silanol groups of the zeolite and orthosilicate species. Even though they are small, they are an indication that the formation of siloxane bonds does occur during the DRS process.

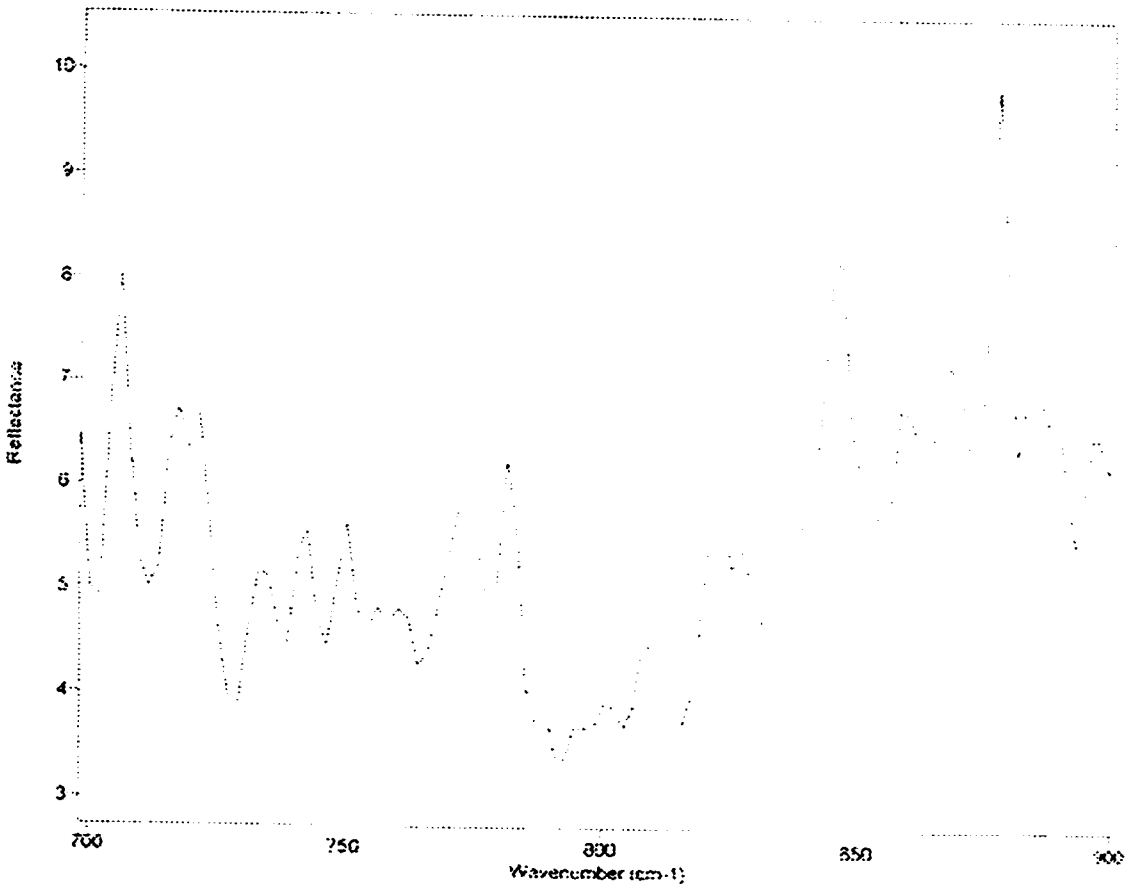

Figure 4.12 Drifts Spectra of parent zeolite (H-ZSM-5).Conditions were the following: Resolution of 4 cm^{-1} and 64 scans.

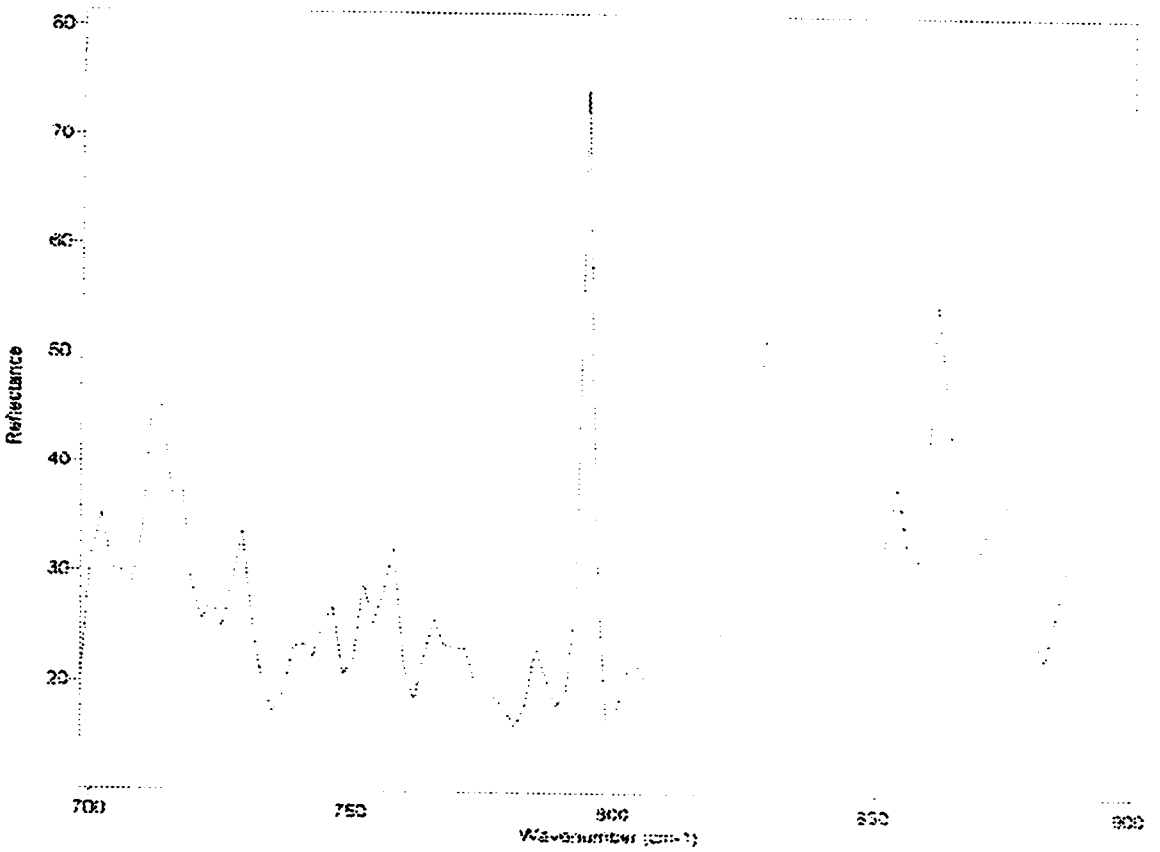

Figure 4.13 Drifts Spectra of Desilicated zeolite (H-DZSM-5). Conditions were the following: Resolution of 4 cm^{-1} and 64 scans.

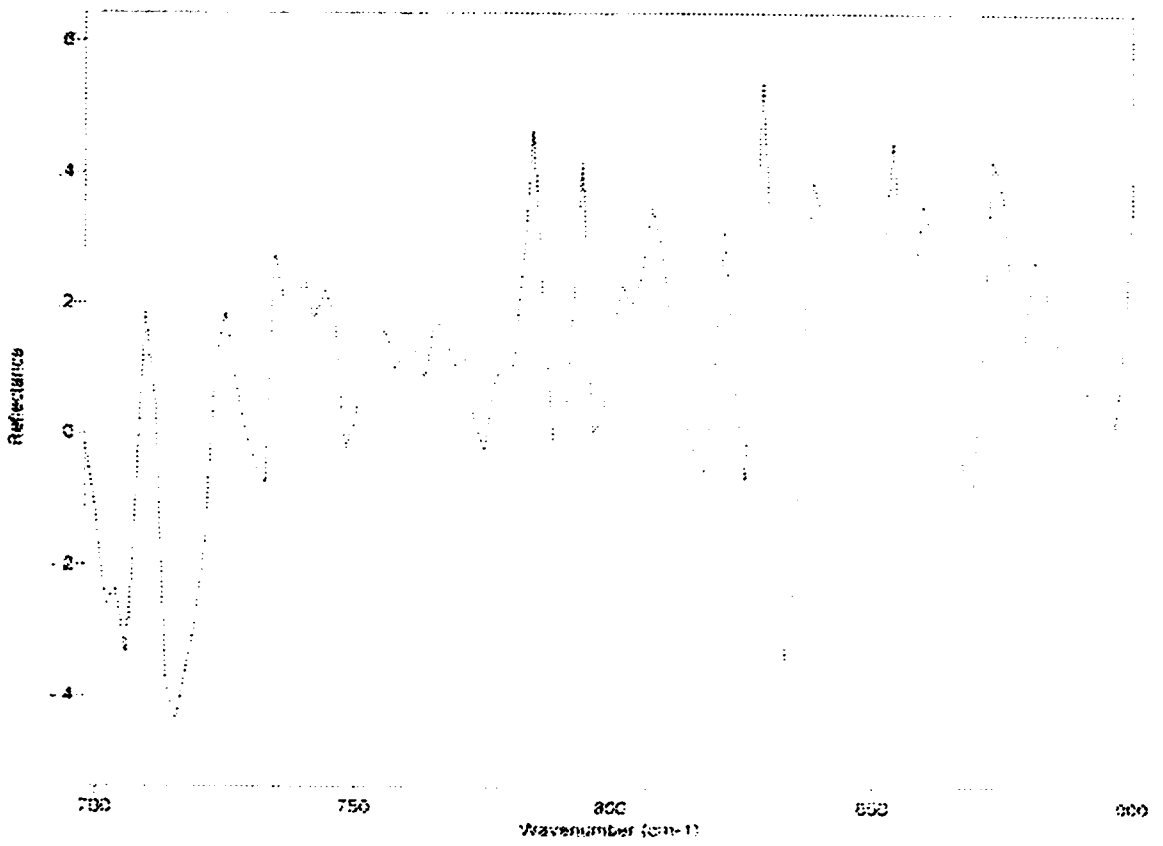

Figure 4.14 Drifts Spectra of Reinserted sample DRS (8 wt.%).Conditions were the following: Resolution of 4 cm-1 and 64 scans.

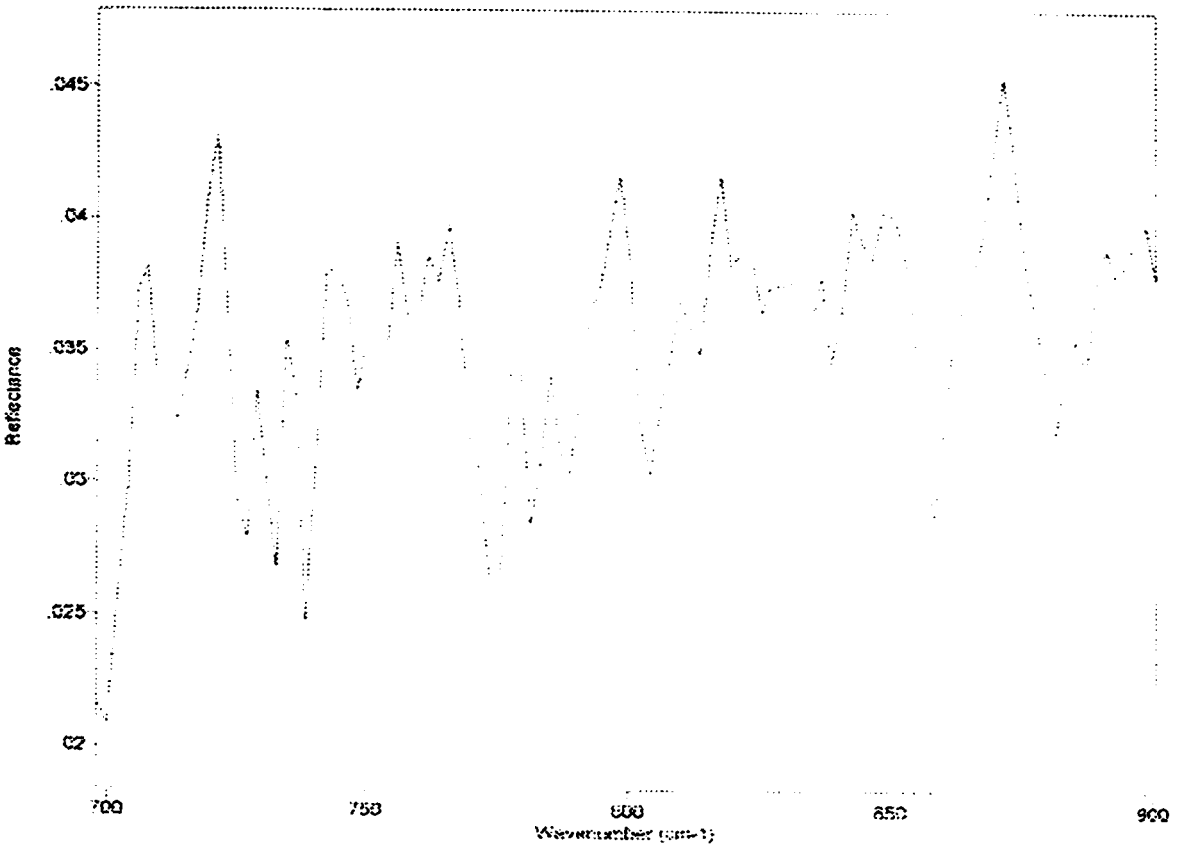

Figure 4.15 Drifts Spectra of sodium orthosilicate. Conditions were the following: Resolution of 4 cm^{-1} and 64 scans.

4.6.6 Differential Scanning Calorimetry and Thermal Gravimetric Analysis (DSC/TGA)

In figure 4.16, the top TGA spectra of the DRS (8 wt.%) has a pore size of 4.4Å. The loss of weight at 478.57°C is due presumably to the dehydroxylation of the zeolite's silanols. Comparing the DRS of the TGA spectra to that of the H-ZSM-5, we could clearly observe that there is no peak at a temperature of 400°C or over for the time derivative of the weight loss for the parent zeolite.

Another important factor that we need to look at closely, is the total weight loss for both zeolites. In the case of the H-ZSM-5, 2.8% was lost when the sample was heated between 100°C to 900°C. The DRS over the same temperature range lost 7.2% weight. The difference in weight loss between both samples is of 4.4% for the DRS sample. The DRS possesses more silanol groups, a part being provided by the reinserted orthosilicic acid. At 478.6°C, these silanols start reacting (dehydroxylation) and this is why we have a larger weight loss for the DRS sample compared to the H-ZSM-5 zeolite.

Figure 4.17 of the Differential Scanning Coulorimetry (DSC) of the H-ZSM-5 and the DRS sample, shows a very clear difference in the temperature range of 475°C and 600°C. Before these temperatures, heat flow of both samples is very similar. The difference starts occurring with the DRS at 500°C where there is a release of energy (exothermic). This is due to the reaction between silanol groups of the zeolite and the orthosilicic acid that gives a siloxane bond. The reaction temperature occurs in the region between 600°C and 625°C. In the case of the H-ZSM-5 zeolite, no release of energy is observed in the region of 475°C and 600°C.

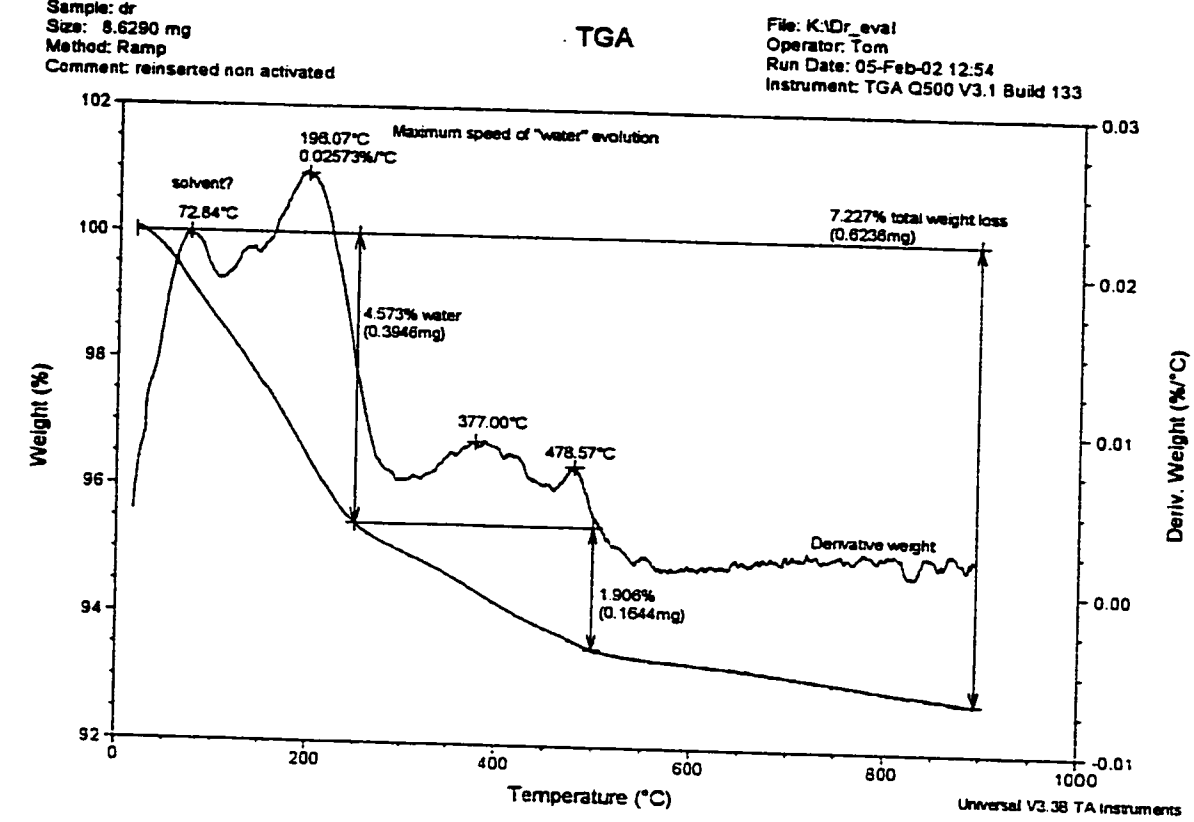

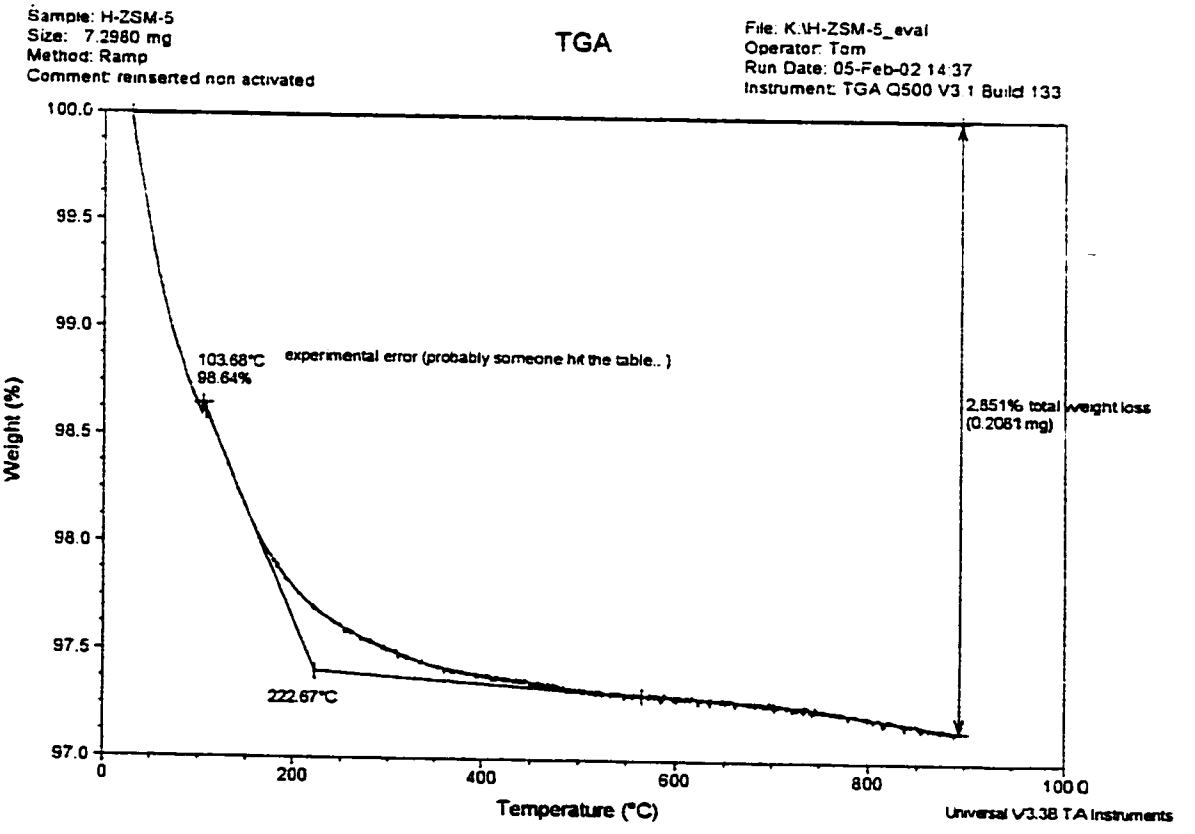

Figures 4.16 TGA analysis of DRS 4.4Å (to) and H-ZSM-5

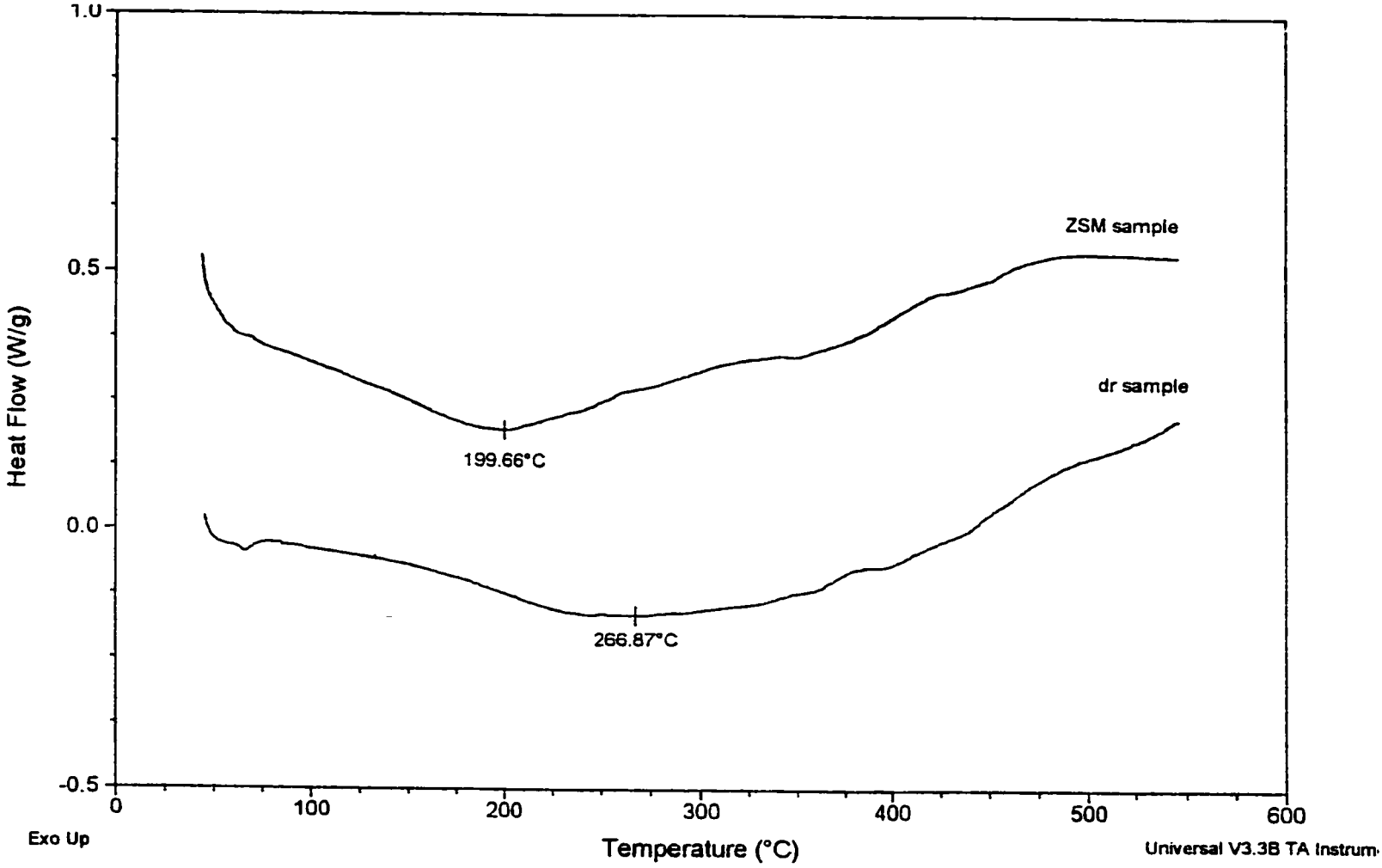

Figure 4.17 DSC analysis of DRS 4.4Å (bottom curve) and H-ZSM-5

4.6.7 Determination of the Constraint Index and the Internal Space for transition States.

The constraint index is defined as the measure of the rate of cracking of n-hexane divided by the rate of cracking of 3-methyl pentane. We decided to test different catalysts on which we performed other types of tests. It was important to see what kind of values we would the constraint index because we wanted to determine if the difference in pore dimension or the amount of strong acid sites was the cause of any change in CI.

The following table, illustrates the results of the conversion as well as the constraint index value and the ratio of isobutane to n-butane. The isobutane to n-butane ratio was recently discussed as being a possible indicator of internal space for the formation of the transition state. [160].

Table 4.21 Results for the Constraint Index and Isobutane/n-butane

Samples	Conversion (%)	Constraint Index	Isobutane/n-butane
DRS (8 wt.%) 4.4Å	67	1.40	1.05
H-ZSM-5	100	10.8	1.29
H-DZSM-5	75	2.45	1.18

The above table, compares the results of three catalysts that have different pore sizes and amount of strong acid sites, while having the same density of total acid sites.

The H-ZSM-5 has a pore opening of 5.6Å and the largest number of strong acid sites, it possesses the highest constraint index value at 10.8.

This gives us the indication that because of its larger number of strong and medium acid sites,

the rate of cracking of n-hexane is much greater than for the 3-methyl pentane. If we compare this result with the one determined for the desilicated sample that has a larger pore size but was determined to contain a very small amount of strong and medium acid sites. The constraint index of the desilicated sample was found to be five times smaller than for the H-ZSM-5. The DRS (8 wt.%) sample that has a pore size of 4.4Å, contains a small number of medium and weak acid sites. It's constraint index value was determined to be smaller than in the case of the desilicated sample. In this case the acidity and the pore size plays a dual role in the CI value.

As for the ratio of isobutane to n-butane, the trend is not dependant on the strength of the acidity but on the available internal room inside the zeolite's pores. The DRS sample that has a 4.4 Å pore size has the smallest isobutane/n-butane ratio. The parent and the desilicated samples both have almost the same size and their values are very close but higher than for the DRS sample.

Dr. McVicker [160] from Exxon Mobil Research does not believe that this parameter is very useful when used with the ZSM-5 zeolite. He believes it is very difficult to extrapolate any useful information when trying to measure CI differences for samples that have pore sizes very close to each other and for samples that have drastic differences in their proportions of strong acid sites. The ideal condition for the CI parameter to be useful would be for samples that have an almost identical number of strong and medium acid sites but with different pore sizes. Then any variation of the CI value would be attributed to the pore size difference.

According to Dr. McVicker[160], the isobutane/n-butane ratio would give us a more reliable indication of the pore size differences. It gives us an indication of the available internal space, with the value being independent of any temperature change or any differences in the number of strong and medium acid sites. Harris et al.[161] discussed the correlation between a low isobutane/n-butane ratio and a high CI value. They explained this by saying that a low isobutane/n-butane ratio is related to a low conversion of 3-methyl pentane.

4.7 Catalytic Applications of the Zeolites Engineered with Orthosilicic Acid

Our goal is to get the most considerable pore size reduction, with the highest rate of success. Using the orthosilicic acid (8 wt.%) in the DRS method, we achieved pore reduction results of 4.4Å and 4.5Å (after washing). Some of our attempts to get pore size reduction were not fruitful but help us and we determined two specific samples that have pore sizes of 5.1Å (medium size) and 5.7Å (larger size). We wanted to use them in the MTG/MTO reaction to determine how the changes in the pore sizes affect this reaction for samples that have had an 8 wt.% reinsertion of orthosilicic acid.

The second application was to assess the molecular sieving effect of the four samples mentioned above with respect to n-heptane and isooctane. Large disks were produced using fibrous sepiolite as matrix which embedded the zeolite particles. These disks had a thickness of 1.5 cm and were made from 50% zeolite and 50% sepiolite.[150]

4.7.1 Product Shape Selectivity in the Methanol Conversion

In this section, we presented tables of results for various catalysts in the methanol conversion reaction. The catalysts which are going to be analyzed are all DRS (8 wt.%) in the extrudate form, made from a proportion of 80% zeolite and 20% bentonite clay. They all differ from their median pore sizes which are: 4.4Å, 4.5Å (washed), 5.1Å and 5.7Å. We also decided to determine the products that were formed due to the bentonite, so we made some extrudates with containing only bentonite. The samples were all tested at a temperature range of 375°C-550°C.

Table 4.22 Distribution of the Product Aromatics for Bentonite (100%) in the MTG Reaction

Selectivity (Catom %)				Distribution of product aromatics (Catom%)					
Zeolite	Rxn. Temp. (°C)	C_2-C_4 Olefins	Arom.	Benz.	Toluene	m-&p-Xylene	o-xylene	C_9	C_{10}^+
Bentonite	375	0	0	0	0	0	0	0	0
Bentonite	450	0	0	0	0	0	0	0	0
Bentonite	550	0.5	4.6	100	0	0	0	0	0

In table 4.22, we could see that the bentonite binder which contains only mesopores and no acidity, did not produce any olefins and aromatics at 375°C and 450°C. While at 550°C, they produced very low amounts of olefins and aromatics.

In the table below (4.23), we are able to determine the activity and effect of the zeolite due to their pore size and acidity in the methanol conversion reaction.

Table 4.23 Distribution of Product Aromatics in the MTG Reaction for DRS (8 wt.%) Samples with Different Median Pore Size Diameter.

Selectivity (Catom %)				Distribution of product aromatics (Catom%)					
Zeolite	Rxn. Temp. (°C)	C_2-C_4 Olefins	Arom.	Benz.	Toluene	m-&p-Xylene	o-xylene	C_9	C_{10}^+
4.4Å	375	2.1	2.6	62.5	37.5	0	0	0	0
4.5Å	375	0	4.7	95.9	4.1	0	0	0	0
5.1Å	375	2.9	5.8	94.5	5.5	0	0	0	0
5.7 Å	375	0.03	0	0	0	0	0	0	0
4.4Å	475	36.4	14.8	1.88	10.5	38.4	3.3	29	17
4.5Å	475	12.8	7.6	27	5.5	30.8	2.2	26	8.5
5.1Å	475	7.6	3.4	69.2	20.1	4.4	0.5	4.6	1.2
5.7 Å	475	9.3	2.7	20.8	29.5	26.8	2.6	18	2.3
4.4Å	550	41.5	21.3	5.3	18.7	49.3	4.8	19	2.9
4.5Å	550	34.9	19.8	3.2	15.1	49.4	4.3	25	3.0
5.1Å	550	23.6	15.0	15.8	7.7	41.7	3.6	23	8.2
5.7 Å	550	30.1	22.8	6.5	8.7	38	3.8	29	14

In the above table, where the temperature of the reaction varied from 375°C to 550°C, we could measure the differences in the selectivity of the olefins and aromatics.

If we look at the olefin production for all the catalysts, we could see that they all reach their maximum at a temperature of 550°C. Knowing that the olefins are thermodynamically more favored, the catalyst with the narrowest pore was found to produce an amount of olefins reaching 41.5%.

In the case of the aromatics, all the analyzed catalysts have their maximum C atom% at a temperature of 550°C. All four catalysts produce roughly the same type of aromatics, but differ in the distribution of these products.

We noticed a few more important details in the results in table 4.25. The catalyst with the median pore size of 4.4Å has formed a large amount of benzene but did not produce any o-xylenes, C_9 or C_{10}^+ aromatics at 375°C. This may be due to the smaller pore size which prevents the formation or outward diffusion of bulky products.

In table 4.24, we compare the production of heavy aromatics for all the catalysts at 550°C by grouping the heavy aromatics.(the sum of the C atom% of o-xylene, C_9 or C_{10}^+ aromatics is tabulated in table 4.24 for all the catalysts tested)

Table 4.24 Heavy Aromatics Production for the DRS (8 wt.%) Catalysts at 550°C

Samples of DRS (8 wt.%)	Heavy Aromatics in C atom %
4.4Å	26.6
4.5Å	32.3
5.1Å	34.8
5.7 Å	46.8

From the above table, we could conclude that the size of the median pore diameter plays a very big role in the production of the heavy aromatics. The sample with the largest pore size produces the largest amount of heavy aromatics, while the one with the narrowest size has the smallest production of that class of aromatics. This makes sense that if there is more internal room, the larger size products will be able to form in greater amounts.

Table 4.25 Production and distribution of light olefins for DRS (8 wt.%) samples

Selectivity (Catom %)				Distribution of product olefins (Catom%)		
Zeolite	Rxn. Temp. (°C)	Arom.	C_2-C_4 Olefins	Ethyl.	Propyl.	Butenes
4.4Å	375	2.6	2.1	48.0	46.8	5.2
	475	14.8	36.4	28.6	57.8	13.6
	550	21.3	41.5	26.9	59.3	13.8
4.5Å	375	4.7	0	0	0	0
	475	7.6	12.8	41.8	47.6	10.6
	550	19.8	34.9	24.4	64.7	10.9
5.1Å	375	5.8	2.9	58.5	35.9	5.6
	475	3.4	7.6	71.5	19.6	8.9
	550	15.0	23.6	28.7	62.7	8.6
5.7Å	375	0	0.03	100	0	0
	475	2.7	9.3	33.7	52.9	13.8
	550	22.8	30.1	23.8	67.8	8.8

From the results above, we could see that at 375°C the catalyst with a 4.4Å is the most selective towards propylene. At higher reaction temperature, the light olefins are more thermodynamically favored. This may explain why all the catalysts produce more of the light olefins at 550°C. The catalyst producing the highest quantity of light olefins is the one with the narrowest pore size (4.4Å). It produces 6.6% more than the catalyst with a 4.5Å pore size.

If we compare the two catalysts that are at extremes of the pore size scale (4.4Å vs 5.7Å), we can see a 27.5% difference in the light olefin production at a reaction temperature of 550°C.

In conclusion, the size of the pore diameter matters in the hydrocarbon production in the methanol conversion reaction. Even though they all had the same DRS treatment with 8 wt.% of orthosilicic acid reinserted, their sizes vary and each samples proportion of strong, medium and weak acid sites differs. This may help explain why there is such variations in the amount of olefin and aromatics produced for the different catalysts.

4.7.2 The Molecular Sieving and Window Effects

We wanted to investigate both the molecular sieving and window effects using the n-heptane, isooctane and an equimolar mixture of the two on three zeolite-sepiolite disks. The zeolites used were: DRS (8 wt.%) (4.4Å), H-ZSM-5(5.5Å) and H-DZSM-5(5.9Å). In figure 4.18, we compare the chromatograms for the tests on the 3 zeolites using n-heptane. All of the n-heptane because of its small size (4.3Å), enters the pores of even the narrowest pore size sample, which in our case is DRS. The fact that all of the n-heptane enters the pores is an evidence of the molecular sieving effect.

In the case of figure 4.20, the isooctane (7.0Å) is injected in each of the disks samples and two peaks are obtained. The first peak represents the isooctane molecules which are rejected by the pores due to the restriction, the second peak appeared when the disks are heated at 300°C, so this induces the desorption of the portion of the isooctane that has entered the pores. The isooctane size is larger than 4.4Å , so when it is injected into the DRS disks, we obtain a rejection ratio of 1.13.The H-ZSM-5 and H-DZSM-5 both gave identical rejection ratios of 0.75. This could be explained by the fact that the latter two zeolite disks are larger than the DRS and they have pore sizes which are very close to one another, so this explains why more isooctane is adsorbed and less of it exits at the start.

When an equimolar mixture of n-heptane and isooctane is injected, two peaks exit and the chromatograms for all three zeolites are shown on figure 4.20. For the DRS sample, the rejection ratio was found to be 4.55. The large value is explained by the fact that n-heptane being smaller has an easier time entering the pore at the expense of isooctane that is larger. For larger size disks, containing H-ZSM-5 and H-DZSM-5 the rejection ratio was

determined to be 0.22 which is much smaller than for the DRS. We could conclude from this that the DRS is much smaller than the other two zeolites, and its size is closer to the one of the n-heptane. The molecular sieving effect is more obvious in the case of the DRS than for the other zeolite disks.

The window effect could be observed when we look at the chromatograms of all three zeolite disks for the separation of the mixture. The retention time of the second and third peaks tend to come out later for the H-DZSM-5 which has a larger pore size than for the other two zeolite disks. The explanation is very simple, the critical length of the molecule probably corresponds to the free length of the H-DZSM-5 cage. The isooctane molecule just fits the cavity. Entrapement in the cage leads to "low mobility for just fitting" molecules such as the isooctane. In the case of the H-ZSM-5 and the DRS, the pore sizes are smaller so the molecule is able to orient itself much more easily to then exit the pore system in a shorter lapse of time than in the case of the H-DZSM-5. We could say that in this case, the window effect is not as pronounced.[162]

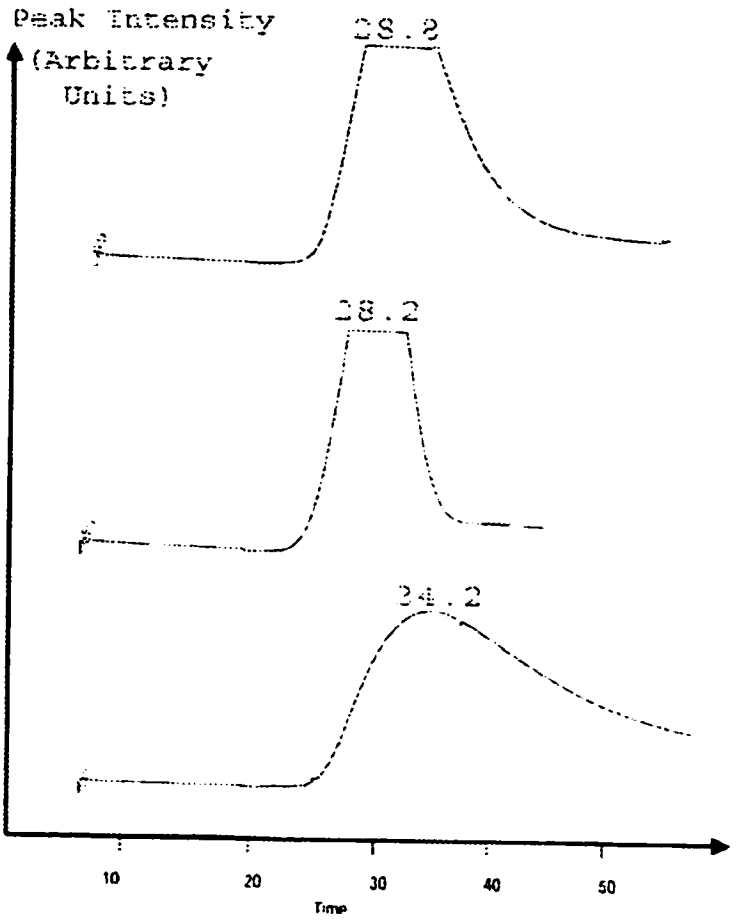

Figure 4.18 Separation of the n-heptane in disks such of: a)H-DZSM-5 (Bottom), b) H-ZSM-5 and c)DRS (8 wt.%) (Top)

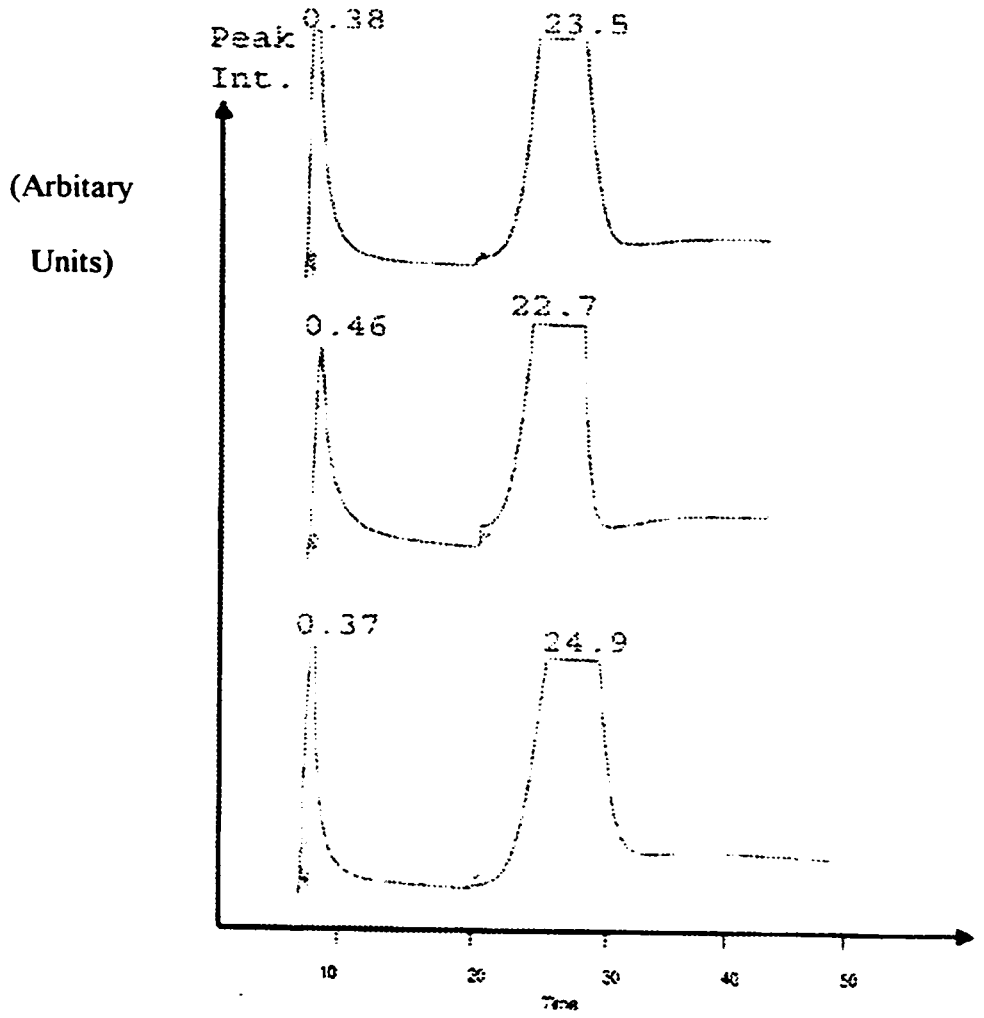

Figure 4.19 Separation of isooctane in disks such of: a)H-DZSM-5 (Bottom) b) H-ZSM-5 and c)DRS (8 wt.%) (Top)

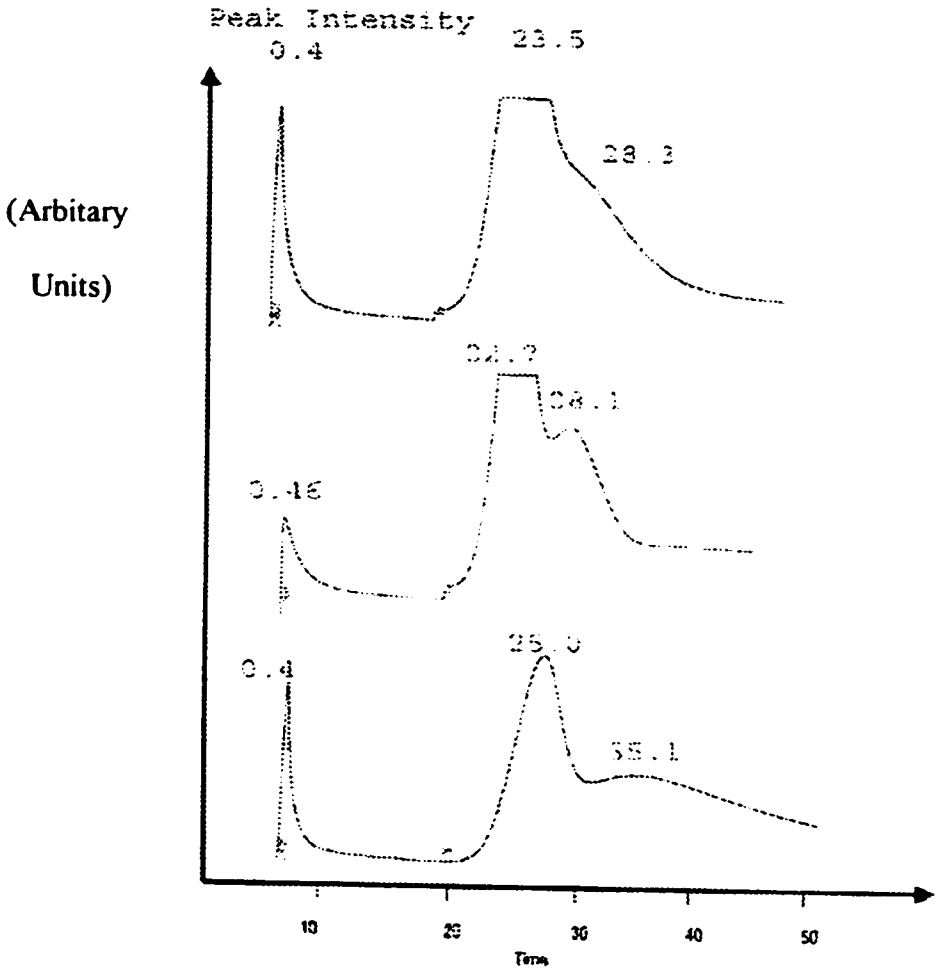

Figure 4.20 Separation of the equimolar mixture in disks such of:

a)H-DZSM-5(bottom),b) H-ZSM-5 and c)DRS (8 wt.%) (Top)

Chapter 5

5.1 Conclusion

The results that were achieved during the M.Sc. project set the foundations for the research that was conducted during the Ph.D project. Our goals were very clear, we had to determine the mechanism of reinsertion of the orthosilicic acid on the desilicated zeolite, the reaction temperature at which this occurs also had to be determined, the success rate of the DRS process had to be improved and if possible we needed to decrease the median pore diameter even more than the 4.9Å that was achieved at the end of the M.Sc. research work.

The optimal desilication procedure for the ZSM-5 zeolite was determined to be with 0.8M sodium carbonate. The DRS process gave the best results, when the sodium form zeolite was ion-exchanged to give a zeolite in the ammonium form. The optimal steps for pore size reduction were determined to be in the following order:

a) desilication with 0.8M sodium carbonate, b) ion-exchange with 5 wt.% of ammonium chloride, c) reinsertion with 5 wt.% of sodium orthosilicate, and d) activation stepwise to 700°C overnight. Using these steps, the median pore diameter was measured to be 4.6Å with a success rate of 80%. The total surface area, micropore area, crystallinity and acid density data all show that the DRS (5 wt.%) structure was very similar to the parent sample so even though some changes were brought onto the structure, it did not change its nature. The Fourier-Transform Infrared Spectroscopy of the pore size engineered sample compared to the parent and desilicated showed a net increase in the intensity of two bands in the region of 850-910 cm^{-1} that characterize strained siloxane bonds.

The product shape selectivity in the methanol conversion was applied to three catalysts of different pore dimensions and decreasing acid strength, they are: H-ZSM-5 (5.2Å), DRS (4.6Å) and the desilicated (5.9Å) sample in a temperature range of 375°C-550°C. Due to the stronger acid strength of the H-ZSM-5, it produces more aromatics than the two others. But it is the desilicated sample that produces the larger size alkylaromatics (C_9-C_{10}^+) because of its greater pore size. The DRS sample because of its smaller median pore size produces less of the bulky alkylaromatics, while producing over 90% of C_5^- aliphatics at temperatures of 450°C and lower.

Membranes were produced using the same three catalysts, using sepiolite as a matrix. We wanted to see how the different pore sizes would alter the adsorption of the BTX aromatics. The desilicated sample adsorbed the BTX completely because of its 5.9Å pore size. The H-ZSM-5 had a small amount of the larger size xylenes that was not totally adsorbed because of its 5.2Å, while the DRS did not adsorb the majority of the larger size xylenes because of it had the smallest pore size of the three.

Knowing that the pore reduction is achieved by a reaction between the silanol groups of the zeolite and the sodium orthosilicate, we decided to use an acid resin, to exchange the sodiums for protons. This would make the reaction between the zeolite's silanols and the orthosilicic acid, this occurs at a reaction temperature that was determined using DSC/TGA instrument to be at about 600°C. The pore narrowing reached 4.4Å for a reinsertion of 8 wt.% of orthosilicic acid in 90% of the tests.

Many characterization tests were performed on the DRS sample and it was confirmed that the crystallinity and the surface area did not change very much when compared to the

desilicated sample. The proportion of strong and medium to weak acid sites was just below the value determined for the H-ZSM-5.

The constraint index and the internal space of the DRS sample, was determined to be lower than for the desilicated and the parent ZSM-5 zeolites.

The product shape selectivity in the methanol conversion was applied to four catalysts of different pore dimensions they are formed from DRS (8 wt.%) but some gave different pore dimensions: 4.4Å, 4.5Å, 5.1Å and 5.7Å in a temperature range of 375°C-550°C. The sample with a 4.4Å pore dimension produced at 550°C the largest amount of olefins, being very selective for propylene (~ 60%). At the same temperature this sample produced the smallest amount of heavy aromatics of all the samples tested with the smaller aromatics being produced in greater amounts than the larger ones. The size of the pore diameter matters in the hydrocarbon production for the methanol conversion. The proportion of strong and medium to weak acid sites may also be used to explain why there is a variation in the amounts and selectivity to the olefins and aromatics for the zeolites investigated.

Using three different pore sizes of zeolites (DRS (8wt.%), H-ZSM-5 and H-DZSM-5), we were able to make disks using sepiolite as a matrix. We were also able to prove that there was a molecular sieving effect caused by these membranes, using n-heptane which has a small enough size to enter the pores of any of these disks. With the isooctane, because of its larger size, a portion was not adsorbed by each of the disks. This amount was larger in the case of the DRS because of the large size difference with the isooctane. The window effect was shown to occur in the case of the H-DZSM-5, when n-heptane or isooctane is passed through the disks. The effect is very simple, because of the size of the

cavities, the molecules have a tougher time getting out and so their retention times, compared to the ones for the H-ZSM-5 and the DRS are much longer. This is clear evidence that when the size of the molecule and of the cavity are very close, it makes it more difficult for that molecule to exit.

APPENDIX

AP.1 Atomic Absorption Spectroscopy

A.1.1 Theory

Atomic Absorption spectroscopy (A.A.S.) was used for elemental analysis of Al, Na and Si which is expressed as SiO_2 was obtained by subtracting the sum of the Al_2O_3 and Na_2O percentage from 100%. Since the relative quantities of each of these elements will directly affect the catalytic and adsorptive properties of the molecular sieves. We could classify zeolites according to the ratio of Si/Al tetrahedra in their framework.

A.A.S. is based on the principle that metal atoms absorb electromagnetic radiations at frequencies which are characteristic of each metal, and the amount of light absorbed is a function of the metal concentration. This is one of the most used analytical tools in the modern analytical laboratory, mainly by the use of the hollow-cathode discharge lamp as a light source and the use of atomizers to provide rapid and efficient atomization of liquid samples. With current instrumentation, however the method is not suitable for qualitative or simultaneous multi-element analysis.[163]

Qualitative analysis by A.A.S. is based on the measurement of the radiant energy absorbed by free atoms in their gaseous state. Because the spectra of gaseous atomic species consist of well-defined narrow lines at a wavelength characteristic of the element involved, it is known to be a high selectivity technique. The solution samples are vaporized, commonly by flames, electrical heating or lasers; and on further heating the vapor dissociates into free atoms. From figure AP.1, we could see a schematic presentation of this process.

Since the element of interest does not usually exist as free atoms in any common

solution but is in the ionic state or in a molecular form, it is necessary to generate a population of free neutral atoms of the element of interest in order to observe A.A signals. The metal atoms are then capable of strongly absorbing radiations at discrete characteristic wavelength, which coincide with the narrow emission lines of the particular metal generally provided by a hollow cathodes lamp. Hence, the theory of A.A concerns the formation of free atoms from the sample, which are in an unexcited ground-state level and this absorption of radiation.[164])

Because most of the atoms remain in the ground-state, absorption is greatest for resonance lines resulting from transitions originating from the ground-state and this therefore, greatly restricts the number of absorption lines that can be used in the atomic absorption. The degree of absorption depends on the population of atoms in the ground-state and the ability of these absorbing atoms. Such a degree of absorption is an expression of the line intensity and represents the probability that an atom will undergo a transition per unit time.

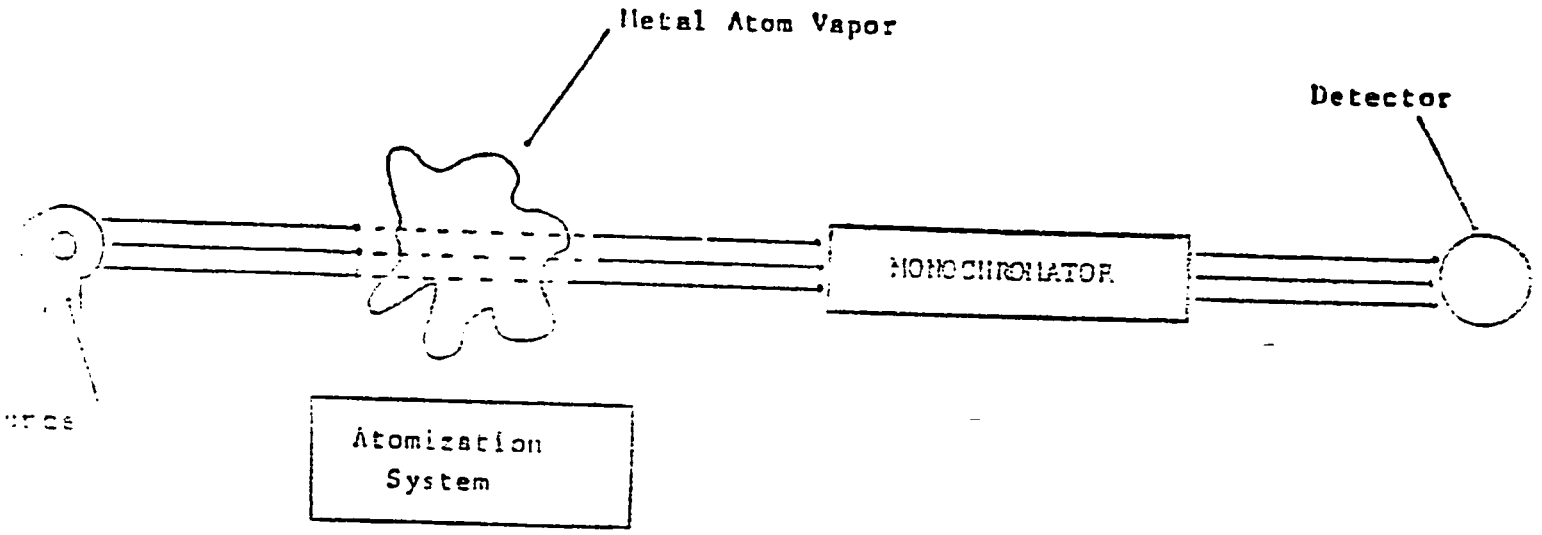

Figure AP1. A schematic Presentation of the Concept of Atomic Absorption Spectroscopy.

The degree of absorption is a function of the concentration of the metal in the sample while the absorption follows the Beer's Law where the absorbance is directly proportional to the path length in the flame. Both of these variables are difficult to determine. However, the path length can be held constant and the concentration of the atomic vapor is directly proportional to the concentration of the analyte in the solution being aspirated. [165,166]

Similarly to Lambert's law, we have:

$$I = I_0 \exp(-K_\nu B)$$

Where: I = intensity transmitted by the sample

I_0 = incident Beam

K_ν = absorption coefficient characterizing the intensity

B = horizontal path length of the flame or thermal source

Since the physical property actually is measured in absorbance A, we then have:

$$A = \log(I_0 / I) = K_\nu \log e = 0.4343\ K_\nu B$$

The absorbance is directly proportional to the absorption coefficient K_ν which is directly proportional to the number of absorbing atoms and therefore to the concentration of the solution. Thus, plots of absorbance at the specified wavelength against concentration should yield a linear relationship.

A.1.2 Instrumentation

There are two parts with essentially different functions: the means whereby the population of ground-state atoms is produced from the sample and the optical system. The basic components of an A.A spectrometer include: 1) A radiation source to emit the spectral line of the element of interest, 2) An atomization system (flame or furnace) to provide sufficient energy for analyte dissociation and vaporization as free atoms, 3) A monochromator for spectral dispersion and isolation of the spectral lines to be measured and 4) A detector and data- logging device to measure, amplify and display the results.

The most critical component of an A.A spectrophotometer is the source. The hollow cathode lamps which have been used almost exclusively as the radiation source for most elements, emitting strong sharp lines of appropriate wavelength characteristic of the desired element. This radiation then passes through a flame into which the sample solution is sprayed as a fine mist. Under the experimental conditions, the predominant ground-state atoms, thermally generated by the flame, absorb the resonance radiation from the source lamp and reducing hence the intensity of the incident beam.[167]

The monochromator and the slits isolate the desired resonance line from other radiations emitted by the source and allow it to fall in the photomultiplier detector which then converts the light signal into an electrical one. Since the range of wavelengths detected is determined primarily by the hollow-cathode source, the monochromator and slits serve primarily to minimize the detected background radiation from the flame and also to remove extraneous lines emitted by the hollow cathode filler gas. The emitted radiation corresponding

in wavelength to the monochromator setting is inevitably present in the flame, due to excitation and emission by the analyte atoms. The thermally excited emission by the analyte atoms is therefore discriminated by modulating the source of radiation and using an AC amplifier: the unmodulated emission is not detected. The signals generated by the photoelectric detector are amplified by an amplifier tuned to the frequency of modulation while the radiation emitted by the flame is not modulated, and gives therefore no resulting output signal. [168]

Since reducing the sample to the free atomic state, it is necessary to achieve absorption by atoms, the most common atomization device spectroscopy consists of a nebulizer and a burner.[169] The nebulizer converts a sample solution into a fine spray or aerosol which is then fed into the flame. The analyte solution is first aspirated from the sample container through a capillary tube by suction (Venturi action) caused by the rapid flow of support gas (oxidant) past the capillary tip. The resulting aerosol is then mixed with the fuel and flows past a series of baffles which remove all but the finest droplets. The flame evaporates the solvent, decomposes and dissociates the molecules into the ground-state atoms. Its use as the atom cell in analytical A.A is at present, by far the most widely used method to obtain a population of free analyte atoms.

A.1.3 Atomic Absorption Analysis

A Perkin-Elmer model 503 AA spectrophotometer utilizing a double-beam optical system and Perkin-Elmer 56 digital recorder were used. The dispersion optical system included also a high quality diffraction grating monochromator.

A laminar flow (Premix) burner was used, equipped with two single-slot burner heads: a 10-cm long for air-acetylene and 5-cm long for nitrous oxide-acetylene, respectively. The burner heads were held in place by stainless steel cables and a safety pin interlock. [170]

AP.2 X-Ray Powder Diffraction (XRD)

A.2.1 Theory

X-Ray diffraction is a very powerful technique, it is used for phase identification, quantitative phase analysis, structure determination and the study of the crystallinity of solids. Knowing that zeolites are crystalline micropore solids whose catalytic properties, such as unique shape-selectivity, homogeneity and porosity, depend on their structural integrity and crystallinity, so it is important that zeolites exist in a form in which they possess their highest crystallinity, chiefly for the purpose of exercising their maximum advantages in shape selective catalytic reactions. [171]

We could define a crystal type in terms of the lengths of the sides of its smallest repeating structure which is called a unit cell. The regular repetition of he unit cell gives rise to planes throughout the crystal and so each crystal structure is characterized by a very unique set of families of parallel planes at different orientations. The d-spacing is the distance between two adjacent planes of a given family (see figure AP 2). So each crystalline material is characterized by a unique set of d-spacings. Since the wavelengths of x-ray are of the same order of magnitude as the interplanar spacings and can be constructively scattered from them to give a diffraction pattern, a unique x-ray pattern for each crystalline material can be obtained which allows for the identification of the crystalline materials. [172]

An x-ray beam incident on a crystal will be diffracted by the regularly repeating array of scattering centers which are electron clouds surrounding the atomic nuclei in the crystal. As shown from figures AP 3 and AP 4, the angle throughout which the x-ray diffracts depends upon the spacing between planes of the atoms in the crystal.

Hence, Bragg's equation was derived as follows:

$$N\lambda = 2d \sin \theta$$

where: N= an integer expressing the order of diffraction.

λ = x-ray wavelength

θ = angle of diffraction

d = interplanar spacing

One of the methods which is the most frequently used for phase identification is the powder method. The single crystal diffraction method is much better suited for crystal structure determination. We could get a diffraction pattern of all possible planes, if a monochromatic beam of x-rays strikes a fine homogeneous powder, which is formed from an enormous number of small crystallites randomly oriented in every possible direction. What is expected is that a certain number are oriented in such a way that Bragg's condition for diffraction is fulfilled from every possible interplanar spacing.

The main objective of an x-ray powder diffractometer is to measure the intensity of the diffracted x-rays as a function of the angle θ between the incident beam and the surface of the sample. The θ angle is called the Bragg angle and typically instruments give the intensity of x-rays versus 2θ. The 2θ values which are the angles between the incident beam and the diffracted beam can be converted to d-spacings using Bragg's relation. [173]

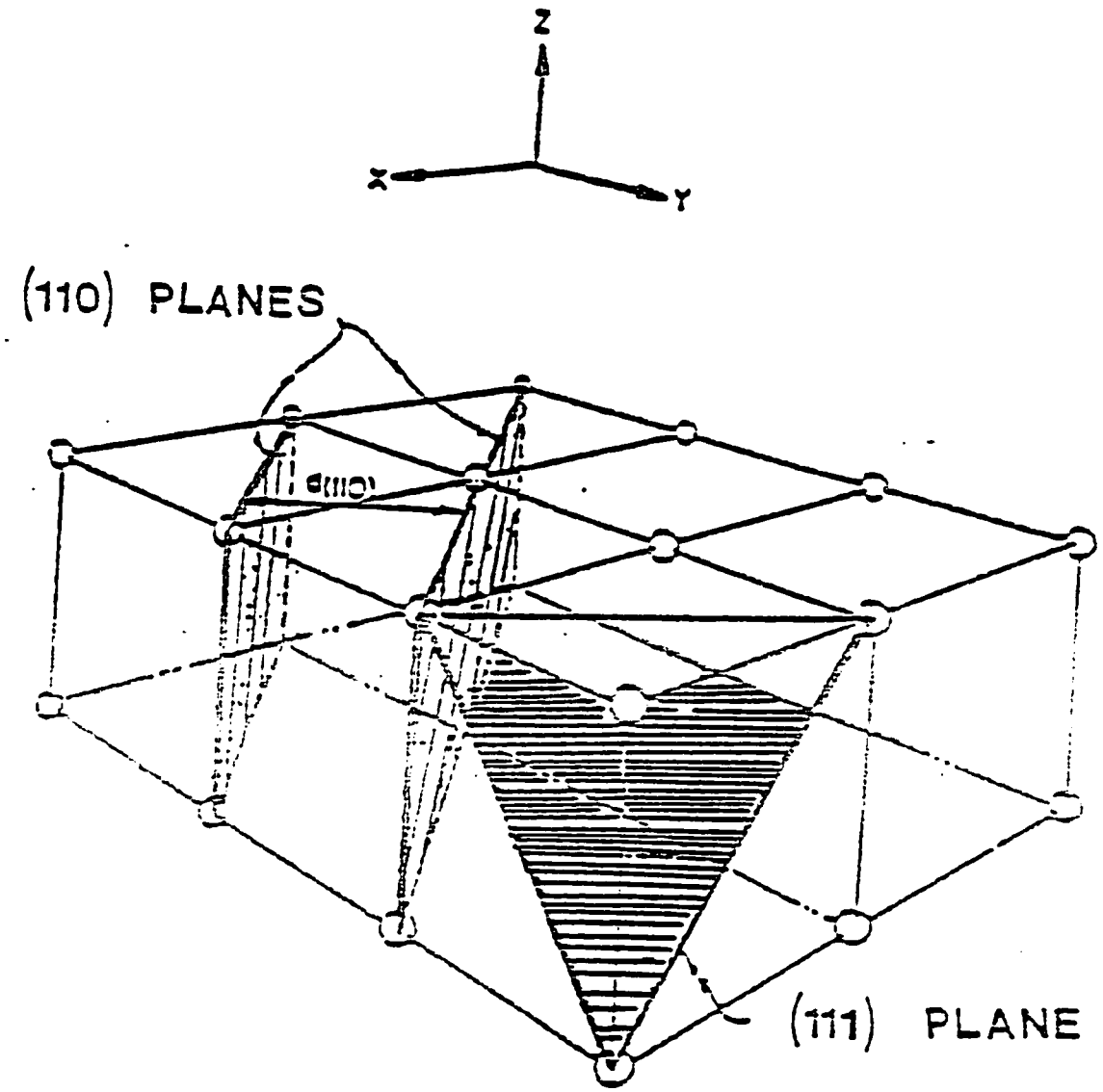

Figure AP 2 Representation of a Simple Cubic Crystal Structure Showing Atoms, two adjacent (110) planes and the interplanar spacings d(110) between them.

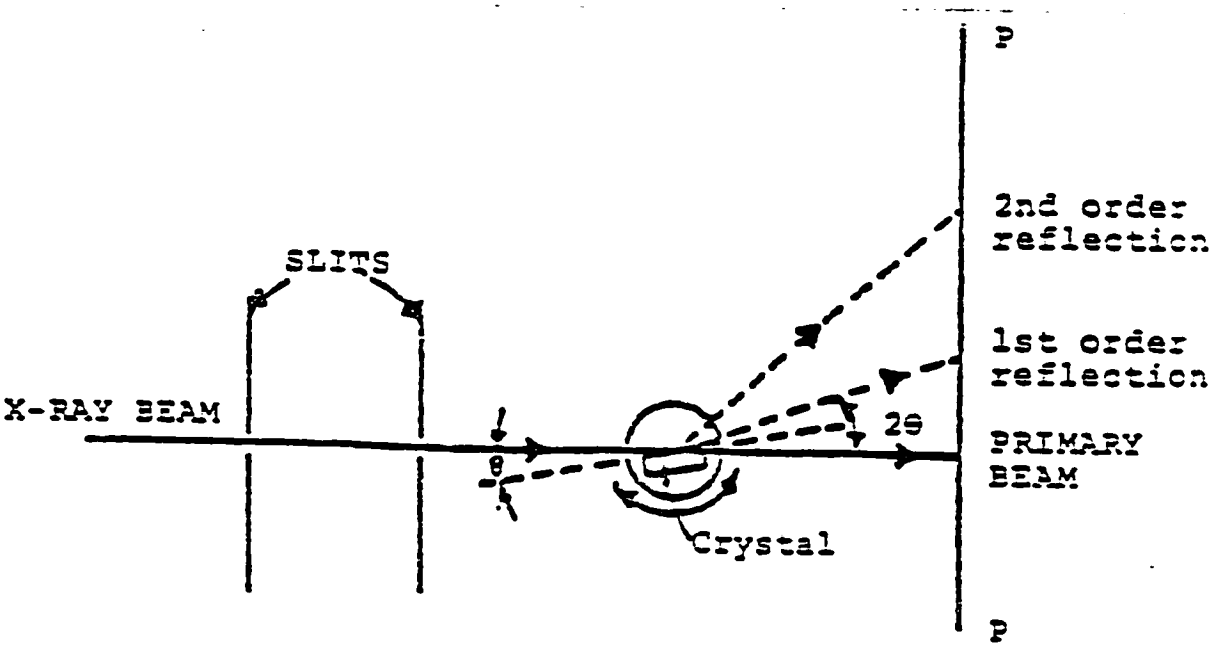

Figure AP 3 Diffraction of Radiation from a Crystal

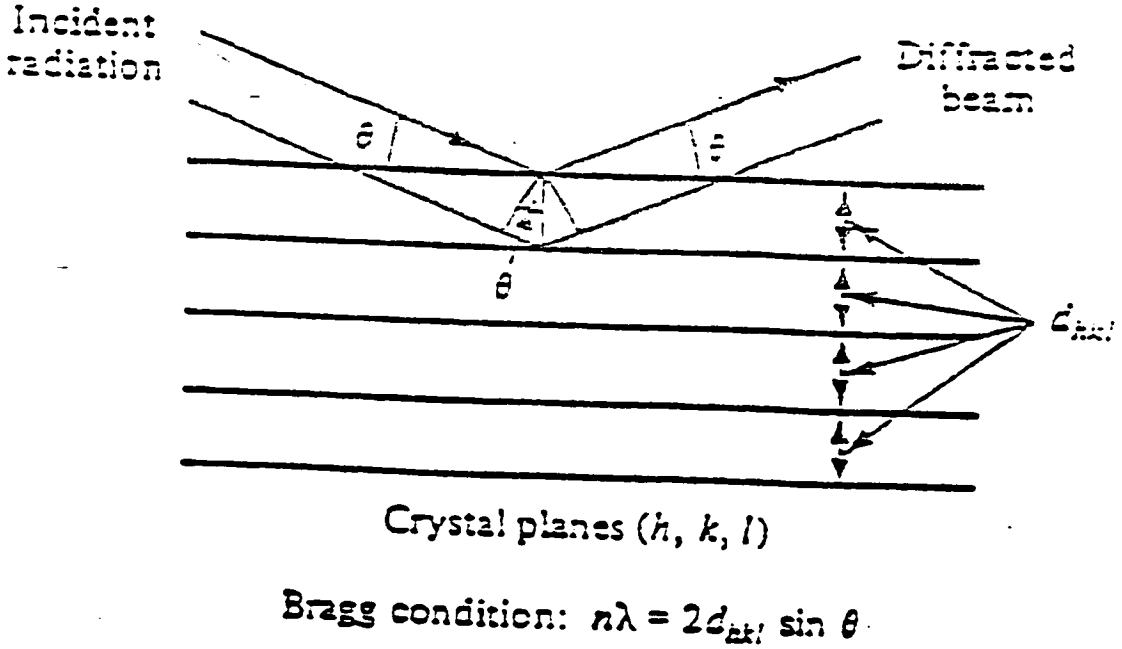

Figure AP 4 Reflexion Analogy of X-Ray Diffraction

A.2.2 XRD Analysis

We used a Phillips PW 1050/25 automated x-ray powder diffractometer which was powered by a Phillips x-ray generator line focusing goniometer and a scintillation counter. The measurements were done using a Philips long fine focus copper x-ray tube. Copper K_α monochromatic radiation with $\lambda = 1.5418$Å was obtained by using a nickel filter. The data acquisition was carried out using the step scanning mode and was computer controlled using the Sie 112 software from Sietronics. Peak determination and background removal was all done using the Sie 112 software. [174]

AP 3 Differential Scanning Calorimetry and Thermal Gravimetric Analysis

A.3.1 Theory

Almost all physical and chemical phenomena come with a certain amount of thermal energy. Heat is the most common energy form. Reactions of combustion or nuclear give off large amounts of heat, but other reactions that give off smaller amounts of thermal energy are probable as important. There are two points that need to be considered: a) From a point of view of thermodynamics where the time factor id not considered, there is a measure of the exchanged energy between a system and its external environment. This helps us determine the interatomic and intermolecular bond energies.

b) From the thermokinetic point of view, the time factor is considered.

What is important to determine is the amount of thermodynamic energy produced, this will help us better understand the solid materials.

The methods that are used to study these phenomena are called :

1)Differential Thermal Analysis(DTA) and 2) Thermal Gravimetric analysis (TGA)

Differential Thermal Analysis involves the measure of the physical-chemical change of solid materials that are put in conditions are gradual increases of heat, which is then followed by exothermic or endothermic energy. This technique works by measuring the temperature difference between a reference material are measured in function of the temperature. While both of these materials are put through the same heating conditions. The information that is determined, tells us something about the energetics of the sample.

The principal on how the technique work is very simple, it consists of heating a sample and a reference which is usually inert as shown in figure AP 5. The difference in energy between the two is measured and the difference in temperature is recorded as ΔT. The temperature the sample is put through is constantly measured as shown in the figure.

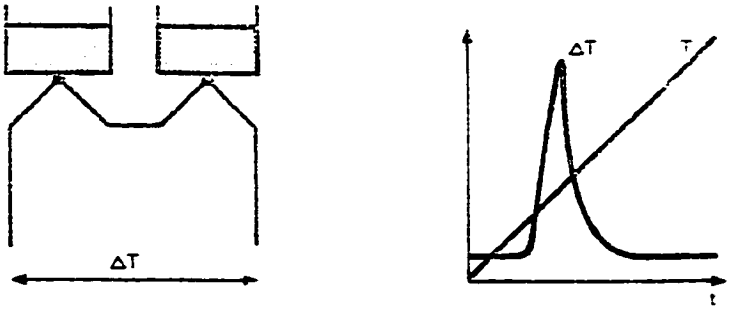

Figure A.P 5 The Principal of the DTA Technique with the Results Graph it Produces.

This is fundamentally different from what is learned from the gravimetric analysis (TGA). Most physical and chemical phenomena are characterized by variations in the weight of the sample when they are heated for example. A precise weight is taken at the start before any heating. Then, while heating is occurring the weight is constantly measured. Thermogravimetric analysis is the study of a sample from its variations of weight when this sample is put through a specific thermal environment. The method considers that the variation in weight will occur between the sample, its external environment and vice versa.
This method uses a magnetic balance, which measures the weight continuously and precisely. An oven that could go up to fairly high temperatures is used and it is linked to a computer with the proper software that converts the information into curves that will help us understand the sample's characteristic.[175]

Differential Scanning Calorimetry (DSC) measures the direct heat. It inform us on the transformation energies of the sample. This method works well for gases, ionized solutions or a heterogeneous solid. Determining the thermodynamic energies that are involved when a sample is heated will give us information on the enthalpy, specific heat produced and these will help us determine the entropy and the internal energy.

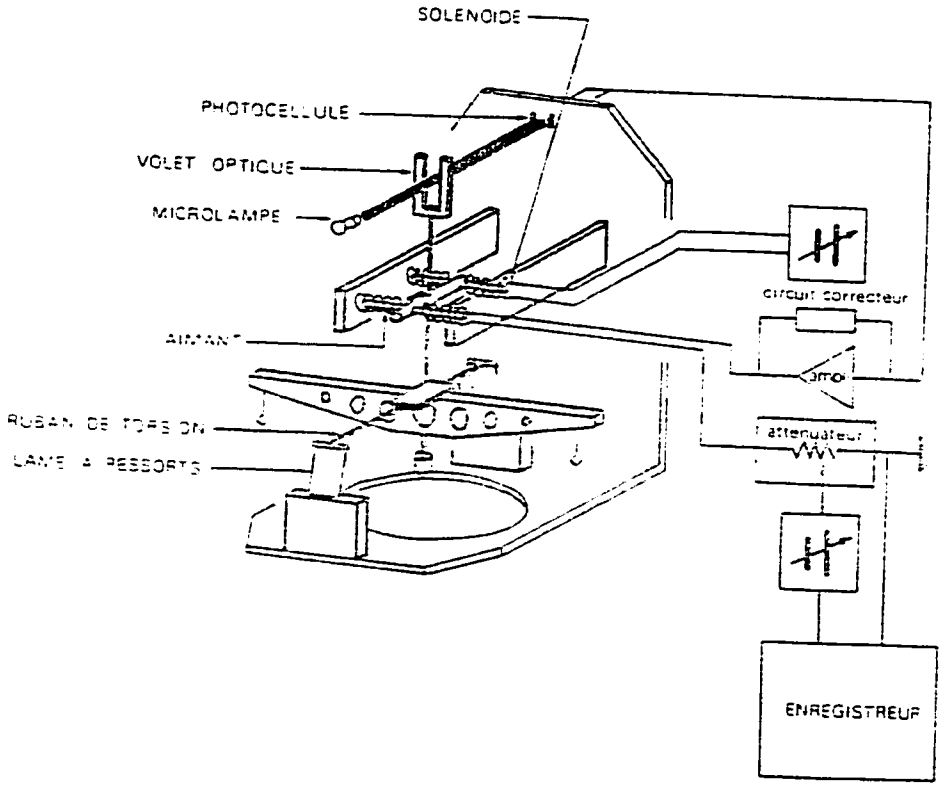

Figure A.P 6 Representation of a Typical Balance used in the DTA TGA instrument

A.3.2 DTA/TGA Analysis

We used the Universal V3.3B DSC/TGA Instruments to perform the analysis of our samples. The crucibles used were made of aluminum.

AP 4 The B.E.T Method

A.4.1 Specific Surface Area

The most useful method to determine the total surface area of solid material which requires non-specific physical adsorption, is called the B.E.T method for Brunauer, Emmett and Teller. The surface area is a very important textural parameter of a solid, can be used to define the morphology and surface characteristics. The specific surface area (A) is the measure of the accessible surface area per unit mass of solid, where the surface is the sum of the internal surface area associated with pores and of the external surface area developed by the outer boundary of the particles.[176,177]

The determination of A includes the following steps:

1) Setting up the adsorption isotherm by measuring the volume of nitrogen adsorbed versus the relative pressure of the adsorbate, 2) Evaluating the monolayer capacity (V_m) from the isotherm, 3) Converting V_m into A by means of the molecular area (A_m).

The theory of B.E.T is based on a kinetic model of the adsorption developed by Langmuir (A_{14}) in which the surface of the solid is regarded as an array of adsorption sites. The B.E.T theory is based on the following three assumption:

A) There is no interaction between molecules adsorbed in the first layer of a homogeneous surface with equivalent sites for localized adsorption. B) Each molecule in the first layer is a possible site for adsorption of a molecule in the second layer, and so on in order to get multilayer adsorption. C) With the exception of the first layer, the heat of adsorption is equal to the molar heat of condensation and the evaporation-condensation conditions are identical in all others.

The physical and mathematical treatment of these hypothesis leads to the following B.E.T equation:

$$P/V(P_0-P)= (C-1)P/V_mCP_0 +1/V_mC$$

where: P = is the equilibrium pressure of the adsorbate.

P_0 = Saturated vapor pressure of the adsorbate in the condensed state.

V = Volume of the gas adsorbed at Standard Temperature and Pressure.

V_m = Volume of gas at STP corresponding to the formation of a monolayer coverage.

C = A constant varying with the adsorbent-adsorbate interactions which is related to the differential heat of adsorption E_a, and to the heat of liquefaction E_L, by the following:

$$C = Exp.\ (E_A-E_L)/RT$$

Where: R = Ideal Gas Constant

T = Absolute Temperature

The graph of $P/V(P_0-P)$ versus P/P_0 at a pressure range of $(0.05<P/P_0<0.35)$ should give a straight line hence, from which one should be able to derive C and V_m. As mentioned previously, the B.E.T method for calculation of a specific surface area (A) involves two additional steps:

A) Evaluation of the monolayer capacity (V_m) from the isotherm. To obtain a reliable value of Vm from the isotherm, it is necessary that the monolayer be virtually complete before the build up of additional layers start: which is met if the B.E.T parameter C is neither too low not too high.

B) Conversion of V_m into A by means of the molecular area (A_m). Since nitrogen comes the closest to meeting these conditions when adsorbed on an extensive range of solids, it has become the most generally used adsorbate for surface area determination. The specific surface area of the adsorbent is then given by:

$$A = A_m (V_m * N)/V$$

Where: N = Avogadro's Number

A_m = Area occupied by one molecule of adsorbate A_m (N_2) of 16.2Å^2 is the widely accepted value.

A.4.2 Pore Size Measurement

The pore size distribution is defined as the distribution of the specific area versus the pore size . It is an important textural parameter for the determination of morphology and pore structure of a porous solid . Depending on the pore size range of a solid , the appropriate technique is applied. [178]

Techniques based on nitrogen adsorption/desorption isotherms make use of the desorption loop of an adsorption isotherm to relate the amount of adsorbate lost in a theoretical desorption step to the average size of a the pore emptied in the step. A pore loses its condensed liquid adsorbate at a pressure related to the pore radius by the Kelvin equation on the assumption of cylindrical pores when the adsorbate surface tension, contact angle and molar volume being known for the adsorption temperature .

However , even when a pore has been emptied of condensed liquid , multi-layers of adsorbed molecules remain on the inner surface of the pores and these multi-layers continue to thin

down as desorption proceeds . Therefore , the measured desorption is made up of removal of condensed liquid from some pores , plus the adsorbate lost from the surfaces exposed in earlier steps .

The classical method consists of adsorption of N_2 at saturation under liquid nitrogen and then by applying vacuum , the adsorbed adsorbate is generally removed . At $P/P_0 \rightarrow 1$ where P_0 is the saturation pressure , all the pores are completely filled with adsorbed and condensed nitrogen . When the pressure is lowered by small increments , a small amount of nitrogen will first evaporate from the meniscus formed at the ends of the larger pores . Hence , a desorption isotherm of volume desorbed versus pore radius is established . The pore size distribution of a mesoporous solid may be calculated from the desorption isotherm of a vapor with the help of the Kelvin equation :

$$\ln P/P_0 = -2\, nV/RT * 1/r_K \cos\theta$$

Where : P/P_0 = the relative pressure of vapor in equilibrium with a meniscus having a radius of curvature r_K .

n = the surface tension of liquid adsorbate .

V = the molar volume of liquid adsorbate

R = ideal gas constant

T = the absolute temperature

θ = the contact angle between the capillary condensate and the adsorbed film on the walls .

The concept of capillary condensation and its quantitative expression in the Kelvin equation is , indeed the basis of virtually all the various procedures for the calculation of pore distribution.[179] When capillary condensation occurs during the course of isotherm determination, the pore walls are already covered with an adsorbed film , having a certain thickness (t) determined by the value of the relative pressure . Capillary condensation therefore , does not occur directly in the pore itself but rather in the inner core (fig. AP 7).

The conversion of an r_K value to a pore size requires recourse to a model of shape and a knowledge of the angle of contact θ (it is assumed that $\theta = 0$ hence $\cos \theta = 1$) .
Several methods which make use of Kelvin's equation and attempts to correct the Kelvin radius have been proposed . However , all these computation methods can give an accurate assessment and measurement of the macro- and mesopores but not the micropores .

Pore size distributions can be computed using a simplified model proposed by Pierce [220] , based on the application of Kelvin's equation to nitrogen desorption isotherms, from which the following is proposed :

1) All pores have cylindrical geometry .

2) The Kelvin equation is applicable for computing the pore radii from the relative pressures at which desorption occurs .

3) The film thickness remaining on pore walls after the inner capillary volume is desorbed in the same manner as on a non-porous surface at the same relative pressure (area of the core walls is identical to the area of the pore walls , as desorption progresses) .

By summing the values of pore area , γA_P , for each successive group of pores over the whole pore system , a value of cumulative surface area Scum = $\Sigma \gamma A_P$ is obtained [180] . And this

cumulative surface area reports the total area of macro- and mesopores and excludes the pore are of micropores since the validity of Pierce's method only extends down to a pore radius of 15Å .

A.P 4.3 Horvath-Kawazoe Method for Micropore Size Measurement

Dollimore and Heal [181] gave a criticism of the previous methods that were used for the calculation of pore size distribution. They pointed out that these methods also had some problems when pores approached molecular dimensions, because of the use of the Kelvin equation.

Horvath and Kawazoe [182] used molecular-sieved activated carbon which usually contains slit-like pores of the order of 1Å and the distances between the walls of the slits are of the interest from the standpoint of separation processes.

In the micropore domain, the so-called "outer surface" of carbon atoms may be regarded as " the effective radius of the carbon atom".[182] Therefore, the pore size itself must be called "effective pore size". This definition by Everett is in use in the case of micropores.

The micropores of molecular sieve materials are usually considered to be slits between two graphitized carbon layer planes.[184] Supposing that the potential field of these layers can be approximated by a potential of the graphite layer, simple mathematical expressions may be used.

$$RT \ln (P/P_0) = V_0 + P_a \qquad (1)$$

where: Pa = adsorbate-adsorbate-adsorbent interaction

V_0 = Adsorbent-adsorbate interactions

The potential function [183] over a graphite surface, which is the interaction energy between a gas molecule and an infinite graphite layer :

$$\Phi = 3.06\ \Phi^* [- (\sigma/r)^4 + (\sigma/r)^{10}] \qquad (2)$$

where: σ = distance between a gas atom and the surface at zero interaction energy.

r = distance from surface.

N_s = Number of atoms per unit of surface

A_s = Constant given by Kirkwood-Muller

$\Phi^* = (N_s A_s / (3.06) (2\sigma^4)$

The potential function between 2 parallel layers in the case of one adsorbate molecule is :

$$\Phi = [(N_s A_s/(2\sigma^4)] [- (\sigma/r)^4 + (\sigma/r)^{10} - \{\sigma / (l-r)\}^4 + \{\sigma / (l-r)\}^{10} \qquad (3)$$

where : l = distance between the nuclei of the 2 layers

The Frenkel-Halsey-Hill theory [184-188] uses the Kirkwood-Muller expressions for the calculation of adsorption potential. A similar expression is used for the present case of adsorption on 2 parallel surfaces. The potential originated from the interaction of the adsorbate molecules in a pore, increases the interaction energy. The potential function between the two carbon layers filled with adsorbate is:

$$\Phi = N_s A_s + N_A A_A / 2\sigma^4 * [- (\sigma/r)^4 + (\sigma/r)^{10} - \{\sigma / (l-r)\}^4 + \{\sigma / (l-r)\}^{10} \qquad (4)$$

They end up with the following equation:

$$RT \ln (P/P_0) = K N_a A_a + N_A A_A / \sigma^4 (l-d) * [- (\sigma^4/3(l-d/2)^3 + (\sigma^{10}/9(l-d/2)^9 - \{\sigma^4 / 3(d/2)\}^3 + \{\sigma^{10} / (d/2)\}^9] \qquad (5)$$

(where $l > d$) , this gives a finite value for P/P_0 and P_c/P_0

Having used the data of nitrogen isotherm at liquid nitrogen temperature, where the $W/W_\infty = q(P)$. The expression is :

$$W/W_\infty = f(l-d_a) \qquad (6)$$

This function gives us the effective pore size distribution, since W is considered as the mass of the nitrogen adsorbed into pores smaller ($l-d_a$), the pore size distribution is obtained.

Dollimore and Heal [181] have stated that about 15Å is the lower limit of their method in the case of cylindrical pores, and in the lower interval it gives undoubtedly poor values. The Horvath-Kawazoe model gives poor values for larger pores. The 2 models together cover the full range of pore sizes.

A.4.4 Measurement For Micropores

For macroporous (pore sizes > 500 Å) and mesoporous (pore sizes within the range of 20-500 Å) , the BET surface area can be obtained without limitations . However in the presence of large quantities of micropores (pore sizes < 20 Å) such as the ones we find in the ZSM-5 zeolite , it becomes more practical to apply the Langmuir isotherm for estimating the Langmuir surface area . Since the size of the adsorbate molecules is of the same order as the pore sizes , a free multilayer adsorption such as occurs in the BET theory does not occur without perturbation by interactions between the Walls of the zeolite . Because the Langmuir treatment gives a more practical assessment of surface area , the Langmuir surface area has also been reported .

The micropore size distribution was determined by the adsorption of argon at 87K using the Micrometrics model ASAP 2000m and the data interpretation model by Horvath Kawazoe [177] .

A.4.4 Instrument Used

The ASAP 2000 system , as shown in figures AP 8 and AP 9 , is used for macro and meso pores analysis and it consists of either one or two analyzers and a multi-function control module . The separate internal vacuum systems are included in the analyzer : one port for sample analysis and two ports for sample preparation. Between the vacuum pump and the manifold in both the degassing and the analysis system, are located next to the in-line cold traps. The sample saturation pressure (P_0) tube is located next to the sample analysis port beneath which is conveniently located the automatically operated

elevator with the liquid nitrogen (LN_2) Dewar mount. Connectors are put near each sample preparation port for the mounting of heating mantles and thermocouples . Controls and indicators on a swing-open control panel can provide operation of the vacuum system , degas valves and heating mantles for sample preparation. The control module consists of a computer equipped with ASAP 2000 software.

For the micropore size measurement , we used the Micrometrics model ASAP 2000m . It determines the micropore size distribution by adsorption of argon at 87K and interprets the data using the model by Horvath and Kawazoe. The ASAP 2000m looks very similar to the ASAP 2000 , but the only difference lies in the fact that at the analysis port , the Dewar mount is filled not with N_2 but with liquid argon. The other obvious difference is that we have adsorption of argon instead of nitrogen .

The micropore size and distribution of the desilicated zeolites used for the optimization of the desilication procedure , and all other zeolite samples studied by this technique thereafter in this thesis, were calculated using more suitable values of the interaction parameter (IP) . These new values gave more accurate results than the empirical values to obtain the average values of the micropore sizes in the first samples studied by this technique. [189]

Moreover for the measurements of the BET and Langmuir surface area and for micropore size determination , an out gassing temperature of 150°C was used in order not to favor any advanced healing process which was observed to occur at high temperatures of activation. [189]

The interaction parameter as recommended by Horvath Kawazoe was 5.89 * 10^{-43} ergs/cm^4 for microporous solids [190] and by Micrometrics Corporation for zeolites was 3.19 * 10^{-43} ergs/cm^4 [191]. We found that for the ZSM-5 zeolites the best value for the IP was found to be 4.9 * 10^{-43} ergs/cm^4 for the Y zeolite 4.6 * 10^{-43} ergs/cm^4 and for the X zeolite 5.2 * 10^{-43} ergs/cm^4.

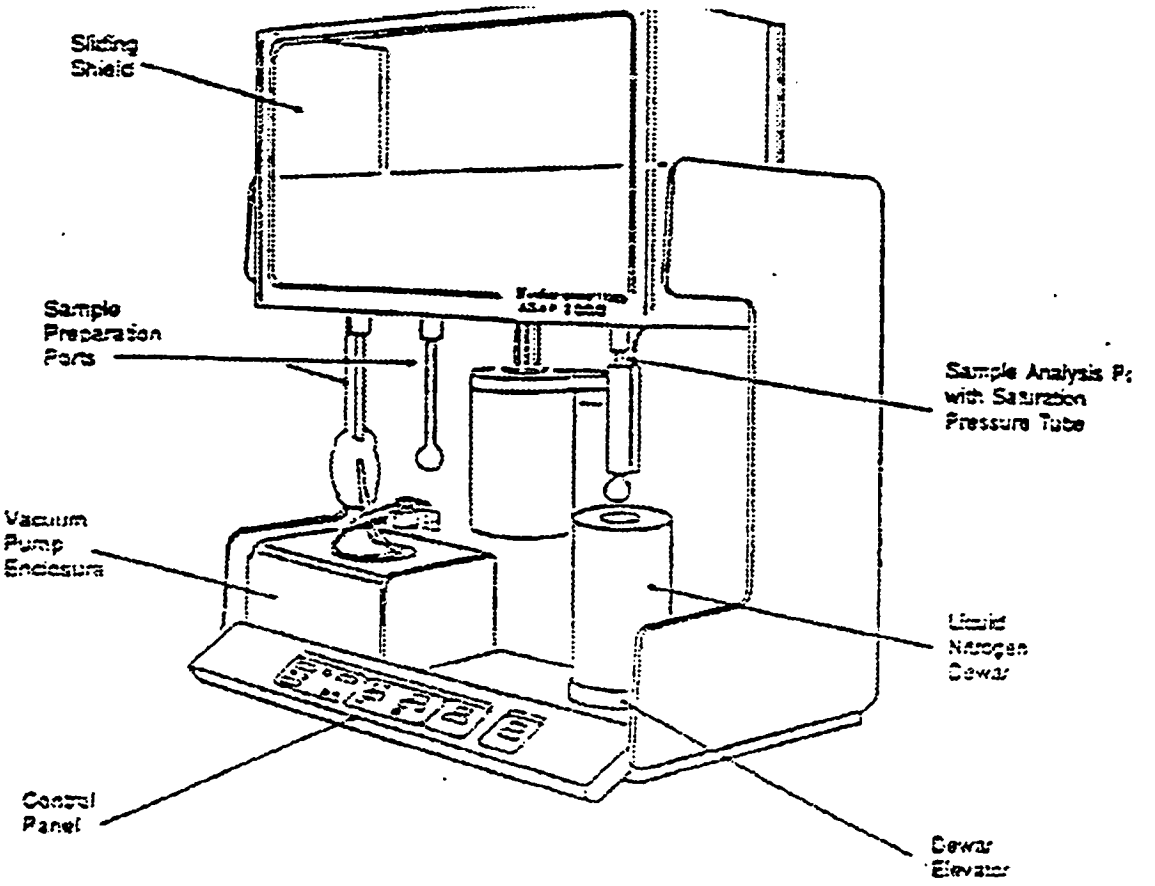

Figure AP 7 ASAP 2000 System

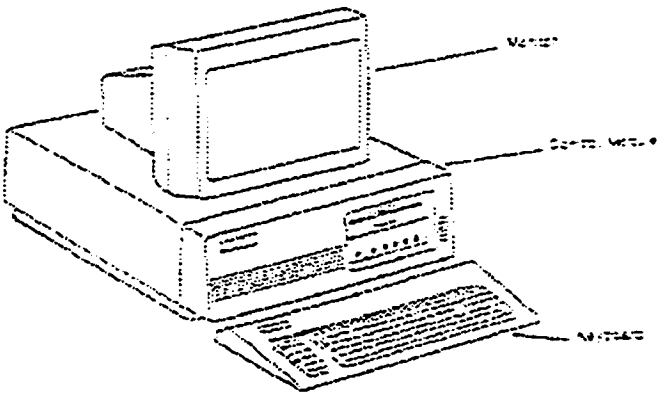

Figure AP 8 The Control Module

AP 5 The Fourier Transform InfraRed Spectroscopy

A.5.1 Introduction

For a long time, Infra-Red (IR) spectroscopy had been the mainly used spectroscopic technique to characterize zeolite and zeolite/adsorbate systems. Their study was reported in the literature before 1975 and they have been extensively reviewed by Ward. [192]

The main areas of application of IR spectroscopy have been and still are : i) investigation of framework properties, ii) study of sites of the zeolite lattice, being relevant, e.g., for adsorption or catalysis, iii) characterization of zeolite/adsorbate systems, and iv) measurements related to the motion of guest molecules in the pores and cavities of the zeolites. [193]

A.5.2 Some Theoretical Background

The electromagnetic section of the electromagnetic radiation covers the wavelength range from about $9x\ 10^2$ nm to $5x10^5$ nm. The units reciprocal centimeters or wavenumbers are usually preferred in IR spectroscopy. The range from 12000 cm^{-1} to 4000 cm^{-1} is called near infrared, that from 4000 cm^{-1} to 400 cm^{-1} is the far infrared region In order to interact with the e lectromagnetic radiation in the infrared range, the species exposed to it must have a permanent or induced dipole. Then the radiation can be adsorbed and excite certain states.

A.5.3 Principle of the FTIR Spectrometer

IR spectrometers measure the energy of the radiation transmitted through a sample as a function of the frequency. One distinguishes between dispersive and non-dispersive Fourier Transform Infrared spectrometers. The older design of dispersive instruments employs prisms or gratings as monochromators in order to select IR radiation of a certain frequency from the originally continuous radiation generated by the source. The dispersive spectrometers are generally double-beam instruments, where one beam (I_0) does not transmit the sample and is used for comparison. Due to a continuous rotation of the monochromator, which is coupled with the movement of the recorder device, radiation of successively changed frequency is directed to the exit slit, transmits the sample and reaches the detector. According to the interactions of the radiation with the molecules of the sample as the resonance frequencies the energy I received by the detector is, in comparison with that of the second beam I_0, lower at these frequencies. A plot of the transmittance vs. the frequencies provides the conventional IR spectrum with typical bands of decreased transmittance at certain frequencies.

The concept of a Fourier transform IR spectrometer is completely different. Here, the whole spectrum is obtained via a process of interference. The interference is provided by an "interforemeter" device, e.g., a Michelson interforemeter (see figure AP 10).
The polychromatic light, made parallel by the collimator, is directed to the sample S. One part of the light transmitted through the sample is reflected by the beam splitter and thrown to the fixed mirror, M1. The other part reaches the moving mirror, M2. Both partial beams are returned to point C where they interfer. After interference, half of the radiation is re-directed

to the source and is lost, the other half is directed to the detector. If, for a particular λ_i of the polychromatic light, the total pathway difference created by the movement of the mirror M2 is just λ_i, then the corresponding waves will be enhanced by the interference. If the total pathway difference is for instance $\upsilon_i/2$, the interference for that particular wave is destructive, the wave is extinct. Thus, after reflection at point C, the radiation of wavelength λ_i will create at the detector D a sinusoidal fluctuation of the energy. This holds for any wave of wavelength λ_i being included in the polychromatic light and transmitted through the sample. All the partial energy fluxes corresponding to the various λ_i's are superimposed to give the total energy arriving at the detector, thus generating a complex interferogram (see figure A.P 10).[194]

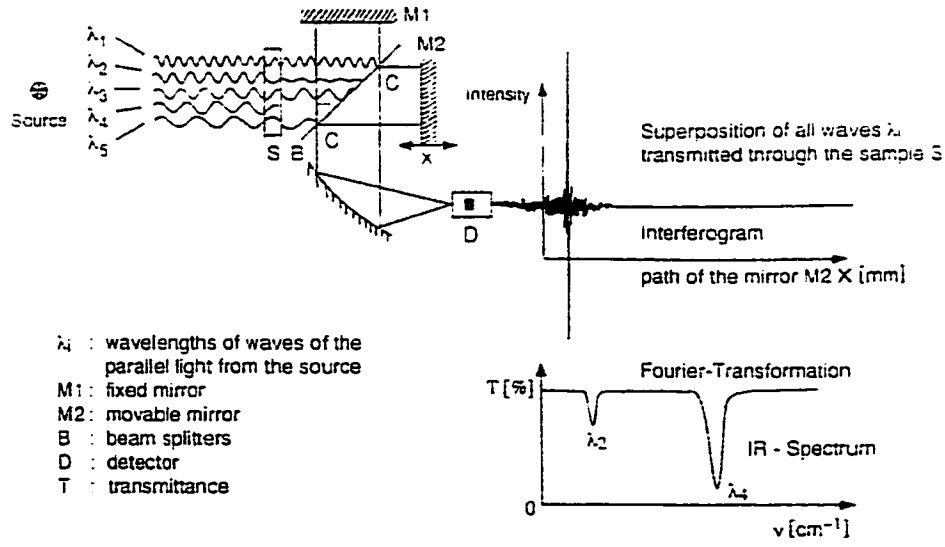

Figure AP 9 Scheme of the Principle of a Fourier Transform Infrared Spectrometer

A.5.4 Diffuse Reflectance IR Spectroscopy (DRIFT)

For a long time, IR spectroscopic studies on zeolites were almost exclusively carried out in the transmission mode. During more recent years diffuse reflectance spectroscopy, which used to play an important role in UV-visible spectroscopy on zeolites, has also been employed in IR studies. Pioneering work in this area was done by Kazansky and co-workers.[194-196] This method is especially helpful in exploring the near infrared region, where the transmission techniques essentially fail due to the severe scattering of the zeolite samples. However, this region is of great interest because, for example, of the occurrence of overtone and combination modes of the hydroxyls which might be studied with or without the use of probe molecules.

Two important requirements for successful diffuse reflectance measurements must be fulfilled: i) the sample must be sufficiently thick and large to avoid light loss by forward scattering at its edges; ii) scattering must be predominant compared with absorption so that illumination is essentially diffuse.

A.5.5 Instrument Used

The instrument used is a MB series Fourier Transform Spectrometer from Bomen. The MB series spectrometer is controlled by an acquisition software running on an external PC computer running Microsoft Windows®.

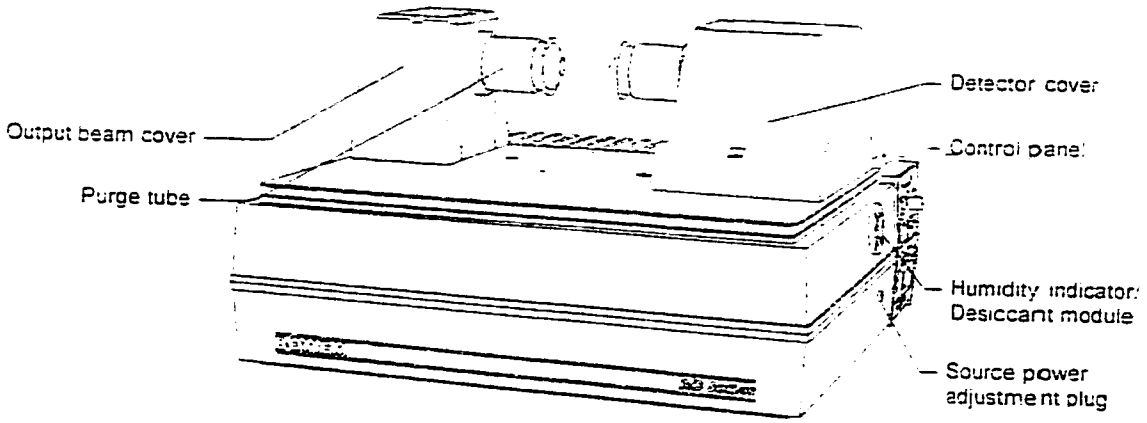

Figure AP10 MB Series Spectrometer with Arid-Zone Sample Station

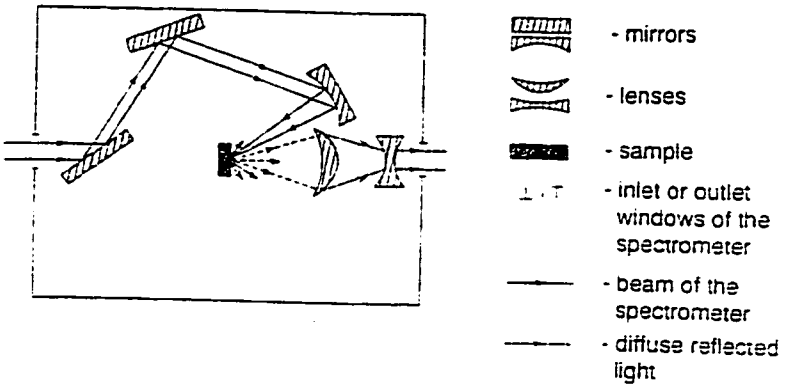

Figure A.P 11 Scheme of a unit for Diffuse Reflectance Infrared Spectroscopy

References

1. D. Breck, Zeolite Molecular Sieve-Structure, Chemistry and use, John Wiley and Sons; New York, 147 (1974).

2. E.F Vansant, " Pore Size Engineering in Zeolites", John Wiley and Sons; 8,113 (1990).

3. R. Le Van Mao, G. Denes, N.T.C. Vo, J.A Lavigne and S.T Le, "Production of porous materials by dealumination of alumina-rich zeolites", in Advances of porous materials Research Symposium; 371,**125** (1995).

4. J. Weitkamp and L. Puppe; Catalysis and Zeolites, "Fundamental and Applications", 357-358 (1999).

5. E.M Flanigen, H.A Szymanski and H. Khatami; adv. chem. ser.;101, 210 (1971).

6. A. Ramsaran, " Desilication ZSM-5 Zeolite as Catalyst for the dehydration of ethanol", Ph.D Thesis, Concordia University, 12 (1996).

7. Bruce C. Gates, "Catalytic Chemistry", John Wiley and Sons; New York, 397 (1992).

8.Bruce C. Gates, "Catalytic Chemistry", John Wiley and Sons; New York, 399 (1992).

9. D.E.W Vaugh, Chemical Engineering Progress, 25 (Feb.1988).

10. Von Ballmoos, R. Higgins, "Collections of Simulated X-Ray powder patterns for Zeolites"; International Zeolite Association Butterworth: London (1990).

11. N.Y Chen, T.F Degnan and C. Morris Smith; " Molecular Transport and Reaction in Zeolites"; 10-12 (1994).

12. R. Szostak, Molecular Sieves: "Principles of Synthesis and Identification",Van Nostrand reinhold Catalysis series, New York; 31 (1989).

13 N.Y Chen, T.F Degnan and C. Morris Smith; " Molecular Transport and Reaction in Zeolites"; 15 (1994).

14. J.T Richardson, "Principles of Catalyst Development", Plenum Press, New York and London; 177(1989).

15. Louis Hegedus, Alexis T. Bell, N.Y Chen and Werner O. Hagg, "Catalysis Design and Progress and Perspectives", Wiley Science Publications; 114 (1987).

16 M.E. Davis, Industrial Engineering Chemical Resources; 1775,**30** (1991).

17. D. Breck, Zeolite Molecular Sieve-Structure, Chemistry and use, John Wiley and Sons; New York, 475 (1974).

18. P.R Pujado, J.A Rabo, G.J Antos and S.A Gembicki, Catalysis Today; 13,**113** (1992).

19. N.Y Chen, T.F Degnan and C. Morris Smith; " Molecular Transport and Reaction in Zeolites"; 14 (1994).

20. J.T Richardson, "Principles of Catalyst Development", Plenum Press, New York and London; 177(1989).

21. Louis Hegedus, Alexis T. Bell, N.Y Chen and Werner O. Hagg, "Catalysis Design and Progress and Perspectives", Wiley Science Publications; 114 (1987).

22. D.E.W Vaughn, Chemical Engineering Progress; 27 (Feb 1988).

23. W.A Hagg, "Zeolites and Related Microporous Materials", State of the Art Studies in Surface Science Catalysis; 1375, **84** (1994).

24. R.J Farrauto, R.M Heck and B.K Speronello,"Hydrocarbon Processes"; 71, **31** (1992).

25. M. Iwamoto, "Zeolites and Related Microporous Materials": State of the art studies in Surface Science Catalysis"; 1395, **84** (1994).

26. A.T Bell, Chemical Engineering Progress; 26 (February 1995).

27. S. Ainsworth, Chemistry and Engineering; 34 (January 1994).

28. J. Armor; Chemtech 557 (September 1992).

29. M.E Davis, Industrial Engineering Chemical Resources; 1675, **30** (1991).

30. Z.Li, C. Lai and T.E Mallouk, Inorganic Chemistry; 178, 28 (1989).

31. S.M Scicsery, Zeolites; 202, **4** (July 1984).

32. R. Morrison and R. Boyd, Organic Chemistry 3rd edition, Allyn and Bacon inc.; 32-34 (1979).

33. S.M Scicsery, Zeolites; 206, **4** (July 1984).

34. Bruce C. Gates, Catalytic Chemistry, Wiley and Sons U.S.A; 269-270 (1992).

35. D.H Olson, W.O Haag and R.M Lago, Journal of Catalysis; 390, **61** (1980).

36. R. Morrison and R. Boyd, Organic Chemistry 3rd edition, Allyn and Bacon inc.; 32 (1979).

37. C.N Satterfield, "Heterogeneous Catalysis in Industrial Practice ", McGraw-Hill, 205 (1991).

38. R. Le Van Mao, S. Xiao and S.T Le, "Thermal Stability of the Platinum Bearing Superacidic Sulfate-Promoted Zirconia in the Presence of Hydrogen"; Catalysis Letters; 107-108, **35** (1995).

39. R. Morrison and R. Boyd, Organic Chemistry 3rd edition, Allyn and Bacon inc.; 40-41 (1979).

40. E. Brunner, K. Breck, M. Koch, H. Pfifer, B. Staudte and D. Zscherpel, "Zeolites and related Microporous Materials": State of the art studies of Surface Science Catalysis; 357,**84** (1994).

41. A. Ramsaran, "Desilicated ZSM-5 zeolite as Catalyst for the dehydration of ethanol", Ph.D thesis, Concordia University, 26 (1996).

42. H.Pfeifer, D.Freude and M.Hunger; Zeolites, 274, **5** (Sept. 1995).

43. J. Scherzer, Octane Enhancing Zeolite FCC Catalysts, Marcel Dekkar inc. 44 (1990).

44. A. Ramsaran, "Desilicated ZSM-5 zeolite as Catalyst for the dehydration of ethanol", Ph.D thesis, Concordia University, 28-29 (1996).

45. C.N Satterfield, "Heterogeneous Catalysis in Industrial Practice ", McGraw-Hill, 173 (1991).

46. D. Barthomeuf, Zeolites; 394, **14** (July-August 1994).

47. Bruce C. Gates, Catalytic Chemistry, Wiley and Sons U S.A, 470 (1991).

48. P. Batamack, C. Doremieux-Morin, R. Vincent and J. Fraissard, Journal of Physical Chemistry; 9779, **97** (1993).

49. J. Scherzer, Octane Enhancing Zeolite FCC Catalysts, Marcel Dekkar inc. 45 (1990).

50. R.M Dessau, E.W Valyocsik and M. Goeke, Zeolites; 776,12 (1992).

51. Bruce C. Gates, Catalytic Chemistry, Wiley and Sons U.S.A, 271 (1991).

52. N.Y Topsoe, K. Pedersen and E.G Derouane; Journal of Catalysis; 41,**70** (1981).

53. J.C Vedrine, A. Auroux, V. Bolis, P. Dejaive, C. Nacchache, P. Wierzchowski, E.G.B Derouane, J. Nagy, J.P Gilson, J.A.C Van Hoof, J.P Van de Berg and J.Wolthuisen, Journal of Catalysis; 248,**59** (1979).

54. M.E Davis, Acc. Chem. Res.; 111,**26** (1993).

55. D.H Olson, W.O Haag and R.M Lago, Journal of Catalysis; 390,**61** (1980).

56. W.O Hagg, " Zeolites and Related Microporous Materials", State of the art Studies in Surface Science Catalysis; 1375,**84** (1994).

57. D. Barthomeuf, Zeolites; 396,**14** (July and August 1994).

58. H. Pfeifer, Journal of Chemical Soc. Faraday Trans.; 3777,**84** (1988).

59. A. Ramsaran, "Desilicated ZSM-5 zeolite as Catalyst for the dehydration of ethanol", Ph.D thesis, Concordia University, 12-13 (1996).

60. C.N Satterfield, "Heterogeneous Catalysis in Industrial Practice ", McGraw-Hill, 171-173 (1991).

61.C.N Satterfield, "Heterogeneous Catalysis in Industrial Practice ", McGraw-Hill, 179 (1991).

62. S.M Sciesery, Zeolites; 202,**4** (July 1984).

63. D.W Breck, "Zeolite Molecular Sieves-Structure", Chemistry and Use, 2nd edition, Robert E. Krieger, Malabar Florida; 633-645 (1984).

64. B.B Bird, W.E Stewart and E.N Lightfoot, " Transport Phenomena", John Wiley and Sons, New York; 19-26 (1960).

65. R.C Reid, J.M Sherwood, "The Properties of Gases and Liquids", McGraw and Hill, New-York; 23-24 and 678-679 (1977).

66. D.W Breck, "Zeolite Molecular Sieves-Structure", Chemistry and Use, 2nd edition, Robert E. Krieger, Malabar Florida; 651 (1984).

67. C.N Satterfield, "Heterogeneous Catalysis in Industrial Practice ", McGraw-Hill, 207 (1991).

68. N.Y Chen, W.E Garwood and F.G Dwyer, "Shape Selective Catalysis in Industrial Applications, Marcel Dekkar inc.; 26-27 (1989).

69. Bruce C. Gates, Catalytic Chemistry, Wiley and Sons U.S.A, 269-270 (1991).

70. Bruce C. Gates, Catalytic Chemistry, Wiley and Sons U.S.A, 274 (1991).

71. J.A Moulin, P.W.N.M Van Leeuwen, R.A Santen, Studies in surface science and Catalysis; 262,**79** (1993).

72. R.L Gorring, " Diffusion of Normal Paraffins in Zeolite T", Journal of Catalysis, 17-24,**31** (1973).

73. C.D Chang, A.J Silvestri; Journal of Catalysis; 249,**47** (1977).

74. L. Bernhard, A. Martin, H. Gunsehel and S. Nowak; " Formation of lower Olefins from Methanol and Hydrocarbons over modified zeolites", Microporous and Mesoporous Materials; 145,**29** (1999).

75. C.T-W. Chu and C.D Chang; " Methanol Conversion to Olefins over ZSM-5"; Journal of Catalysis; 299,**86** (1984).

76. C.D Chang in: " Handbook of Heterogeneous Catalysis"; ed. H. Knozinger, J. Weitkamp;1894, **4** (1995).

77. M. Stocker; "Methanol-to-Hydrocarbons: Catalytic Materials and their Behavior"; Microporous and Mesoporous Materials; 27,**29** (1999).

78. C.N Satterfield, "Heterogeneous Catalysis in Industrial Practice ", McGraw-Hill, 254 (1991).

79. C.N Satterfield, "Heterogeneous Catalysis in Industrial Practice ", McGraw-Hill, 267 (1991).

80. W.G Appleby, J.N Gibson and G.M Good; Ind. Eng. Chem. Process Development; 102,**1** (1962).

81. E.G Derouane; Studies in Science Catalysis; 221,**20** (1985).

82. J.B Butt, S. Delgado-Diaz and W.E. Muno; Journal of Catalysis; 158,**37** (1975).

83.J.B Butt; Journal of Catalysis; 190,**41** (1976).

84. M.Guisnet, P. Magnoux; Pure Applied Catalysis; 59,**1** (1989).

85. C.N Satterfield, "Heterogeneous Catalysis in Industrial Practice ", McGraw-Hill, 254 (1991).

86. E.F. Vansant, " Pore Size Engineering in Zeolites", John Wiley and Sons, New-York, 1 (1990).

87. A. Dyer, "Introduction to Zeolite Molecular Sieve", John Wiley and Sons, New-York, 125 (1988).

88. N.Y. Chen, W.W. Kaeding and T. Dwyer; Journal of American Chem. Soc.; 6783,101 (1979).

89. A. Corma, "Zeolites in Oil Refining and Petrochemistry in zeolite microporous solids: Synthesis, structure and reactivity, Kluswer Academic, The Netherlands, 173 (1983).

90. W.W Kaeding, L. Chu, C. Young, L.B. Weinstein, S.A Butter; Journal of Catalysis; 159,**67** (1981).

91. N.Y Chen; Journal of Catalysis; 17,**114** (1988).

92. L.B Young, S.A Butter and W.W Kaeding; " Shape-Selective Reactions with Zeolite Catalysts", Journal of Catalysis; 421,**76** (1982).

93. G. Mirth, J. Lercher; " On the Role of Product Isomerization for Shape- Selective Toluene methylation over H-ZSM-5", Journal of Catalysis; 199,**147** (1994).

94.D. Zakett, A.E Schoen, R.W Kondrat, R.G Cooks; " Para-Aromatic reactions over Shape- Selective molecular Sieve Catalysts"; Journal of American Chemical Society; 22,**101** (1979).

95.G. Mirth and J.A Lercher; Journal of Catalysis; 24,**132** (1993).

96. D. Zakett, A.E Schoen, R.W Kondrat, R.G Cooks; " Para-Aromatic reactions over Shape-Selective molecular Sieve Catalysts"; Journal of American Chemical Society; 24,**101** (1979).

97. L.B Young, S.A Butter and W.W Kaeding; " Shape-Selective Reactions with Zeolite Catalysts", Journal of Catalysis; 422,**76** (1982).

98. W.W Kaeding, L. Chu, C. Young, L.B. Weinstein, S.A Butter; Journal of Catalysis; 163,**67** (1981).

99. T. Hibino, M. Niwa, Y. Murakami; Journal of Catalysis; 554,**128** (1991).

100. N.Y Chen, William E. Garwood and Francis G. Dwyer; Shape Selectivity on Industrial Applications; 97 (1989).

101. N.Y Chen, W.W Kaeding and T. Dwyer; Journal of American Chemical Society; 6784,**101** (1979).

102. M.B Sayed and J.C Vedrine; Journal of Catalysis; 43,**101** (1986).

103. N.Y Chen; Journal of Catalysis; 17,**114** (1988).

104.C. Benzouhanova, C. Dimitrov, V. Sinova, B. Spassov and H. Lerchert; Applied Catalysis; 149,**21** (1986).

105. G. Mirth and J.A lercher; Journal of Catalysis; 26,**132** (1993).

106. L.B Young, S.A Young and W.W Kaeding;" Shape-Selective Reactions with Zeolite Catalysts"; Journal of Catalysis; 422,**76** (1982).

107. T. Hibino, M. Niwa, Y. Murakami; Journal of Catalysis; 554,**128** (1991).

108. N.Y Chen, W.W Kaeding and T. Dwyer; Journal of American Chemical Society; 6783,**101** (1979).

109. T. Yashima, Y. Sakaguichi and S. Namba; "Proc. 7th Congr. Cat."; (1981).

110. J-H Kim, S. Namba and T. Yoshima; Bull. Chem. Soc. Japan; 105,**61** (1988).

111.D.Theodorou and J. Wei; "Diffusion and Reaction in blocked and High Occupancy Zeolite catalysts"; Journal of catalysis; 205-206,**83** (1983).

112.W.Karge; "Influence of the Zeolite pore structure on the Kinetics of the Disproportionation of ethylbenzene"; Microporous and Mesoporous materials; 113-119, **36** (2000).

113.N.R Meshram, S.G hedge and S.B Kulkarni; " Active sites on ZSM-5 zeolites for Toluene Disproportionation; Zeolites; 41,**6** (1986).

114. W.W Kaeding, C. Chu, L.B Young and S.A Butter; Journal of Catalysis; 392,**69** (1981).

115.L.B Young, S.A Butter and W.W Kaeding; " Shape-Selective Reactions with Zeolite Catalysts", Journal of Catalysis; 424,**76** (1982).

116.W.O Hagg and D.H Olson; U.S patent: 4,117,026 (1978).

117.P.B Weisz; Pure Applied Chemistry; 2091,**52** (1980).

118.W.W Kaeding, C. Chu, L.B Young and S.A Butter; Journal of Catalysis; 392,**69** (1981).

119.T. Hibino, M. Niwa, Y. Murakami; Journal of Catalysis; 551,**128** (1991).

120.T. Hibino, M. Niwa, Y. Murakami; Journal of Catalysis; 553,**128** (1991).

121. R.M Dessau, E.W. Valyocsik and N.H Goeke; Zeolites, 776,**12** (1992).

122.G. Letz, K.H. Schnabel, G. Peuker, W.Storck and J. Volter; Journal of Catalysis, 562,**170** (1994).

123. R. Le Van Mao, A. Ramsaran, S. Xiao and J. Yao; " pH of the sodium carbonate solution used for the desilication of zeolite materials"; Journal of Material Chemistry, 533, **5(3)** (1995).

124. R. Le Van Mao, S. Xiao, A. Ramsaran and J. Yao; " Selective Removal of Silicon form the Zeolite framework using sodium carbonate"; Journal of Material Chemistry, 609-610,**4(4)** (1994).

125. D.W. Breck, Potential uses of Natural and Synthetic Zeolites in Industry, Union Carbide Corporation Brochure, 25 (1979).

126. R. Le Van Mao, S. Xiao, J. Yao and A. Ramsaran; "Selective Removal of Silicon from Zeolite Frameworks Using sodium Carbonate", Journal of Material Chemistry, 605,**4(4)** (1995).

127. R. Le Van Mao, S. Xiao, A. Ramsaran and J. Yao; " Selective Removal of Silicon form the Zeolite framework using sodium carbonate"; Journal of Material Chemistry, 609-610,**4(4)** (1994).

128. R. Le Van Mao, P. Levesque, B. Sijiariel, N.T Do; Canadian Journal Chemical Engineering ; 462,**64** (1986).

129. R. Le Van Mao, E. Rutinduka, C. Detellier, P. Gougay, V. Hascoet, S. Tavakoliyan, S.V Hoa, T. Matsuura; Journal Of Material Chemistry, 783,**9** (1999).

130. D.W Breck, Zeolite Molecular Sieves: Structure, Chemistry, and use, Wiley and Sons, New-York , 634 (1974).

131. G. Horvath and K. Kowazoe,Journal of Chemical Engineering in Japan, 474,**16** (1983).

132.Tuan S. Le; " Development of Zeolite Based Acid Catalysts for the Synthesis of MTBE", Ph.D Thesis Concordia University, 67 (2000).

133. P.K Kipkemboi, "Preparation and Characterization of Leached Asbestos Materials", Msc. Thesis Concordia University, 177 (1988).

134.G.W Skeels and D.W Breck, " Proceedings of the 6th International Zeolite Conference", Butterworth-Heinemann, Stoneham Mass., 87 (1984).

135. S.B Kulkarni, V.P Shivalkan, A.N Kotasthane, R.B Borade and P.Ratnasamy, Zeolites,313, **2** (1982).

136.E.F. Vansant, " Pore Size Engineering in Zeolites", John Wiley and Sons, New-York, 16 (1990).

137.D.W Breck, Zeolite Molecular Sieves: Structure, Chemistry, and use, Wiley and Sons, New-York , 509 (1974).

138.S.I Jones and T.V Harris; Microporous and Mesoporous Materials,35-36, 34 (2000).

139. Dr. Le Van Mao and David Ohayon; " Methods for Pore Size Engineering in ZSM-5 Zeolite", Applied Catalysis A, 242, **217** (2001).

140.C.Doremieux-Morin, A. Ramsaran, R. Le Van Mao, P. Batamack, L. Heeribout, V.Semmer, G.Denes and J.Fraissard, Catalysis Letters,139, **34** (1995).

141.C. Doremieux-Morin, A. Ramsaran, R. Le Van Mao, P. Batamack, L. Heeribout, V.Semmer, G.Denes and J.Fraissard, Catalysis Letters,142, **34** (1995).

142.D.W Breck, Zeolite Molecular Sieves; Structure, Chemistry and use, Wiley and Sons N-Y,517-518 (1974).

143. R. Le Van Mao, D.Ohayon in M.M.J. Treacy, B.K Marcus, M.E Bischer, J.B Higgins; Proceedings of the 12th International Zeolite Conference, Materials Research Society, 1543,**3** (1999).

144.D.W Breck, Zeolite Molecular Sieves; Structure, Chemistry and use, Wiley and Sons N-Y,517-518 (1974).

145.R.Le Van Mao, T.S. Le, M. Fairbain, A. Muntassar, S. Xiao, G. Denes; Applied Catalysis, 41, **185** (1999).

146.R. Le Van Mao, S.T. Le, D. Ohayon, F. Caillibot, L. Gelebart, G. Denes; Zeolites, 270,**19** (1997).

147. C.D Chang in Handbook of Heterogeneous Catalysis, 1894,**4** (1995).

148.C. Doremieux-Morin, A. Ramsaran, R. Le Van Mao, P. Batamack, L. Heeribout, V.Semmer, G.Denes and J.Fraissard, Catalysis Letters,140, **34** (1995).

149.C. Doremieux-Morin, A. Ramsaran, R. Le Van Mao, P. Batamack, L. Heeribout, V.Semmer, G.Denes and J.Fraissard, Catalysis Letters,142, **34** (1995).

150. Dr. Le Van Mao and David Ohayon; " Methods for Pore Size Engineering in ZSM-5 Zeolite", Applied Catalysis A, 244, **217** (2001).

151.C.V McDaniel, P.K Maher and W.E Bouster, U.S Patent 3,374,058 (1968).

152.P.K Maher, U.S Patent 3,393,049 (1968).

153.A.B Scwartz, U.S Patent 3,244,643 (1966).

154. L.B Sand U.S Patent 3,436,174 (1969).

155. J. Weitkamp and L. Puppe; " Catalysis and Zeolites:"Fundemental and Applications", 329 (1999).

156.A. Chauvel, G. Lefebvre; Petrochemical Processes at Technip Paris,235,**1** (1989).

157.G. Mirth, J. Lercher; " On the Role of Product Isomerization for Shape- Selective Toluene methylation over H-ZSM-5", Journal of Catalysis; 199,**147** (1994).

158.A.Godfried ; "Interfacial Properties" in Energia, 4, 7 (1996).

159.C. Doremieux-Morin, A. Ramsaran, R. Le Van Mao, P. Batamack, L. Heeribout, V.Semmer, G.Denes and J.Fraissard, Catalysis Letters,139, **34** (1995).

160.G.McVicker and R. Beyerlein, Journal of Physical Chemistry, 1967-1970, **92** (1988).

161.J. Weitkamp and L.Puppe, "Catalysis and Zeolites (Fundemental and Applications), 329 (1999).

162. R.L Gorring, " Diffusion of Normal Paraffins in Zeolite T", Journal of Catalysis, 17-24,**31** (1973).

163. D.A Skoog, "Principles of Instrumental Analysis", 3rd ed. Saunders College Publishing, 464 (1985).

164. J.W Robinson, Analytical Chemistry, 32, 17A (1960).

165.D. Freude, " Studies in Surface Science Catalysis, 169, **52** (1989).

166. H. Kahn, Chemical Education, 43, A7 (1966).

167. J.W Robinson, Analytical Chemistry, 32, 17A (1960).

168. M.E Pillon, Spectrochem Acta, 821,**36B** (1981).

169. A. Walsh, Pure and Applied Chemistry, 1621, **49** (1977).

170. R.D Dresser, Journal of Chemical Education, 52,**A403** (1975).

171. W.M Meir and D.H Olson in " Atlas of Zeolite Structure Types", Butterworth-Heinemann, 3rd edition, London, 138 (1992).

172. Sie Ray 112, X-Ray Diffractometer Automation System Software 2.1 M.D U.S.A.

173.D.A Skoog, "Principles of Instrumental Analysis", 3rd ed. Saunders College Publishin.

174.Sie Ray 112, X-Ray Diffractometer Automation System Software 2.1 M.D U.S.A.

175. J.C Vedrine and Boris Imelik, " Les Techniques Physiques d'etude des catalyseurs", The Catalysis Research Institute, Technip ed. 823-824,856-857 (1980).

176. D.W Breck, Potential uses of Natural and Synthetic Zeolites in Industry, Union Carbide Corporate Brochure, 25 (1979).

177. G. Horvath and K Kowazoe, Journal Chemical Engineering in Japan, 470,**16**(6) (1983).

178.R. Le Van Mao, N.T Vu, S. Xiao and A. Ramsaran, " Modified Zeolites for the Removal of Calcium and Magnesium from hard water", Journal of Materials Chemistry, 1143, **4**(7) (1994).

179.G. Englehard and D. Michel, " Solid State NMR of Silicates and Zeolites", John Wiley and Sons, 157-161 (1977).

180.B.H Davis, Chemtech 19 (January 1991).

181. Dollimore D. and G.R Heal; Journal of Applied Chemistry;109, **14** (1964).

182. G. Horvath and K Kowazoe, Journal Chemical Engineering in Japan, 470,**16**(6) (1983).

183. Walker P.L : " Chemistry and Physics of Carbon"; 349,**2**, Marcel Dekker, N-Y (1966).

184.Frankenburg, W.G , V.I. Komarewsky and E.K Rideal, Eds: "Advancemes in Catalysis", 211,**11** (1952).

185. Frenkel J. : "Kinetic Theory of Liquids", Clarendon Press, Oxford (1946).

186. Halsey G.D : Journal of Chemical Physics; 931,**16** (1948); Journal of American Society; 1082,**74** (1952).

187. Hill T.L; Journal of Chemical Physics; 590,668, **17** (1949).

188. Pierotti R.A and H.E Thomas: "Surface and Colloid Science; 242,**4**, Wiley-Interscience,N-Y (1971).

189.Israel E. Wachs, "Characterization of Catalytic Materials", Manning Publishing 135(1992).

190.J.M Ward in Rabo, Zeolite Chemistry and Catalysis in American Chemical Society, 171 Washington D.C,118 (1976).

191.J. Weitkamp and L. Puppe; " Catalysis and Zeolites:"Fundemental and Applications", 201 (1999).

192.J. Weitkamp and L. Puppe; " Catalysis and Zeolites:"Fundemental and Applications", 204-205 (1999).

193.H.G Karge, Physical Chemistry, N.F 103,**122** (1980).

194. H.G Karge, K. Klose, Physical Chemistry, 92,**83** (1973).

195. H.G Karge, M. Ziolek, Laniecki M., Proceedings of the 9th IberoAmerican Symposium Catalysis (1984).

196. E. Gallei, E. Shadow, Rev. Scientific Instrument, 1504,**45** (1974).